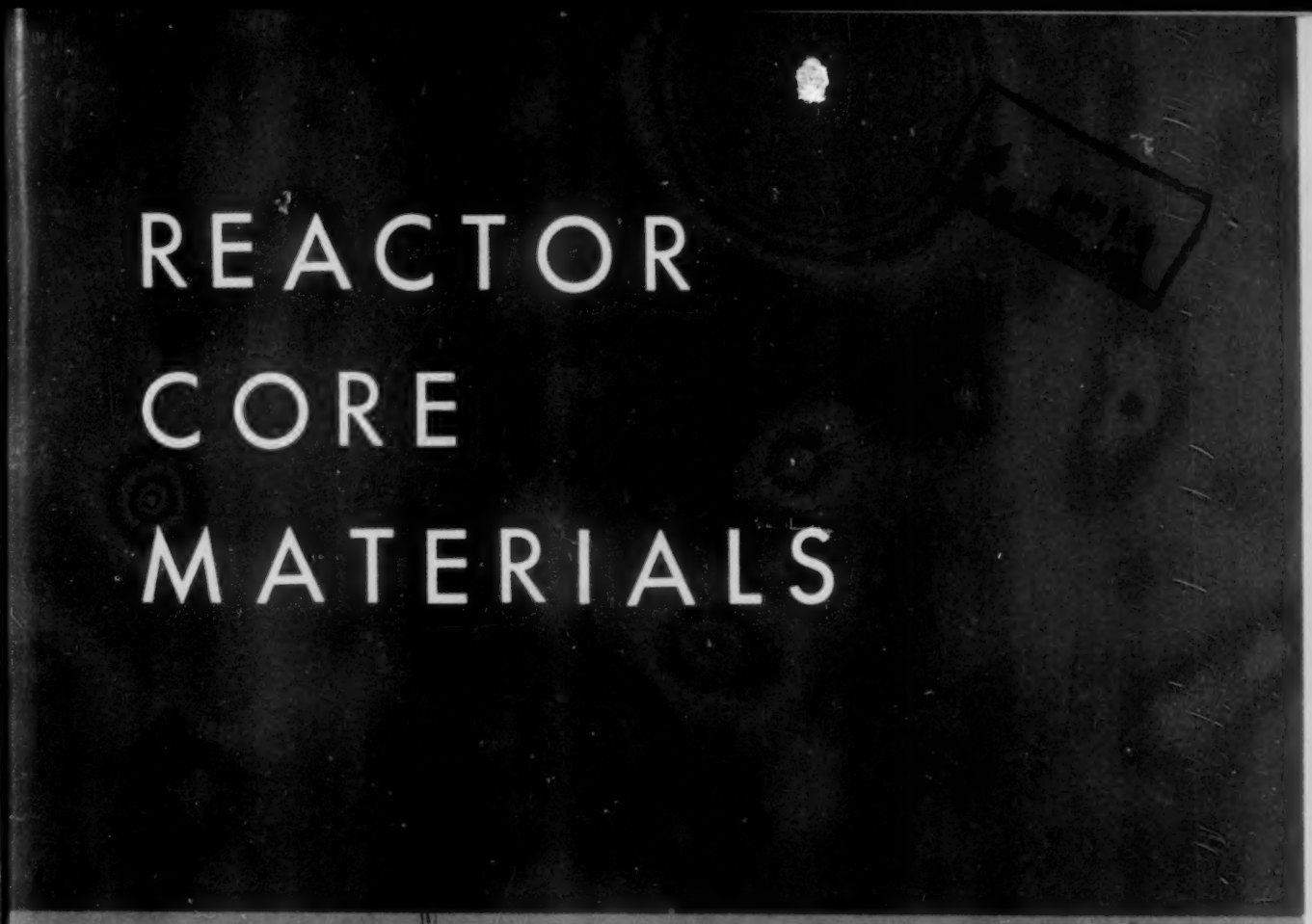

REACTOR CORE MATERIALS

A Quarterly Technical Progress Review

Prepared for U. S. ATOMIC ENERGY COMMISSION by BATTELLE MEMORIAL INSTITUTE

February 1961

● VOLUME 4

● NUMBER 1

TECHNICAL PROGRESS REVIEWS

To meet the needs of industry for concise summaries of current atomic developments, the Atomic Energy Commission is publishing this series, Technical Progress Reviews. Issued quarterly, each of the reviews digests and evaluates the latest findings in a specific area of nuclear technology and science.

The four journals published in this series are:

Nuclear Safety, W. B. Cottrell, editor, R. A. Charpie, advisory editor, and associates, Oak Ridge National Laboratory

Power Reactor Technology, Walter H. Zinn and associates, General Nuclear Engineering Corporation

Reactor Core Materials (covering solid material developments), R. W. Dayton, E. M. Simons, and associates, Battelle Memorial Institute

Reactor Fuel Processing, Stephen Lawroski and associates, Chemical Engineering Division, Argonne National Laboratory

Each journal may be purchased ($2.00 per year for subscription and individual issues $0.55) from the Superintendent of Documents, U. S. Government Printing Office, Washington 25, D. C. See back cover for remittance instructions and foreign postage requirements.

Availability of Reports Cited in This Review

Unclassified AEC reports are available for inspection at AEC depository libraries and are sold by the Office of Technical Services, Department of Commerce, Washington 25, D. C. Some of the reports cited are not available owing to their preliminary nature; however, the information contained in them will eventually be made available in formal progress or topical reports.

Unclassified reports issued by other Government agencies or private organizations should be requested from the originator.

Unclassified British and Canadian reports may be inspected at AEC depository libraries. British reports are sold by the British Information Service, 45 Rockefeller Plaza, New York, N. Y.; Canadian reports (AECL series) are sold by the Scientific Document Distribution Office, Atomic Energy of Canada, Ltd., Chalk River, Ontario, Canada.

Classified U. S. and foreign reports identified in this journal as Classified may be purchased by properly cleared Access Permit Holders from the Office of Technical Information Extension, U. S. Atomic Energy Commission, P. O. Box 1001, Oak Ridge, Tenn. Such reports may be inspected at classified AEC depository libraries.

TK9201
.R415

REACTOR CORE MATERIALS

Prepared for U. S. ATOMIC ENERGY COMMISSION
by BATTELLE MEMORIAL INSTITUTE

● FEB. 1961
● VOLUME 4
● NUMBER 1

foreword

Reactor Core Materials, one of a series of four quarterly reviews broadly covering the field of nuclear science and technology, is prepared by Battelle personnel from worldwide literature and covers materials and fabrication processes applicable to a nuclear reactor core. The coverage of this subject, however, is limited to materials that are solid at reactor operating temperatures. Pure chemistry, physics, core instrumentation, fuel processing, and source materials are not covered by this Review.

The authors and editors of *Reactor Core Materials* attempt to incorporate new developments and significant findings. This Review can serve as a useful summary of current research for both management and the technical specialist. For the latter group of readers, it is intended that the extensive referencing will aid in locating sources of more detailed information.

R. W. DAYTON
E. M. SIMONS
R. W. ENDEBROCK
Battelle Memorial Institute

1
1
1
5
6
6
8
9
10
12
16
16
17
18
22
22
22
30
30
34

contents

Foreword

1 I FUEL AND FERTILE MATERIALS

1 Unalloyed Uranium
1 Alpha-Phase Uranium Alloys
5 Gamma-Phase Uranium Alloys
6 Epsilon-Phase Uranium Alloys
6 Dilute Uranium Alloys
8 Plutonium and Its Alloys
9 Thorium
10 Dispersion Fuel Elements
12 Refractory Fuel and Fertile Materials
16 Mechanism of Corrosion of Fuel Alloys
16 Basic Studies of Radiation Effects in Fuel Materials
17 Metal-Water Reactions
18 References

22 II MODERATOR MATERIALS

22 Graphite
22 Beryllium
30 Beryllium Compounds
30 Solid Hydrides
34 References

36 III NUCLEAR POISONS

36 Burnable-Poison and Control Dispersion Materials
37 Control-Rod Alloys
39 References

40 IV CLADDING AND STRUCTURAL MATERIALS

40 Corrosion
46 Selected Mechanical Properties of Cladding and Structural Materials
49 Selected Metallurgical Aspects of Cladding and Structural Materials
52 Diffusion Studies
53 Radiation Effects in Nonfuel Materials
58 References

63 V SPECIAL FABRICATION TECHNIQUES

63 Melting, Casting, Heat-Treatment, and Hot Working
64 Cladding
68 Explosion Forming
71 Welding and Brazing
72 Nondestructive Testing
73 References

Issued quarterly by the U. S. Atomic Energy Commission. Use of funds for printing this publication approved by the Director of the Bureau of the Budget on November 1, 1960.

Section I

FUEL AND FERTILE MATERIALS

Unalloyed Uranium

The transformation temperatures of high-purity uranium were determined at Argonne National Laboratory (ANL)[1] by thermal analysis and dilatometry. Two thermal-analysis methods were used: one in which the rates of heating and cooling were controlled by a differential thermocouple, and another in which repeated thermal analyses were made at independently controlled rates. The solid-state transformation temperatures and the logarithm of the heating or cooling rates at relatively low rates are related linearly. The extrapolated functions intersect at a point where the disturbing effects of hysteresis, superheating, and undercooling disappear, i.e., at the equilibrium temperature. The mean transformation temperatures are 667°C for $\alpha \rightleftharpoons \beta$ and 775°C for $\beta \rightleftharpoons \gamma$. The mean temperature for melting and freezing is 1132°C.

In another study,[2] ANL workers observed that the self-diffusion coefficient of uranium decreases from 3×10^{-9} cm^2/sec at 785°C (gamma phase) to 2.1×10^{-11} cm^2/sec at 760°C (beta phase), dropping by a factor of 150 on crossing from the gamma into the beta phase. Even at temperatures high in the beta phase, there are indications that self-diffusion in beta uranium does not take place by isotropic volume diffusion alone. (M. S. Farkas)

Alpha-Phase Uranium Alloys

British workers have found[3] that the alpha and beta uranium phases exhibit high solubility for neptunium. The room-temperature solubility of neptunium in alpha uranium is 43 wt.%. There is some uncertainty as to whether complete solid solubility exists between gamma uranium and gamma neptunium; however, if there is a miscibility gap, it is very restricted. There is one intermediate phase in the system, stable to about 650°C and existing between 75 and 48 wt.% neptunium. Its crystal structure is simple cubic (a = 10.6 A), and it is isomorphous with the zeta phase in the plutonium-uranium system.

The uranium-molybdenum equilibrium diagram has been redetermined up to 19 wt.% molybdenum and below 900°C.[4] The eutectoid transformation $\beta \rightleftharpoons \alpha + \gamma$ was located at 639 ± 5°C. The limit of the $\beta + \gamma$ field was placed at 4.5 wt.% molybdenum at the eutectoid temperature. The gamma phase undergoes a eutectoid transformation at 10.5 wt.% molybdenum and 565 ± 5°C, to $\alpha + \delta$. The tetragonal structure of the delta phase was confirmed, with c_0 = 9.854 A, a_0 = 3.427 A, and c/a = 2.876. It is considered probable that the delta phase is formed by a congruent transformation.

Nuclear Metals[5] has reported findings regarding the aqueous corrosion of diffusion-annealed Zircaloy-2-clad uranium–2 wt.% zirconium fuel rods. Interdiffusion heat-treatment overcame the deleterious effect of a 7-mil-diameter defect when the element was exposed to high-temperature water, even though the defect, created before or after the heat-treatment, exposed the core. The following conclusions were reached by the investigators.

1. There is no unique range of temperature for effective heat-treatment. Various temperatures could be used if sufficient time is allowed, e.g., 1.5 hr at 950°C.

2. If a bond is inadequate, a defected sample will fail despite a normally adequate diffusion anneal, although failure has been prevented in specimens with weak bonds by the use of a more drastic diffusion treatment.

3. The severity of the diffusion anneal necessary to overcome the effect of a defect in-

creases as the cladding thickness decreases. Even the most severe treatment may not overcome the effect of a defect if the cladding is less than about 10 mils thick.

4. In order for the diffusion anneal to be effective, any reduction in cladding thickness must be compensated for by strengthening of the core-cladding bond.

5. After the diffusion anneal, the thermal history may undo the beneficial effect of the diffusion anneal. The effect of the diffusion anneal is counteracted by subsequent exposure to temperatures between about 700 and 550°C, either by slow cooling or by subsequent heat-treatment. Therefore, rapid cooling is necessary after the diffusion treatment.

6. The corrosion resistance of the Zircaloy-2 cladding is not adversely affected by diffusion annealing at 880 and 900°C.

7. The problem of uranium diffusing to the surface of the Zircaloy cladding can be eliminated by proper choice of heat-treatment and cladding thickness. The standard 7-hr diffusion anneal at 880°C does not increase the uranium concentration in the outer 4 mils of 15-mil-thick Zircaloy cladding.

8. A complete explanation for the protective action of the diffusion-anneal technique has not been established. The evidence accumulated indicates that bond strength, cladding stiffness, and cladding strength play major roles, whereas the corrosion resistance of the core plays a lesser role.

Other studies[6] on the retention and metastability of the beta phase in dilute uranium alloys have been completed. It is anticipated that, because of greater strengths, beta-phase uranium alloys will possess greater resistance to swelling during irradiation than either the alpha-phase or gamma-phase alloys. Among the alloys investigated, the uranium–0.3 wt.% chromium, uranium–0.3 wt.% chromium–0.3 wt.% niobium, and uranium–0.3 wt.% chromium–0.3 wt.% molybdenum alloys exhibited the best retention and stability properties. Calculations indicate that, if neutron-induced phase reversion occurs, more than 90 per cent beta would be retained in these alloys during irradiation at 400 to 500°C and fission rates of about 10^{14} fissions/$(cm^3)(sec)$.

In order to determine whether a correlation exists between out-of-pile strength properties and in-pile irradiation behavior, investigators[7–9] are determining the high-temperature tensile and creep properties of dingot uranium and a uranium–1.5 wt.% molybdenum alloy. Tables I-1 and I-2 give the tensile properties of the dingot uranium and the uranium–1.5 wt.% molybdenum alloy, respectively, and their creep properties are given in Table I-3.

Atomics International[10] has developed fuel alloys for use in the Organic-Moderated Reactor (OMR). The specifications of a uranium alloy of slight enrichment which can be clad and bonded to aluminum and which is capable

Table I-1 TENSILE PROPERTIES OF DINGOT URANIUM[8]

History	Temp., °C	Strength, psi: Yield (0.2% offset)	Strength, psi: Ultimate tensile	Elongation in 2 in., %	Reduction of area, %
Beta treated*	RT†	37,000	64,100	3.7	6.3
Beta treated and aged‡	RT	33,100	84,400	11.3	13.0
Beta treated and aged	RT	32,600	84,800	11.9	13.1
Beta treated	150	35,500	63,200	28.2	38.1
Beta treated and aged	150	32,600	61,150	31.9	50.0
Beta treated	400	21,200	25,500	19.5	65.2
Beta treated and aged	400	18,400	23,200	30.8	71.6

*720°C, 10 min, air cooled.
†RT = room temperature.
‡343°C, 24 hr; 399°C, 24 hr, in argon to simulate thermal conditions associated with corrosion acceptance test.

Table I-2 TENSILE PROPERTIES OF URANIUM–1.5 WT.% MOLYBDENUM[7]

History	Temp., °C	Strength, psi: Yield (0.2% offset)	Strength, psi: Ultimate tensile	Elongation in 2 in., %	Reduction of area, %
As cast	RT	61,500	124,000	21.8*	30.3
		57,500	121,000	19.7*	34.8
		65,800	127,000	14.7*	20.7
Extruded rod, heat-treated†	RT	69,700	134,000	17.5	23.2
	150	72,000‡	107,000	18.7	36.0
	300	53,500	67,300	17.2	51.7
	400	47,500	59,600	21.4	55.4
	500	28,200	37,400	23.0	67.1

*Gauge length ¾ in.
†775°C, 15 min, furnace cooled to 620°C, held for 1 hr, then air cooled.
‡Load-deformation curves were obtained from head travel; yield-strength values are therefore questionable.

Table I-3 STRESS-RUPTURE TEST RESULTS FOR EXTRUDED MATERIALS[9]

Material	Heat-treatment	Temp., °C	Stress, psi	Rupture time, hr	Elongation in 2 in., %	Reduction of area, %	Minimum strain rate, in./(in.)(hr)
Dingot uranium	720°C, 10 min, air cooled, aged at 343°C for 24 hr plus 400°C for 24 hr in evacuated Vycor tube	350	25,000	3.9	18.8	58.5	1.7×10^{-2}
		475	10,000	3.9	25.1	75.0	3.1×10^{-2}
		535	10,000	0.13	37.0	62.4	
Uranium–1.5 wt.% molybdenum	As cast	530	25,000	16.8	15.8	50.0	2.8×10^{-3}
Uranium–1.5 wt.% molybdenum	775°C, 15 min, furnace cooled to 620°C, held for 1 hr, then air cooled	400	40,000	75.1			5×10^{-5}
		425	40,000	116.3	17.5	43.6	9.4×10^{-6}
		450	40,000	16.2	20.6	57.2	5.6×10^{-3}
		475	25,000	118.3	16.7	46.2	3.6×10^{-4}
		475	25,000	115.7	24.8	38.0	5.0×10^{-4}
		530	25,000	1.4	11.8	41.0	2.8×10^{-2}
		550	10,000	92.6	16.8	26.7	4.7×10^{-4}
		565	10,000	19.9	9.8	43.5	2×10^{-3}

of 3000 Mwd per metric ton of uranium average burnup (5000 Mwd per metric ton of uranium peak burnup) at a peak temperature of 850°F have apparently been obtained. Investigation has shown that the addition of 3.5 wt.% molybdenum to uranium improves the thermal-cycling stability of the base material and eliminates the alpha-to-beta phase transformation. In addition, 3.5 wt.% molybdenum increases the ultimate and yield strengths of as-cast uranium by a factor of 5. The addition of 0.1 wt.% aluminum to the binary further increases these properties by a factor of about 7, whereas additions of 0.1 to 0.5 wt.% silicon did not appreciably improve the tensile properties of the binary alloy. The creep strength of uranium is increased significantly by the addition of 3.5 wt.% molybdenum and is improved further by the addition of 0.1 to 0.5 wt.% aluminum or silicon. The uranium–3.5 wt.% molybdenum–0.1 wt.% aluminum alloy showed the highest creep strength of all the low alloys tested. The results of these high-temperature tensile and creep tests are presented in Tables I-4 and I-5, respectively. On the basis of creep tests, three alloys were selected: uranium–3.5 wt.% molybdenum, uranium–3.5 wt.% molybdenum–0.5 wt.% silicon, and uranium–3.5 wt.% molybdenum–0.1 wt.% aluminum. Irradiation of test elements at OMRE showed that both the uranium–3.5 wt.% molybdenum and the uranium–3.5 wt.% molybdenum–0.5 wt.% silicon alloys were dimensionally stable up to 2300 Mwd per metric ton of uranium. The uranium–3.5 wt.% molybdenum–0.1 wt.% aluminum alloy was stable to an estimated 4000 Mwd per metric ton of uranium.

Further results[11] of irradiation tests on uranium binary alloys containing less than 0.2 wt.% cerium, vanadium, chromium, beryllium, and yttrium have been reported. The test was designed to show the effect of alloy additives of different atomic size than uranium. Because of the strains around the alloy atoms when they are in solid solution, these atoms may attract and be bound to fission-gas atoms, decrease the gas-atom mobility, and therefore decrease

Table I-4 RESULTS OF TENSILE TESTS AT 900°F[10]

Alloy composition (balance U), wt.%	Strength, 1000 psi				Elongation in 2 in., %
	Ultimate tensile	Yield (0.2% offset)	Yield (0.1% offset)	Yield (0.02% offset)	
3.5 Mo–0.1 Al; average of 6 tests	110.1	81.4	67.1	46.8	1.4
3.5 Mo–0.5 Si; average of 4 tests	79.5	59.8	50.9	35.8	1.1
3.5 Mo; average of 10 tests	91.5	61.3	51.8	37.2	5.6
3.5 Mo–0.1 Si; average of 2 tests	71.9	55.5	42.4	23.7	0.5
3.5 Mo–0.5 Al; average of 3 tests	51.8			45.3	0.2

Table I-5 RESULTS OF CREEP TESTS OF VARIOUS AS-CAST URANIUM-BASE ALLOYS[10]

Alloy composition (balance U), wt.%	Test temp., °F	Minimum creep rate at indicated stress level (1000 psi), %/hr							Duration of test, hr
		10	15	20	30	40	45	50	
3.5 Mo–0.1 Al	900	0.0025	0.0025	0.004					218
	900				0.0032	0.0057	0.0084	0.026	148
	900			0.003	0.003	0.0065		*	355
	900			0.005	0.006	0.013	0.023*		
	800			0.001					
	900			0.002					
	1000			0.018					192
	800				0.0025				
	900				0.007				190
3.5 Mo–0.5 Al	900	0.003	0.003	0.003					599
3.5 Mo–0.5 Si	900		0.0038	0.0043		0.0045			426
	900			0.004		0.0048			460
	900			0.0055		0.012	0.027		
	900						0.0076	0.021	164
3.5 Mo	900	0.0054		0.013					164
	900			0.012	0.023				233
	900		0.009			0.033			
	900			0.007					137
	1000			0.175					22
	900						0.037		54
	900							0.166	24
	900		0.007						

* Specimen ruptured at indicated stress.

Table I-6 DATA FROM URANIUM-BASE ALLOYS[11] IRRADIATED TO 0.25 At.% BURNUP AT 700 TO 1100°F

Element	Atomic size as a pure metal, A	Size mismatch with U, %	Fuel composition, wt.%	% ΔV/0.1 at.% burnup (av. for the alloy)
U	1.38	0	U	15.7
Cr	1.25	−10	U–0.2 Cr	5.7
Ce	1.82	+32	U–0.1 Ce	8.5
V	1.31	−5	U–0.2 V	9.2
Be	1.11	−20	U–0.04 Be	7.6
Y	1.80	+30	U–0.1 Y	6.4

the fuel swelling. The swelling for 0.1 at.% burnup varies from 5 to 17 per cent, as shown in Table I-6, with uranium-chromium samples showing the best resistance to swelling. Some of the suggested reasons for the decrease in swelling are as follows:

1. A decrease in the fission-gas mobility (the chromium has relatively high solubility at the irradiation temperature, which is necessary for the proposed mechanism)

2. Fuel strengthening (chromium is known to decrease irradiation growth, which is probably partly due to an increase in the fuel strength during irradiation)

3. A difference in grain size (the uranium-chromium alloys show the smallest subgrain size)

Examination of two irradiated Experimental Boiling-Water Reactor (EBWR) Core I fuel elements was performed by Argonne.[12] These two Zircaloy-2-clad uranium–5 wt.% zirconium–1.5 wt.% niobium alloy fuel elements had a maximum burnup of 0.11 and 0.39 at.%, respectively. Both elements were disassembled and sampled for the evaluation of the effects of in-pile irradiation and radiation damage to the fuel. The fuel elements were in good condition, with no ruptures of the cladding, no core-cladding nonbonds, and no excessive fuel-plate swelling or warpage.

Thin samples cut from the fuel plates in the element which received 0.39 at.% burnup warped and cracked, suggesting a relieving of locked-in stresses and indicating that the fuel cores were hard, brittle, and highly stressed. The rate of fuel-plate volume increase due to the burnup of uranium was 6 to 7 per cent ΔV per atomic per cent burnup. Annealing studies on

sections of fuel plate at 500 and 550°C indicated bulk-volume increases of 1 to 2 per cent and 5 to 10 per cent, respectively, after 500 hr. A 600°C anneal of a fuel plate with a 0.35 at.% burnup resulted in a bulk-volume increase of 17 per cent after 45 hr. For burnups ranging from 0.005 to 0.11 at.%, the corrosion resistance of irradiated fuel alloy is superior to that of the unirradiated material.

Several unusually well-presented and complete reviews of the aqueous corrosion of uranium and its alloys have been included in the compendium of papers[13] from the AEC-Euratom Conference in Brussels. (M. S. Farkas)

Gamma-Phase Uranium Alloys

Uranium-Niobium

The results of studies of the role of lattice mismatch between the oxide and base metal in the corrosion behavior of uranium–10 wt.% niobium and uranium–10 wt.% niobium–0 to 10 wt.% zirconium alloys are presented by Chirigos.[14] The degree of mismatch is found to control the thickness of oxide-layer buildup and the time at which flaking of the oxide layer occurs. It is concluded that there is good evidence that lattice mismatch has an important influence on corrosion life of these gamma-phase alloys.

Uranium-Molybdenum

In a study[15] of the effect of irradiation on the U_2Mo phase, plates of U_2Mo composition were homogenized and then annealed at 500°C for seven days to obtain the ordered U_2Mo phase. The plates were then irradiated in thermal-neutron fluxes of 2×10^{10} to 2×10^{12} neutrons/(cm^2)(sec) below 65°C. The irradiation resulted in the disappearance of the X-ray lines associated with the ordered structure and a change to the cubic gamma structure. The data indicate that the transition is continuous.

The results[8] of the irradiation of a series of uranium-molybdenum alloys prepared by Atomics International are shown in Table I-7. Resistance to swelling increases markedly with increasing molybdenum content. Also, damage to the uranium–10 wt.% molybdenum alloy increases rapidly with increasing temperature between 1100 and 1300°F.

Oxidation rates for the uranium–10 wt.% molybdenum alloy at 600°F in air are given as 0.079, 0.051, 0.043, 0.032, and 0.015 mg/(cm^2)(hr) after 1, 2, 4, 8, and 24 hr, respectively. Rates at 900°F at these same intervals are 0.075, 1.22, 1.31, 1.64, and 1.75 mg/(cm^2)(hr).

Table I-7 EFFECT OF TEMPERATURE ON RADIATION DAMAGE IN URANIUM-MOLYBDENUM ALLOYS[11]

Alloy (balance U), wt.% Mo	Typical temp., °F		Burnup, Mwd/metric ton of U	Increase in diameter per 3300 Mwd/metric ton of U, %	Decrease in density per 3300 Mwd/metric ton of U, %	Increase* in volume per 3300 Mwd/metric ton of U, %
	Surface	Center				
3	745	940	2100	0.4	0.9	1.1
3	775	990	2500	4.1	4.0	9.6
3	875	1120	2500	1.6	3.4	3.7
3	900	1160	2600	1.0	4.8	2.5
3	955	1235	3200	5.8	15.1	14.7
3	980	1260	2900	5.9	6.8	7.8
3	1035	1370	3500	1.2	6.8	4.5
5	850	1100	3200	1.1	2.6	2.6
5	910	1180	3200	3.0	2.9	6.7
5	1075	1410	3900	0.9	5.4	3.2
7.5	855	1125	3100	0.0	0.9	0.2
7.5	1045	1380	3900	0.7	2.1	2.0
7.5	1065	1400	3900	0.7	1.7	1.9
10	780	1040	3000	0.2	0.1	0.5
10	800	1060	2600	0.1	0.0	0.4
10	850	1130	2800	0.3	0.3	0.4
10	990	1330	3300	0.3	0.8	0.7
10	990	1330	3900	0.5	1.1	1.5
10	1025	1370	4000	0.4	1.3	1.2

* Calculated from measured dimensional changes.

Studies of the corrosion of the uranium–10 wt.% molybdenum alloy in various environments are reported by Battelle.[16] Data are shown in Table I-8.

Table I-8 CORROSION OF URANIUM–10 Wt.% MOLYBDENUM ALLOY IN VARIOUS ENVIRONMENTS[16]

Exposure time, days	Weight loss in indicated environment,* mg/(dm²)(day)		
	Humidity	Humidity-freeze	Salt spray†
7	0.53	0.09	23.4
14	0.26	0.14	35.8
21	0.17	0.16	39.9
28	0.14		42.8

* Humidity: saturated air at 120°F with condensation. Humidity-freeze: saturated air at 165°F, with condensation for 20 hr; freeze at −50°F for 4 hr; daily cycle. Salt spray: 20 wt.% NaCl at 95°F.

† Specimens severely roughened.

A few pits were noted at random positions on specimens exposed to the humidity and cyclic humidity-freezing conditions. Pitting and corrosion were severe in the salt-spray environment.

At Atomics International,[11] it was found that 96 heats were required to produce 3856 acceptable uranium–10 wt.% molybdenum fuel slugs having dimensions of 0.590 ± 0.005 in. in diameter and 12.000 ± 0.010 in. in length. A 44-cavity mold was used for the major portion of the castings. Average mold life was one mold per 10 heats, with two heats per 16-hr day. Representative metal yields and losses per heat were:

	Total charge, %
Finished casting yield	80.0
Total nonrecyclable scrap	7.1
Total recyclable scrap	12.9

A 24-hr heat-treatment at 900°C is reported to produce a fully gammatized structure in cast uranium–10 wt.% molybdenum material. Transformation of this material begins within 24 hr at 370°C. The optimum heat-treatment for gammatization of this as-cast alloy is reported as 8 hr at 1000°C. A 250-hr heat-treatment at 475°C is the optimum condition for producing transformation from the gamma phase.

The metallographic procedures for the preparation of uranium–0.5 to 10 wt.% molybdenum alloys are reviewed in a French paper.[17] Information concerning the various phases and their characteristics is included. (A. A. Bauer)

Epsilon-Phase Uranium Alloys

Uranium-Silicon

The dimensional changes obtained by ANL[18] after irradiating specimens of U_3Si are summarized in Table I-9. Exposure of irradiated specimens in 260 and 290°C water showed that the corrosion rates were not drastically affected by irradiation, although the specimens eventually disintegrated. Specimens tested in 315°C water showed higher corrosion rates after irradiation, with hydrogen evolution accompanying corrosive attack.

Uranium-Zirconium

The gamma-to-epsilon transformation has been studied at Battelle[19] in zirconium alloys containing 22 to 70 wt.% uranium. In this range of compositions the gamma phase can be retained by quenching. Transformation to the epsilon phase occurs by a nucleation-and-growth process. The diffusion of atoms to preferred sites to yield a partially ordered structure apparently controls the rate of transformation. Alloys outside the equilibrium-epsilon composition range transform initially to a supersaturated form of epsilon; equilibrium epsilon forms by the precipitation of the alpha-uranium and alpha-zirconium phases.

(A. A. Bauer)

Dilute Uranium Alloys

Aluminum-Uranium

As a part of a program of fuel-material evaluation, Phillips Petroleum[20] has irradiated aluminum-uranium alloy specimens containing 18, 23, and 25 wt.% uranium. Some of the 18 wt.% uranium alloys contained natural boron in varying amounts, some contained Gd_2O_3, and some contained both boron and Gd_2O_3. These specimens were irradiated at ambient reactor temperatures to U^{235} burnups which ranged from

Table I-9 EFFECTS OF IRRADIATION ON U_3Si (U–3.8 WT.% Si) ALLOY[18]

Specimen	Zircaloy-2 cladding thickness, in.	Ingot	Method of fabrication	Heat-treatment	Burnup, at.%	Irradiation temp., °C: Surface	Irradiation temp., °C: Center	Length change, %	Growth rate,* G_1	Diameter change, %	Weight change, mg
AB-111	None	UA42	Cast	66 hr at 800°C	0.09	130	200	−1.44	−16	2.88	
AB-110	None	UA42	Cast	66 hr at 800°C	0.25	280	450	2.05	8.1	1.80	
BB-2	None	Y16F-123	Cast	2 hr at 825°C	0.14	220	290	0.92	6.6	2.34	−0.6
BB-3	None	Y16F-123	Cast	2 hr at 825°C	0.35	510	700	−1.40	−4.0	2.35	−2.6
BB-1	None	Y16F-123	Cast	2 hr at 825°C	0.45	650	890	3.18	7.0	32.5	35.8
CE-4-1	None	UA111	Extruded at 850°C	7 days at 700°C	0.067	90	100	0.77	11	1.25	−1.2
CE-3-1	None	UA111	Extruded at 850°C	7 days at 700°C	0.085	120	140	0.72	8.5	1.50	−0.6
CE-1-1	None	UA155	Extruded at 850°C	7 days at 700°C	0.10	140	150	2.92	29	0.70	0.7
CE-2-1	None	UA155	Extruded at 850°C	7 days at 700°C	0.13	140	160	3.00	23	0.70	1.0
CE-4-2	0.030	UA111	Extruded at 850°C	7 days at 700°C	0.067	100	110	2.78	41	−1.9	1.8
CE-3-2	0.030	UA111	Extruded at 850°C	7 days at 700°C	0.085	130	150	2.99	35	−0.05	−1.6
CE-1-2	0.030	UA155	Extruded at 850°C	7 days at 700°C	0.10	140	170	3.88	38	−0.23	1.7
CE-2-2	0.030	UA155	Extruded at 850°C	7 days at 700°C	0.13	150	180	3.94	30	0.02	1.3

* G_1 = μin./in. per fission/10^6 total atoms.

15 to 50 at.%. As a result of these irradiations, volume changes were only nominal (0.43 per cent increase at 30 to 50 at.%). Hardness increases were noted in cladding, matrix, and fuel compound particles, with the greatest increase being noted in the matrix and the fuel particles. In the case of aluminum, these data indicate that fission products have a large effect on the properties. This means that, if such a material is to be used as a matrix, it must be exposed to fission products as well as to fast neutrons if the test is to be realistic.

The results reported by Phillips indicate that the aluminum–18 and 25 wt.% uranium alloy can be irradiated under Materials Testing Reactor (MTR) conditions to a reasonable burnup without damage, provided that it has been properly fabricated. This seems to be corroborated by the fuel-damage incident at the Westinghouse Testing Reactor (WTR).[21] Examination of the failed element led to the conclusion that the failure resulted from poor core-to-cladding bonding in an area of the element. Inspection control will naturally be tightened, and it is possible that an ultrasonic-test requirement will be included in the specifications.

An evaluation of tin and zirconium ternary additions to the aluminum–35 wt.% alloy has been completed at Battelle.[22] The following briefly summarizes the results of this evaluation.

Casting. Fluidity is improved by the addition of either zirconium or tin. However, the best fluidity is achieved by the addition of 2 wt.% tin.

Stabilization of UAl_3. Both tin and zirconium stabilize UAl_3; however, in the amounts studied (up to 3 wt.%), the zirconium addition was the most effective.

Extrusion Pressure and Strength. The retention of UAl_3 decreased the pressure needed to extrude the alloys, but these additions also caused a decrease in tensile and creep rupture properties. This reduction of strength is most noticeable at elevated temperatures (200 and 250°C).

Corrosion. The ternary additions have no effect on the corrosion behavior of the basic binary in 150°C demineralized water.

Niobium-Uranium

Niobium-base binary alloys containing 10 to 60 wt.% uranium have been exposed to 600°F

water for 336 days. Most of the alloys lost weight, although the 20 and 60 wt.% uranium alloys showed a weight gain. Analysis of the data indicates that the higher the initial oxygen content the more corrosion occurs. Battelle[16] discontinued these tests in water, as well as those in 1500°F sodium. After 1500-hr exposure to the sodium, very little attack was noted on the 10 and 20 wt.% uranium alloys. In the case of the other alloys, the weight change increased generally as uranium content increased, e.g., 1.7 mg/cm^2 for the 30 wt.% uranium alloy to 4.45 mg/cm^2 for the 60 wt.% uranium alloy. Stress-rupture-test results indicate good creep resistance for the niobium–10 and 20 wt.% uranium alloys at 1600 and 1800°F.

Recrystallization studies were completed on 80 per cent cold-worked material. The niobium–30 wt.% uranium alloy begins to recrystallize after 1 hr at 1800°F, and it is completely recrystallized after 1 hr at 1900°F. Recrystallization of the niobium–10 and 20 wt.% uranium alloys begins after 1 hr at 2000°F, and it is complete after 1 hr at 2100°F. The addition of uranium to niobium lowers the thermal conductivity by a significant amount, as is illustrated by the following tabulation:

Temp., °F	Thermal conductivity, Btu/(hr)(ft)(°F)		
	Unalloyed Nb	Nb–10 wt.% U	Nb–20 wt.% U
200	26.9	14.0	10.2
1800	34.2	28.7	27.2

Difficulties have been continually encountered in fabricating alloys containing over 30 wt.% uranium. Careful study[23] has indicated that the material is hot short, which seems to be caused by segregation on a microscale of uranium-rich alloy. Several casting techniques will be examined briefly in an attempt to prevent crack formation. (R. F. Dickerson)

Plutonium and Its Alloys

Micron-sized plutonium powder has been produced at Hanford[24] in 20-g batches by hydriding massive metal and then grinding and decomposing the hydride.

Aluminum-Plutonium

Hanford[25] has irradiated aluminum–5, 10, 15, and 20 wt.% plutonium alloys to total atom burnups of 0.1 and 0.2 at.%. Dimensional changes of dejacketed alloy cores burned up to 0.1 at.% are seen in Table I-10.

Table I-10 DIMENSIONAL CHANGES OF FUEL CORES[25]

(Fuel Cores Are About 0.5 In. in Diameter by 1.98 In. in Length)

Fuel alloy, wt.%	Δ diameter, in.		Δ length, in.	Δ volume, %
	Top	Bottom		
Al–5 Pu	0.0028	0.0027	0.0113	2.7–2.8
Al–10 Pu	0.0006	0.0025	0.0116	1.1–2.6
Al–15 Pu	0.0006	0.0016	0.0090	0.9–1.7
Al–20 Pu	0.0025	0.0036	0.0112	2.5–3.4

In an effort to determine the effects of purity and casting conditions on corrosion, Hanford[26] examined aluminum–2 wt.% nickel–1.8 wt.% plutonium alloys cast under varying conditions and prepared using two grades of aluminum (99.9 and 99.45 per cent aluminum). No differences in corrosion resistance were found, indicating that aluminum purity and casting conditions are not critical in the range tested. Also, the effect of extrusion temperature on the corrosion resistance of an aluminum–2 wt.% plutonium–1 wt.% silicon–1 wt.% nickel alloy was investigated.[27] Rods extruded at 450, 500, and 550°C showed no variation in corrosion properties.

Chalk River[28] is attempting to develop a low-plutonium alloy (approximately 5 wt.% plutonium) with corrosion properties equivalent to those of an aluminum–20 wt.% plutonium alloy. Ternary alloying with uranium, silicon, nickel, and zirconium is being investigated for this purpose. Preliminary tests in 340°C water indicate that aluminum–5 wt.% plutonium–15 wt.% uranium, aluminum–5 wt.% plutonium–15 wt.% silicon, and aluminum–5 wt.% plutonium–1 wt.% nickel alloys are comparable to the aluminum–20 wt.% plutonium alloy. An aluminum–5 wt.% plutonium–2 wt.% zirconium alloy failed rapidly in 340°C water.

Plutonium-Uranium

A peritectoid reaction occurs on the high-plutonium end of the plutonium-uranium system

at a temperature between 115 and 118°C. Time-temperature-transformation (T-T-T) curves obtained at Hanford[29] for plutonium–3, 7, and 15 wt.% uranium alloys were simple "C" curves similar to those describing unalloyed plutonium, with a maximum rate of transformation at –20°C. The T-T-T curves for the plutonium–3 and 7 wt.% uranium alloys are shown in Figs. 1 and 2. The curve for the 7 wt.% uranium alloy is shifted significantly to the right of that describing the 3 wt.% uranium alloy. No transformation upon cooling was observed in the plutonium–15 wt.% uranium alloy.

(V. W. Storhok)

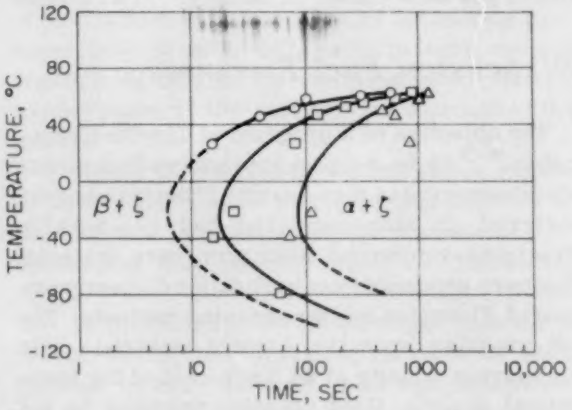

Figure 1—T-T-T curves of a plutonium–3 wt.% uranium alloy.[29] ○, transformation start; □, 50 per cent transformed; Δ, apparent completion.

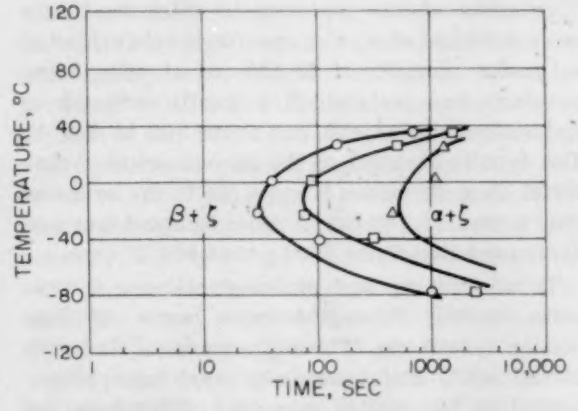

Figure 2—T-T-T curves of a plutonium–7 wt.% uranium alloy.[29] ○, transformation start; □, 50 per cent transformed; Δ, apparent completion.

Thorium

Confirmation of previous reports that complete solubility exists between the face-centered cubic (fcc) allotropes of thorium (fcc up to 1330°C) and lanthanum (fcc between 330 and 865°C) has been made by Evans et al.[30] Lattice-parameter measurements indicating complete solubility were obtained on samples of alloys quenched from a temperature at which the face-centered cubic solid solution is stable.

Graham and McTaggart[31] have investigated compounds of thorium with elements of Group VI-B. The compounds Th_2S_5 and Th_2Se_5 were found to have tetragonal symmetry; $ThTe_3$ was found to be monoclinic; and Th_2Te_3 was found to be hexagonal.

The vapor pressure has been determined[32] over a temperature range of 1757 to 1956°K for solid thorium containing less than 30 ppm oxygen. Over this temperature range, but below the melting point of thorium, the vapor pressure is given by the expression:

$$\log P = -28{,}780\ T^{-1} + 5.991$$

where P is the vapor pressure of thorium in atmospheres and T is temperature in degrees Kelvin. The heat of sublimation of thorium was calculated to be:

$$\Delta H^{\circ}_{298} = 137 \text{ kcal/mole}$$

The recrystallization temperature of thorium alloys containing 5 to 20 wt.% uranium is reported[33] to be about 100°C higher than that of unalloyed thorium. The thorium-uranium alloys, on being cold-reduced 90 per cent, recrystallized after less than 5 min at 725°C. A study of the effects of alloying elements upon the corrosion resistance of thorium-uranium alloys in water at 200°C has led to the conclusion that the best that can be achieved is a twofold decrease in the corrosion rate.

Battelle reports[34] that the creep strength of thorium-uranium alloys at 700°C decreases with increasing uranium content, as is to be expected in a two-phase alloy when the amount of a phase that is very weak at elevated temperatures is increased. Ternary alloy additions which are known to strengthen uranium are beneficial in improving the creep strength of thorium-uranium alloys, as shown in Table I-11.

Table I-11 CREEP STRENGTHS OF THORIUM-URANIUM ALLOYS AT 700°C[34]

Nominal alloy composition (balance Th), wt.%	Stress for 0.01% deformation per hour, psi
5 U	1700
10 U	1100
20 U	480
10 U + 1.5 Mo	1600
10 U + 2 Nb	1200

Subsequently, it has been reported[17] that hot-hardness tests show that a thorium–10 wt.% uranium–0.5 wt.% aluminum alloy is 65 per cent harder at elevated temperatures than unalloyed thorium, a thorium–10 wt.% uranium–2 wt.% molybdenum alloy, or a thorium–10 wt.% uranium–4 wt.% niobium alloy. A thorium–10 wt.% uranium–0.1 wt.% beryllium alloy shows a creep strength of 6300 psi for a creep rate of 0.01%/hr at 600°C and a creep strength of 1900 psi for a creep rate of 0.01%/hr at 700°C. As can be seen from the above data, this latter alloy is the strongest of those being tested and is almost twice as strong as the binary thorium–10 wt.% uranium alloy.

It is also reported[16] that ThN-UN alloys react with moisture to produce ammonia gas, metal oxides, and probably hydrogen gas.

A series of experiments has been run by Neymark[35] to outline the compatibility of thorium-uranium alloys with stainless steel for short times at very high temperatures, such as might be encountered during reactor excursions. A thorium–7.6 wt.% uranium alloy showed only slight alloying with stainless steel at 2000°F in 4 min. Severe alloying by eutectic formation occurred in less than 4 min at 2200°F and in less than 2 min at 2300°F. When sodium bonded to stainless steel, a thorium–7.6 wt.% uranium alloy reacted by eutectic formation at 1800°F in 14 min and at 2000°F in 7 min.

Irradiated thorium has been annealed[36] at 750°C for 1 to 100 hr. The unirradiated thorium had a tensile elongation of 45 per cent, the irradiated thorium had a tensile elongation of 10 per cent, and the irradiated and annealed thorium had a tensile elongation of 40 per cent. It was noted that the tensile curves for the irradiated material after annealing fell below the tensile curves for unirradiated material. This indicates a loss of toughness as a result of these treatments.

Additional confirmation of the excellent radiation stability of thorium-base alloys has been obtained[37] at temperatures below about 1200°F. A thorium–5.4 wt.% uranium alloy was irradiated to a maximum burnup of 1300 Mwd per metric ton of alloy at a temperature not in excess of 1000°F. The irradiated fuel alloy showed no warp in the form of slugs 6 in. long and ¾ in. in diameter, no diameter changes, less than 0.5 per cent change in length, and less than 1 per cent change in density. (W. Chubb)

Dispersion Fuel Elements

The objective of a program at Clevite Corporation[38–40] is to develop procedures that utilize aluminum-coated fuel-bearing Fiberglas as core material in aluminum-clad fuel elements. Fiberglas-reinforced aluminum core material has been produced by consolidation of aluminum-coated Fiberglas by two pressing methods. The hot-pressing operation yielded materials with an average density of 98.5 per cent of the theoretical density. Cold pressing followed by hot pressing produced materials with an average density of 99.1 per cent of the theoretical density.

Hot-pressed compacts were produced with 60.8 wt.% aluminum and 39.2 wt.% Fiberglas. Specimens of this material in which the fibers were oriented along the specimen axis exhibited a tensile strength of 25,250 psi at room temperature and maintained a tensile strength of approximately 18,450 psi from 250 to 800°F. The tensile strength of the as-hot-pressed material in a direction transverse to the oriented fibers was 16,700 psi at room temperature and decreased rapidly to 4500 psi at 600°F.

Three dummy fuel plates containing a uranium-bearing Fiberglas core were cut into tensile specimens. These plates were clad with Alclad 6061. The specimens were taken longitudinal to the rolling direction. Therefore the tensile stress was perpendicular to the fiber orientation. The tensile strength of the clad plates decreased at temperatures above 400°F. For example, the average tensile strengths for two of the plates were 25,350, 23,125, and 12,075 psi at 250, 400, and 600°F, respectively.

At 600°F, commercial 6061 aluminum has a tensile strength of 4500 psi, whereas Alclad 6061 dummy fuel plates have exhibited a tensile strength of 11,400 psi. A series of experiments

demonstrated that aluminum-coated Fiberglas can be rolled directly into sheet with a resulting density of 97.6 per cent of the theoretical density.

An Oak Ridge annual progress report[41] describes achievements on several programs pertinent to dispersion fuel elements. It was the purpose of one program to propose an analytical model that would permit quantitative predictions of the achievable burnup for stainless steel–UO_2 fuels and to compare the effect of the following parameters on the burnup lifetime: UO_2 density, UO_2 particle size, volume fraction of UO_2 in the stainless-steel matrix, temperature of the matrix, and strength of the matrix.

A theory formed from representative results predicts a decrease in the burnup lifetime of the fuel with increasing volume fraction of UO_2, decreasing UO_2 particle size, and increasing temperature. Decreasing the UO_2 particle density is predicted to be the strongest parameter in increasing the performance of these fuels because of the "built-in" void space provided for the fission gases by the lower density UO_2 particles.

The objective of another Oak Ridge program is to develop an optimum fuel material for thin-plate aluminum-base research-reactor fuel elements that are limited to uranium with a maximum enrichment of 20 per cent of the U^{235} isotope. Previous results have shown that, for this application, uranium-aluminum alloys in the range of 40 to 50 wt.% uranium are inherently expansive and difficult to fabricate. Dispersions of UC_2 corrode catastrophically when exposed to water, and UO_2 was rejected because of its reaction with aluminum during fabrication and, possibly, during reactor operation. Dispersions of U_3O_8 in aluminum were developed for this application and successfully tested to an estimated U^{235} burnup of 30 to 50 per cent.

After evaluating the properties and costs of the potential fuel sources, it was concluded that a dispersion of U_3O_8 in aluminum is an optimum fuel material for use in a research-reactor fuel-element application where 20 per cent enriched uranium is required.

The objective of another Oak Ridge program is to investigate the irradiation behavior of dispersions of UO_2 and U_3O_8 in aluminum in reactors of high specific power operating with temperatures up to 315°C. Dispersions both with and without burnable poisons are being studied. Preparatory to the fabrication of the irradiation specimens, preliminary investigations have been conducted to evaluate fabricating procedures and the homogeneity of boron and uranium in the dispersion type fuel plate.

The boron homogeneity is satisfactory; however, the uranium is generally superior, being within ±2 at.% of nominal. Dispersions containing U_3O_8 with a mesh size of −140 +200 showed variations as high as ±4 at.% of nominal. No correlation appears to exist between segregation and hot-working temperatures.

Postirradiation examination of the first plate type UO_2 stainless-steel fuel elements which have operated successfully in the active lattice of the Stationary Medium Power Plant No. 1 (SM-1) reactor is nearing completion. The elements were developed and fabricated at Oak Ridge as part of the first core loading of the SM-1 reactor. Two elements which contained 26 wt.% UO_2 dispersed in stainless steel were removed from the reactor after 10 Mw-years, and, although the fuel elements had operated without incident, it was felt advisable to examine them in detail.

The average burnups of U^{235} due to fission were 13 and 18 at.%, respectively, for the stationary and control-rod fuel elements; maximum burnups of 31 and 32 at.%, respectively, were observed. Qualitative examination revealed no gross damage. The integrity of the stainless-steel matrix appears good, and the only evidence of the relatively high burnup of the U^{235} is the appearance of voids in the UO_2.

Still another program deals with reactor fuel cores consisting of UC or UO_2 dispersed in a matrix of depleted uranium-molybdenum alloy. These are presently being developed for advanced fuel elements for the Enrico Fermi fast-breeder reactor. The work has centered on developing procedures for producing suitable uranium–10 wt.% molybdenum plus 25 vol.% UO_2 and uranium–13.5 wt.% molybdenum plus 35 vol.% UO_2 cores to be roll clad into plate type fuel elements and in developing matrix materials for irradiation testing.

Nuclear Materials and Equipment Corporation[42] is attempting to develop coating techniques for UO_2 powder which will stop UO_2-matrix reactions and provide barriers for corrosion penetration in reactors. After UO_2 powder was coated with chromium, 10 wt.% UO_2 was dispersed in a Zircaloy-2 matrix by mixing and cold compacting. The compacts were then suc-

cessfully extruded without any stringering or reaction with the matrix. The coating was applied by vapor-deposition techniques on 20- to 30-mesh UO_2 particles to a thickness of 5 to 6 μ. The extrusion temperature was 1375°F, and a 25:1 reduction ratio was used in forming a rectangular strip of this UO_2–Zircaloy-2 core clad with Zircaloy-2. Although the chromium coating had been porous after deposition, extrusion densified it.

In the course of coating UO_2 with niobium by the halide reduction process, it was found that some agglomeration of the coated particles resulted and that the form of the agglomerates could be controlled to some extent. Initial efforts indicated that porous plates, cylinders, and disks could be formed. By using stainless-steel wire mesh as a mold and employing a reduced pressure at one end of the agglomerate, niobium was pulled into the pores so that 80 per cent of the voids were filled. It was felt that similar techniques could be developed with materials such as tungsten substituted for niobium.

Battelle[23,43] reports modulus of rupture values ranging from 12,000 to 22,500 psi on 80 vol.% UO_2–molybdenum, chromium, and type 302B stainless-steel cermets. The 0.375-in.-diameter test specimens were prepared by green pressing powder mixes, followed by gas-pressure bonding for 3 hr at 2200 to 2300°F under a helium-gas pressure of 10,000 psi. Surfaces were prepared by grinding. Modulus of rupture testing was done over a 2-in. span, and the loading rate was 110 lb/min. Test-specimen densities ranged from 88.5 to 97.4 per cent of the theoretical density.

Thermal-conductivity values of 0.095, 0.091, 0.091, and 0.095 watts/(cm)(°C), respectively, at 200, 500, 700, and 900°C are reported for an 80 vol.% UO_2–niobium cermet of 93.5 per cent of the theoretical density.

The irradiation testing of cermet fuels containing 60 to 90 vol.% UO_2 combined with refractory-metal matrices is planned. On the basis of physical and mechanical properties of fabricated cermets, the cermet fuels appear to be superior to ceramic UO_2 and possess excellent potential for use in applications where a relatively high fuel loading is required.

The development of techniques for the fabrication of cermet fuels embodying UN has been initiated. Compatibility studies are being conducted to select the most promising matrix materials.

Battelle also reports the results of work, performed in assistance to Alco Products, on the development of fabrication techniques for the preparation of instrumented fuel plates for insertion in the SM-1 and the development of fuel, absorber, and suppressor materials for the SM-2. Techniques have been developed for the fabrication of an instrumented fuel plate for insertion in the SM-1. The instrumented plate is of a blocked-channel design, consisting of a Zircaloy filler plate sandwiched between two standard SM-1 stainless steel–UO_2 plates. A 3-mil niobium interface is utilized as a barrier between the stainless steel and Zircaloy to prevent formation of a eutectic during the bonding process.

Material and process specifications have been established for the SM-2 fuel plate. The fuel plate consists of a stainless steel–UO_2 core and a stainless steel–Eu_2O_3 end suppressor, clad with stainless steel. Commercially available UO_2 in spheroidal shape and boron burnable poison in the form of ZrB_2 are specified.

Reference and alternate SM-2 fuel specimens contained in nickel capsules have been irradiated in the MTR and ETR. The examination of the specimens has been completed, with the exception of isotopic analyses for determination of burnup. In general, the irradiation induced very small volume, density, and dimensional changes.

Additional specimens contained in instrumented capsules are being irradiated in the ETR. The capsules embody thermocouples and auxiliary heaters to maintain the design temperatures of the SM-2.

Thermodynamic studies are being conducted to determine the mechanism of boron loss during the fabrication of a stainless steel–UO_2 fuel plate incorporating boron as a burnable poison.

(D. L. Keller)

Refractory Fuel and Fertile Materials

Properties and Behavior of Uranium Oxide Fuels

Several review papers published[44–46] during this quarter cover the irradiation behavior of UO_2 and UO_2-ThO_2 fuel.

An excellent Bettis[47] summary of high-burnup studies of sintered, flat-plate UO_2 compart-

mented in Zircaloy and of pellet UO_2 is available. For burnups of 45,000 to 60,000 Mwd per ton of UO_2, the UO_2 crystal lattice is destroyed, and volume increases of 4 to 5 per cent occur. At these burnups, fission-gas release increases 100-fold over the release at a lower burnup of 20,000 Mwd per ton of UO_2.

The thermal expansion of sintered UO_2 pellets has been studied up to the melting point.[48] Some anomaly exists in the 1000 to 1500°C region. Ellington[49] discusses the thermal stress and temperature profile in UO_2-pellet fuel. Calculations show that small pellets will fracture at very low radial-temperature gradients. In a study of UO_2 decomposition at the melting point, the oxygen deficiency was found to depend on the length of time at the molten state.[50] A limiting composition of $UO_{1.86}$ is approached. Work at Chalk River[51] on the effect of small additions of Y_2O_3 on the thermal conductivity of irradiated UO_2 focuses attention on the difficulties in proving a positive effect. No improvement of the mean thermal conductivity over the 350 to 2800°F range was found for ≈ 4 mole % addition. The authors state that it is unlikely that small additions of Y_2O_3 will produce sufficient improvement in the thermal conductivity to be of any practical importance in UO_2 fuel. Russian investigators[52] have reported melting-point determinations of binary mixtures of UO_2 and 13 other oxides in air. Hanford[53] is continuing to study the microstructure of thin films of irradiated UO_2 by electron microscopy.

Postirradiation studies of fission-gas release from UO_2 are continuing at several sites. The effect of particle size on fission-gas release from fused and sintered materials is reported by General Atomic.[54] Results are presented in Fig. 3 for a 20-hr anneal at 1400°C. No difference in the particle-size effect is observed between these two materials for this anneal. Chalk River results[28] from postirradiation-heating experiments with sintered UO_2 may possibly clarify the deviation from linearity observed frequently in plots of the release fraction versus the square root of heating time. When extrapolated to zero heating time, this release curve gives a positive intercept that can be correlated with the oxygen/uranium ratio of the UO_2. The study of reentry of fission gas into UO_2 pellets during irradiation is continuing. The complexity of the reentry mechanism is now evident, since fission-fragment

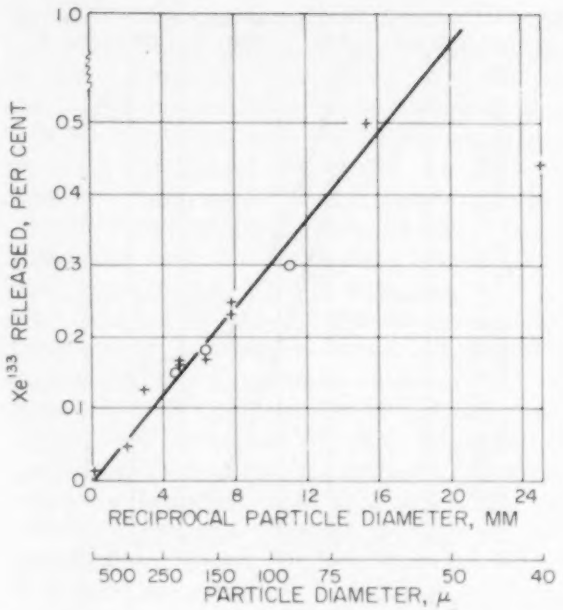

Figure 3—Release[54] of Xe^{133} from sintered and fused UO_2. +, sintered; ○, fused.

collisions with external fission gas do not alone explain the observed results.

Fission-gas release measurements on defected, clad ThO_2–10 wt.% UO_2 pellets during irradiation in the EBWR provide some interesting information on the effect of half life.[55] The fission gases Kr^{85m}, Kr^{88}, Xe^{133}, Xe^{135}, and Xe^{138} are measured in the off-gas stripped from the water circulating over the fuel element. Release rates normalized to the fission yields show an inverse square-root dependency on the decay constant. This same relation was reported earlier by Vallecitos[56] in an in-pile study of defected, clad UO_2 fuel. Fission-product activity in the Pressurized-Water Reactor (PWR) coolant[57] is compared with the Argonne and Vallecitos results, and further support for this correlation with decay constant is obtained.

Oak Ridge has recently reported[58] on investigation of in-pile fission-gas release from unclad plates of UO_2 in a sweep-gas capsule. Iodine release is studied by irradiating at temperature, turning off the capsule heater, and removing the capsule to a low flux. Xenon measurements before and after this procedure give the release rates of xenon and precursor iodine. As shown in Fig. 4, the temperature dependency is the same for xenon and iodine. Diffusion constants for Kr^{88} were calculated from the release as a function of temperature

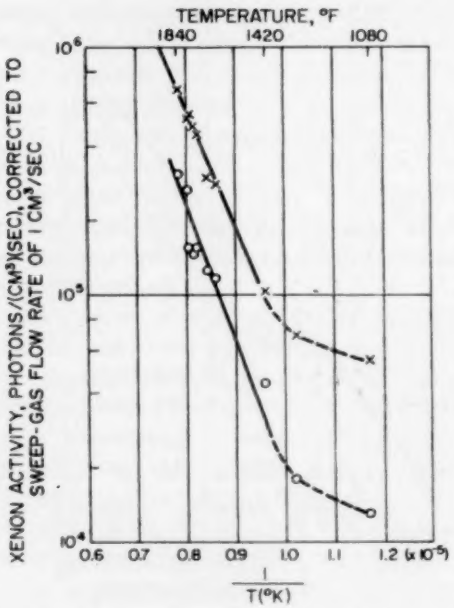

Figure 4—Xenon release from UO_2 fuel and from iodine outside the fuel.[58] ×, xenon evolved from fuel; O, xenon produced from iodine plated onto sweep-gas system. Flux is constant at 33×10^{12} neutrons/(cm^2) (sec).

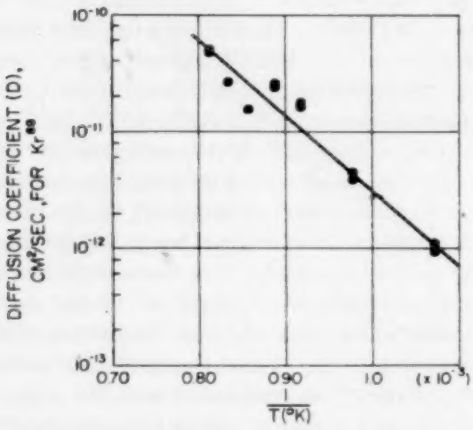

Figure 5—Diffusion coefficients[58] for Kr^{88}. Activation energy is 30 kcal/mole.

for this species and from a slab diffusion model. The data in Fig. 5 give an activation energy of 30 kcal/mole. Evidence of stored energy from irradiation at low temperature is found when the capsule temperature is raised. During the rise, a burst of fission gas is observed. The estimated storage energy is 4 to 6 cal per gram of UO_2.

The phase diagram of the Al_2O_3-UO_2 system is being investigated by General Atomic.[59] Pressed compacts of UO_2 and Al_2O_3 were heated to 1500°C in an oxygen atmosphere at a pressure of 1 mm Hg. No new compounds or measurable ranges of solid solution exist on the oxygen-rich side of the binary Al_2O_3-UO_2. When pressed UO_3 and Al_2O_3 are heated at 1000°C, no new phases appear. (W. S. Diethorn)

Fabrication of UO_2 Materials

Exploratory work on the fabrication of dense, spheroidal UO_2 particles for use in dispersion type fuel elements has been described by Oak Ridge.[60] Batch precipitation of ammonium polyuranates, followed by pyrolysis and sintering at 3300°F in argon-hydrogen atmospheres, allowed preparation of spheroidal, dense (up to 98 per cent of the theoretical density) particles in the size range of 20 to 800 μ.

The final particle size and shape were found to depend on the size and shape of the agglomerates formed during precipitation of the uranates. The use of acetone or sulfuric acid additives during precipitation permitted formation of larger, rounded aggregates, whereas lengthening digestion time resulted in elongated particles. The particles of UO_2 formed by this process in this investigation were not so spherical as those produced by mechanical methods. (H. D. Sheets)

Properties of Refractory Fuels Other Than Uranium Oxides

The increased operating temperature of reactors that employ ceramic type fuel provides several advantages over metallic fuels. However, the physical behavior and, in some cases, the chemical behavior of ceramic fuels have disadvantages. Of the ceramic fuels, the carbides combine some of the advantages of metallic fuels with those of oxides. A summary of known properties of uranium and plutonium carbides is presented by Strasser.[61] Caution must be used in applying published properties, however, because carbide bodies are often not pure or fully dense. Current studies include the evaluation of physical and chemical properties of fuel carbide bodies and the effect of radiation upon these properties. Thermal-expansion data, given in Table I-12, for sintered bodies of UC were obtained at Carborundum.[62] Thermal-conductivity measurements given in Table I-13, of two UC bodies were obtained by Atomics Inter-

Table I-12 THERMAL EXPANSION OF SINTERED UC BODIES[62]

Temperature range, °C	Expansion coefficient, 10^{-6}/°C
30–200	8.0
30–400	9.5
30–600	10.3
30–800	10.6
30–1000	11.2
30–1200	11.75
30–1400	12.4

Table I-13 THERMAL CONDUCTIVITY OF SINTERED UC BODIES[11]

	Thermal conductivity, Btu/(hr)(ft)(°F)		
Carbon content, wt.%	570°F	1110°F	1950°F
4.9	12.7	12.0	11.5
5.3	13.4	13.0	13.4

national[11] at three temperatures. Battelle measurements[63] on the thermal conductivity of UC during irradiation to burnups of 1000 to 20,000 Mwd/ton indicate no appreciable change in thermal conductivity. The electrical resistivity, density, hardness, and microstructure of cast uranium–4.8, 7.0, and 9.0 wt.% carbon alloys have been investigated[23,43,64] after heat-treatment in the temperature range of 1100 to 1500°C for periods up to 1000 hr. Major changes in these properties occur for the 7 wt.% carbon alloy. These changes are associated with the formation of U_2C_3 from UC_2 + UC.

The oxidation stability of UC_2, ThC_2, and solid-solution alloys has been reported by Brett et al.[65] ThC_2 decomposes rapidly in moist air at room temperature, whereas UC_2 is stable in dry air up to 200 to 300°C and in wet argon up to 300 to 400°C. Complete solubility was observed in the ThC_2-UC_2 system in which the chemical activity increases with ThC_2 content. The oxidation product is a UO_2-ThO_2 solid solution. In attempting to improve the corrosion resistance of the uranium carbides, metallic coatings are being investigated.[14] Adherent coatings were obtained by dipping the carbide in melts of copper-silicon and aluminum-silicon. However, the aluminum-silicon melts reacted with the carbide to give products tentatively identified as Al_4C and UAl_4. Corrosion resistance, as well as flexure strength and hardness of UC, is reported[23,64] to be improved by small additions of Mo_2C, VC, ZrC, or NbC. High-temperature creep strength of a 70 mole % ZrC–30 mole % UC hot-pressed body is being determined. At 2300°C and 400-psi load, the creep rate of this mixed carbide was 1.5×10^{-8} cm/(cm)(sec) after an initial creep of 2.5 per cent. The rate with a 2000-psi load was found to be 3.3×10^{-6} cm/(cm)(sec). In other studies at Los Alamos the dissociation pressure of uranium dicarbide [UC_2(solid) → U(gas) + 2C(solid)] was determined at 2336 and 2360°K to be 3×10^{-8} and 1×10^{-7} atm, respectively. Fuel cylinders of UC_2 dispersed in graphite and irradiated to a burnup of 7560 Mwd/ton were investigated at Oak Ridge[66] for dimensional changes. Although the external cans remained unchanged, the cylinders showed a 2 to 5 per cent decrease in diameter and a 3.5 per cent increase in length. Massive uranium carbides containing 4.6, 4.8, and 5 wt.% carbon were found[67] to be dimensionally stable when irradiated in sodium-filled capsules. At the higher carbon content, a change in microstructure indicated that a second phase identified as UC_2 disappears at high temperature and high burnup.

Ceramic oxides, other than uranium oxides, which are of interest as potential reactor fuels include plutonium and thorium oxides. The characteristic temperature for PuO_2 was determined to be 415°K by Roof,[68] using X-ray diffraction line intensity measurements. Reactions between PuO_2 and Al_2O_3 or ZrO_2 have been studied at Hanford.[69] The melting point for the compound $PuAlO_3$ was found to be 1800°C. The addition of 1 mole % PuO_2 to ZrO_2 bodies stabilizes the high-temperature tetragonal modification of ZrO_2 and prevents the disintegration of sintered bodies during thermal cycling. The density and oxidation reduction processes of ThO_2 have been studied by Brown and Chitty.[70] $ThBi_2$ was formed during exposure of ThO_2 to impure bismuth.

The chemical and physical properties of U_3Si_2 are being evaluated at Atomics International[71] with regard to its use as a potential reactor fuel. Oxidation was found to be practically nil in 192 hr at 100°C, but rapid disintegration of U_3Si_2 was observed at 315°C. For heat-treated U_3Si_2, weight-gain data taken at 200°C gave the relation: weight gain (in mg/cm^2) = $0.71t^{0.568}$, t being the time in hours. Specimens of U_3Si_2 exhibited no dimensional changes during a 160

to 1450°F thermal cycle. The Young's modulus of U_3Si_2 was determined to be 7.5×10^6 psi.

(D. A. Vaughan)

Fabrication of Ceramic Fuels Other Than Uranium Oxides

Additional progress was made by various investigators toward the goal of reliable and low-cost methods of preparing and fabricating uranium carbide fuels (references 16, 23, 43, 62, and 72 to 75). Arc melting and casting continued to receive attention in studies of the fabrication of UC fuel slugs (references 16, 23, 43, and 76). After a preliminary investigation of several alternative fabrication methods at Atomics International, the skull melting and casting method was selected for the production of fuel slugs for the Hallam Nuclear Power Facility.[76]

Additional information has appeared on the preparation and fabrication of plutonium compounds.[77-79] The attempt to make PuC and Pu_2C_3 by heating stoichiometric mixtures of PuO_2 and graphite at 1600°C was unsuccessful, but reaction of the metal and carbon at 1550°C produced Pu_2C_3 in apparently good purity.[78] Attempts[79] to produce PuN have thus far resulted only in producing PuO_2. (M. J. Snyder)

Mechanism of Corrosion of Fuel Alloys

The corrosion of unalloyed uranium by water at temperatures to 350°C has been reviewed in a paper from Harwell.[80] The relation to the corrosion mechanism of dissolved oxygen in the water, reaction of corrosion-produced hydrogen with the uranium, heat-treatment and impurity content of the uranium, water temperature, and electrode potentials was among the subjects discussed. The methods of applying protective coatings and their effectiveness in preventing corrosion also were reviewed. (W. E. Berry)

Basic Studies of Radiation Effects in Fuel Materials

Irradiation Effects in Metallic Fuels

Quere and Nakache[81] succeeded in utilizing irradiation-induced electrical conductivity changes in uranium to distinguish between the effects of defect production by irradiation and thermal annealing of defects. From this study, it is reported that the volume of the fission spike is $(2.10 \pm 0.20) \times 10^{-16}$ cm^3.

On the basis of analysis of dimensional instability and reduced in-pile strength at low strain rates for zirconium-uranium alloys, it is proposed[82] that the diffusion of point defects, coupled with anisotropic precipitation of both interstitials and vacancies on different habit planes, provides an improved model for interpreting the observed irradiation phenomena in both uranium- and zirconium-rich uranium alloys.

Experiments[83] to establish a basis for the diffusional theory of the dimensional stability of uranium are reported by Sylvania. The dimensional stability of alpha-uranium rods of constant preferred orientation, but varying grain size, did not vary with grain size as expected. Self-diffusion experiments along different crystallographic directions varied only by a factor of 3, which was within the experimental error. The diffusion coefficients are given below:

$$D_{[1\,0\,0]} = 1.8 \times 10^{-14} \text{ cm}^2/\text{sec}$$

$$D_{[0\,1\,0]} = 0.72 \times 10^{-14} \text{ cm}^2/\text{sec}$$

$$D_{[0\,0\,1]} = 0.66 \times 10^{-14} \text{ cm}^2/\text{sec}$$

A calculation of the energy of solution of rare gases in uranium, based on a method which has given good results in metals,[84] has been made. To do this, the compressibility of the rare gases argon, krypton, and xenon was determined precisely, and the resulting constants were used in the calculation.

A detailed metallographic study of the pore distribution, pore void fraction, and pore densities is reported by Hanford[85] for uranium specimens irradiated to 0.02 to 0.41 at.% burnup at temperatures of 200 to greater than 800°C. The effects of postirradiation heating at 600 to 880°C are also reported. All specimens contained pores greater than 200 A in diameter. This research establishes techniques for postirradiation examination which will yield quantitative data on the mechanisms of swelling in uranium. (F. A. Rough)

Irradiation Effects in Ceramic Fuels

Experiments to stimulate thermal conditions experienced in UO_2 fuel rods during irradiation

have been conducted at Chalk River.[86] These experiments show that growth of columnar grains is induced in high-density sintered UO_2 by the presence of a steep temperature gradient above 1700°C but below the melting point. This growth is believed to result from migration of large transverse voids whose individual widths determine the cross section of the columnar grains formed. These voids migrate up a temperature gradient by a sublimation process, producing (1 1 1) preferred orientation along the grain axes. Migration of these pores results in the formation of a central void in a fuel pin.

Current research at Oak Ridge[41] on diffusion of fission gases in UO_2 has been briefly reviewed. Above about 1600°C, or at 1800 and 2000°C, the release rates of Xe^{133} in postirradiation tests are greater than expected by extrapolation from diffusion coefficients obtained at 1600°C and below. Vaporization appears to contribute to these high releases, but it is proposed that a significant portion of the release is associated with the action of moving grain boundaries (coalescence) sweeping the xenon to the available path for release. Another report[87] reviews all available information on fission-product release from UO_2.

The effects of a short-term reactor irradiation on uranium dioxide specimens of moderate density suggest that reactor irradiation can (1) change the mode of fracture from transcrystalline to intercrystalline, (2) create holes or cracks at grain boundaries, and (3) activate transport mechanisms that distort free surfaces.[88] (F. A. Rough)

Metal-Water Reactions

Further activities in the study of metal-water reactions have been reported by ANL.[89] In condenser-discharge experiments, ANL has used the energy from the discharge to heat or melt wires of various sizes and compositions. The present experiments have been made with 30-mil uranium wire to complement earlier experiments with 60-mil wire. Assuming the reaction $U + 2H_2O \rightarrow UO_2 + 2H_2$ as the only one to occur, the preliminary results indicate that the extent of reaction is independent of the original wire size. This suggests that a linear rate law may be applicable. Runs having initial temperatures in the region between 1900 and 2200°C showed rapid rates of pressure rise. Significant reaction occurred in a few milliseconds. More energetic runs, having explosive pressure rises, were essentially completed in 1 msec. The transition between slow reaction rates and explosive rates is not as striking with uranium as it is with zirconium. The point of transition, however, does coincide approximately with the melting point of the uranium dioxide.

Use of the pressure-pulse method for the study of the isothermal reaction of the molten metals also is being continued.[89] A series of preliminary runs has been completed. Liquid-zirconium samples have been reacted with water vapor at about 20-mm pressure in a temperature range of about 1850 to 2100°C. Since some attack of the liquid zirconium on the thoria crucibles has been found, additional experiments will be run using graphite crucibles. Further experiments will include studies with molten aluminum.

As part of the Transient Test Reactor Facility (TREAT) in-pile testing program to obtain data on metal-water reactions initiated by a nuclear-reactor transient, a comparison is being made of the experimental results and an analog simulation of the experiment.[90] A mathematical model was developed to permit an investigation of metal-water reactions by means of an analog computer. In the first part of the study, four differential equations giving the temperature of the unreacted metal, the temperature of the oxide, the amount of reaction, and the pressure in the vessel as a function of time were solved. In the second part of the study, the temperature in the reacting pin as a function of both time and position was obtained using a finite-difference technique.

The chemical reactions were initiated by nuclear-reactor transients. Flat-top, exponential, and oscillatory neutron bursts were studied. Parametric studies were made of the influence of such factors as the chemical kinetics and heat-transfer coefficients on the temperatures and extent of reaction. Qualitative comparison of experimental results obtained in TREAT shows that there are sufficient similarities in the temperature-time curves and extent of reaction to give promise to the computer approach.

At Oak Ridge,[91] comparative studies of the rate of reaction of highly irradiated uranium with air, CO_2, and steam have been conducted in an investigation of the fission-product-release potential in a loss-of-coolant type accident

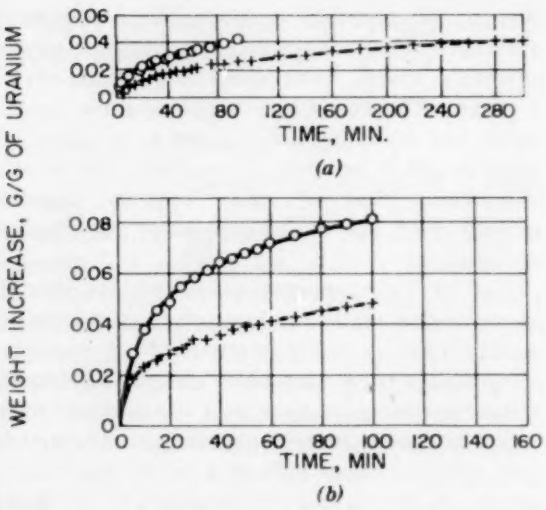

Figure 6—Oxidation rates of irradiated and unirradiated uranium in steam at (*a*) 1000°C and (*b*) 1200°C.[88] O, irradiated uranium in steam-helium (300 cm^3 each of steam and helium per minute). +, unirradiated uranium in steam-helium (300 cm^3 each of steam and helium per minute).

postulated for the plutonium-producing reactors. Oxidation rates of irradiated uranium (0.2 at.% burnup) and unirradiated uranium in steam were compared at 1000 and 1200°C, as shown in Fig. 6. Irradiated uranium oxidized in steam (and in CO_2 and air) more rapidly than did unirradiated uranium, both above and below the melting point. This indicates that oxidation rates measured with unirradiated uranium cannot be applied directly to predict the oxidation behavior of highly irradiated uranium present in operating reactors. All experiments were performed in a vertical continuous-recording thermobalance.

A further comparison between steam-air oxidation data and air oxidation data obtained under the same conditions shows that there was a marked reduction in the rate of oxidation when steam was the predominant gas to which the uranium was exposed, as compared with exposure to air alone at the same temperature. These data show that the choice of water as the extinguishing agent in the Windscale incident, following the unsuccessful use of CO_2, was extremely fortunate. (A. W. Lemmon, Jr.)

References

1. B. Blumenthal et al., The Transformation Temperatures of High-Purity Uranium, USAEC Report ANL-5957, Argonne National Laboratory, June 1960.
2. S. J. Rothman et al., Self-Diffusion in Beta Uranium, USAEC Report ANL-6126, Argonne National Laboratory, July 1960.
3. P. G. Mardon and J. H. Pearce, An Investigation of the Neptunium-Uranium Equilibrium Diagram, *J. Less-Common Metals*, 1: 467–475 (December 1959).
4. A. E. Dwight, The Uranium-Molybdenum Equilibrium Diagram Below 900°C, *J. Nuclear Materials*, 2: 81–87 (March 1960).
5. S. Isserow and R. G. Jenkins, Aqueous Corrosion of Zircaloy-Clad Fuel Elements with High-Uranium Cores, USAEC Report NMI-TJ-23, Nuclear Metals, Inc., Sept. 20, 1959; also in USAEC Report TID-7587, pp. 437–465.
6. A. L. Geary and V. Nerses, Retention of Uranium Beta Phase, USAEC Report NMI-1237, Nuclear Metals, Inc., Aug. 5, 1960.
7. S. Isserow et al., Power Reactor Program. Progress Report to E. I. du Pont de Nemours & Company for the Period March 1, 1960, Through March 31, 1960, USAEC Report NMI-7226, Nuclear Metals, Inc., July 6, 1960.
8. S. Isserow et al., Power Reactor Program. Progress Report to E. I. du Pont de Nemours & Company for the Period May 1, 1960, Through May 31, 1960, USAEC Report NMI-7228, Nuclear Metals, Inc., July 12, 1960.
9. S. Isserow et al., Power Reactor Program. Progress Report to E. I. du Pont de Nemours & Company for the Period June 1, 1960, Through June 30, 1960, USAEC Report NMI-7229, Nuclear Metals, Inc., Aug. 2, 1960.
10. M. H. Binstock, Fuel Element Development for Piqua OMR, USAEC Report NAA-SR-5119, Atomics International, June 30, 1960.
11. Atomics International, Annual Progress Report—AEC Unclassified Programs for Fiscal Year 1960, USAEC Report NAA-SR-5350, August 1960.
12. C. F. Reinke and R. Carlander, Examination of Irradiated EBWR Core-I Fuel Elements, USAEC Report ANL-6091, Argonne National Laboratory, July 1960.
13. AEC-Euratom Conference on Aqueous Corrosion of Reactor Materials, Brussels, Belgium, October 14–17, 1959, USAEC Report TID-7587, July 1960.
14. J. N. Chirigos, The Role of Lattice Mismatch Between Oxide and Metal in the Corrosion Behavior of Gamma Uranium Alloys, in *Physical Metallurgy of Stress Corrosion Fracture*, pp. 70–78, Interscience Publishers, New York, 1959.
15. J. Bloch, Phase Change and Disordering by Irradiation of the Compound U_2Mo, *J. Nuclear Materials*, 2: 90–91 (March 1960) (in French).
16. R. W. Dayton and C. R. Tipton, Jr., Progress Relating to Civilian Applications During June 1960,

USAEC Report BMI-1448(Rev.), Battelle Memorial Institute, July 1, 1960.

17. J. Laniesse and M. Bouleau, Development and Examination of the Micrographic Structures of Alloys of Uranium Containing 0.5 to 10 Wt.% of Molybdenum, Report NP-tr-412 (Translation by M. H. Rand from CEA-Note-269), Commissariat à l'Énergie Atomique, November 1959.
18. J. H. Kittel and K. F. Smith, Effects of Irradiation on Some Corrosion-Resistant Fuel Alloys, USAEC Report ANL-5640, Argonne National Laboratory, May 1960.
19. A. A. Bauer, The Gamma-to-Epsilon Transformation in Zirconium–22 to 70 Wt.% Uranium Alloys, *Trans. Met. Soc. AIME*, 218: 636–644 (August 1960).
20. W. C. Francis and S. E. Craig, Progress Report on Fuel Element Development and Associated Projects, USAEC Report IDO-16574, Phillips Petroleum Co., Aug. 16, 1960.
21. Fuel Damage in WTR Incident, *Nucleonics*, 18(9): 104 (September 1960).
22. N. E. Daniel et al., Preparation and Evaluation of Aluminum–35 Wt.% Uranium Alloys Containing Up to 3 Wt.% Tin or Zirconium, USAEC Report BMI-1454, Battelle Memorial Institute, July 29, 1960.
23. R. W. Dayton and C. R. Tipton, Jr., Progress Relating to Civilian Applications During August 1960, USAEC Report BMI-1464, Battelle Memorial Institute, Sept. 1, 1960. (Classified)
24. G. L. Stiffler and M. H. Curtis, The Preparation of Plutonium Powder by a Hydriding Process—Initial Studies, USAEC Report HW-64289, Hanford Atomic Products Operation, Mar. 10, 1960.
25. L. H. McEwen, comp., Unclassified Research and Development Programs Executed for the Division of Reactor Development and the Division of Research, March 1960, USAEC Report HW-64865, Hanford Atomic Products Operation, Apr. 15, 1960.
26. F. W. Albaugh, Reactor and Fuels Research and Development Operation Monthly Report for July 1960, USAEC Report HW-66237-A, Hanford Atomic Products Operation, Aug. 15, 1960. (Classified)
27. L. H. McEwen, Hanford Atomic Products Operation, Nov. 10, 1959. (Unpublished)
28. W. M. Campbell and E. C. W. Perryman, Atomic Energy of Canada Ltd., 1960. (Unpublished)
29. R. D. Nelson and J. M. Taylor, Preliminary Investigation of the Transformation Rates of Plutonium-Uranium Alloys, USAEC Report HW-62073, Hanford Atomic Products Operation, Jan. 28, 1960.
30. D. S. Evans et al., The Lattice Spacings of Thorium-Lanthanum Alloys, *J. Nuclear Materials*, 2: 121–128 (June 1960).
31. J. Graham and F. K. McTaggart, Observations on the Systems Th-S, Th-Se, and Th-Te, *Australian J. Chem.*, 13: 67–73 (February 1960).
32. A. J. Darnell et al., Vapor Pressure of Thorium, USAEC Report NAA-SR-4512, Atomics International, Feb. 15, 1960.
33. M. S. Farkas et al., Development of Thorium-Uranium-Base Fuel Alloys, USAEC Report BMI-1428, Battelle Memorial Institute, Mar. 18, 1960.
34. R. W. Dayton and C. R. Tipton, Jr., Progress Relating to Civilian Applications During April 1960, USAEC Report BMI-1434, Battelle Memorial Institute, May 1960. (Classified)
35. R. S. Neymark, Rate of Alloying of Uranium Alloys with Stainless Steel, USAEC Report NAA-SR-3278, Atomics International, June 1960.
36. F. W. Albaugh, Reactor and Fuels Research and Development Operation Monthly Report for April 1960, USAEC Report HW-64898-A, Hanford Atomic Products Operation, May 15, 1960. (Classified)
37. J. L. Ballif et al., Engineering Evaluation of a Mixed Alloy Fuel Element Irradiated at Elevated Temperatures in the SRE, USAEC Report NAA-SR-3888, Atomics International, June 1, 1960.
38. R. H. Baskey, Fuel-Bearing Fiberglas in Aluminum-Base Fuel Elements, USAEC Report ORO-273, Clevite Corp., Feb. 15, 1960.
39. R. H. Baskey, Fuel-Bearing Fiberglas in Aluminum-Base Fuel Elements, USAEC Report ORO-313, Clevite Corp., Aug. 16, 1960.
40. R. H. Baskey, Fuel-Bearing Fiberglas in Aluminum-Base Fuel Elements, USAEC Report ORO-316, Clevite Corp., Sept. 2, 1960.
41. Oak Ridge National Laboratory, Metallurgy Division Annual Progress Report for Period Ending July 1, 1960, USAEC Report ORNL-2988, Sept. 30, 1960.
42. Nuclear Materials and Equipment Corp., Final Report on Coating Fuel Elements, November 15, 1958, Through November 14, 1959, USAEC Report NYO-2801, Sept. 15, 1960.
43. R. W. Dayton and C. R. Tipton, Jr., Progress Relating to Civilian Applications During July 1960, USAEC Report BMI-1455, Battelle Memorial Institute, Aug. 1, 1960.
44. J. A. L. Robertson et al., Irradiation Behavior of UO_2 Fuel Elements, *Am. Inst. Mining, Met., Petrol. Engrs., Inst. Metals Div., Spec. Rept. Ser. No. 9*, pp. 45–70, 1959.
45. W. K. Barney, The Swelling of UO_2 at High Burnup, *Am. Inst. Mining, Met., Petrol. Engrs., Inst. Metals Div., Spec. Rept. Ser. No. 9*, pp. 71–74, 1959.
46. L. A. Numark and J. H. Kittel, Irradiation Behavior of ThO_2-UO_2 Fuels, *Am. Inst. Mining, Met., Petrol. Engrs., Inst. Metals Div., Spec. Rept. No. 9*, pp. 83–85, 1959.
47. M. L. Bleiberg et al., Burnup Limitations of Bulk UO_2 Prototype Fuel Elements—An Interim Examination of CR-IV-X-3-1 Test and the CR-V-m Experiment, in USAEC Report WAPD-BT-18,

pp. 107–134, Westinghouse Electric Corp., Bettis Atomic Power Laboratory, April 1960.

48. F. A. Halden et al., Thermal Expansion of Uranium Dioxide — Final Report, USAEC Report TID-5722, Stanford Research Institute, Apr. 15, 1959.
49. J. P. Ellington, Temperatures, Thermal Stresses and Displacements in Solid Uranium Dioxide Rods, *Brit. J. Appl. Phys.*, 11(1): 33–35 (January 1960).
50. J. S. Anderson et al., Decomposition of Uranium Dioxide at Its Melting Point, *Nature*, 185: 915–916 (Mar. 26, 1960).
51. J. A. L. Robertson et al., The Effect of 4 Mole % Y_2O_3 on the Thermal Conductivity of UO_2, Canadian Report CRFD-933, June 1960.
52. S. G. Tresvyatski and V. I. Kushakovskii, The Melting Point Determination of Binary Mixtures of Uranium Oxide with Some Other Oxides in Air, *At. Energ.*, 8: 56 (1960).
53. Hanford Atomic Products Operation, Plutonium Recycle Program Annual Report for Fiscal Year 1959, USAEC Report HW-62000, Oct. 15, 1959.
54. General Atomic and Electric Boat Divs. of General Dynamics Corp., Maritime Gas Cooled Reactor Program, Quarterly Progress Report for the Period Ending June 30, 1959, USAEC Report GA-1099.
55. R. F. S. Robertson, Tests of Defected Thoria-Urania Fuel Specimens in EBWR, USAEC Report ANL-6022, Argonne National Laboratory, May 1960.
56. F. J. Brutschy and R. N. Osborne, Release of Fission Products from Uranium Dioxide Fuel, *Trans. Am. Nuclear Soc.*, 2(2): 10–13 (November 1959).
57. P. W. Frank, Evaluation of the Fission-Product Activities in the Primary Coolant of Shippingport, in USAEC Report WAPD-BT-12, pp. 118–128, Westinghouse Electric Corp., Bettis Atomic Power Laboratory, April 1959.
58. Oak Ridge National Laboratory, Gas-Cooled Reactor Project Quarterly Progress Report for Period Ending June 30, 1960, USAEC Report ORNL-2964, Aug. 22, 1960.
59. General Atomic and Electric Boat Divs. of General Dynamics Corp., Maritime Gas-Cooled Reactor Program, Quarterly Progress Report for the Period Ending September 30, 1959, USAEC Report GA-1183.
60. R. P. Levey, Jr., Preparation of Dense Spheroidal UO_2, USAEC Report Y-1299, Union Carbide Nuclear Co., Y-12 Plant, May 2, 1960.
61. A. Strasser, Uranium Carbide as Fuel, *Nuclear Eng.*, 5(51): 353–357 (August 1960).
62. K. M. Taylor and C. H. McMurtry, Synthesis and Fabrication of Refractory Uranium Compounds, Monthly Progress Report No. 9 for August 1 Through August 31, 1960, USAEC Report ORO-319, The Carborundum Co., Sept. 12, 1960.
63. R. B. Price et al., Irradiation-Capsule Study of Uranium Monocarbide, USAEC Report BMI-1425, Battelle Memorial Institute, Mar. 2, 1960.
64. R. W. Dayton and C. R. Tipton, Jr., Progress Relating to Civilian Applications During September 1960, USAEC Report BMI-1469, Battelle Memorial Institute, Oct. 1, 1960. (Classified)
65. N. Brett et al., Some Investigations of the Uranium-Thorium-Carbon System, *J. Inorg. & Nuclear Chem.*, 13: 44–53 (April 1960).
66. J. G. Morgan and M. F. Osborne, Irradiation Effects on UC_2 Dispersed in Graphite (ORNL-MTR-48-1), Interim Report No. 1, USAEC Report CF-60-6-78, Oak Ridge National Laboratory, Aug. 18, 1960.
67. A. W. Hare and F. A. Rough, Irradiation Effects on Massive Uranium Monocarbide, USAEC Report BMI-1452, Battelle Memorial Institute, July 21, 1960.
68. R. B. Roof, Jr., An Experimental Determination of the Characteristic Temperature for PuO_2, *J. Nuclear Materials*, 2: 39–42 (March 1960).
69. L. H. McEwen, comp.; Unclassified Research and Development Programs Executed for the Division of Reactor Development and the Division of Research, USAEC Report HW-65078, Hanford Atomic Products Operation, May 10, 1960.
70. A. Brown and A. Chitty, Thoria as a Fertile Component for a Liquid-Metal Breeder Blanket, *J. Nuclear Energy: Pt. B, Reactor Technol.*, 1: 145–152 (March 1960).
71. N. R. Koenig, U_3Si_2 Fuel Evaluation. Part I, Oxidation Characteristics, USAEC Report NAA-SR-Memo 5199, Atomics International, Apr. 20, 1960.
72. K. M. Taylor et al., Synthesis and Fabrication of Refractory Uranium Compounds, Monthly Progress Report No. 6 for January 1 Through January 31, 1960, USAEC Report ORO-275, The Carborundum Co., Feb. 8, 1960.
73. K. M. Taylor et al., Synthesis and Fabrication of Refractory Uranium Compounds, Monthly Progress Report No. 8 for April 1 Through April 30, 1960, USAEC Report ORO-276, The Carborundum Co., May 10, 1960.
74. H. S. Kalish and R. B. Holden, Nuclear Fuel Research Fuel Cycle Development Program Quarterly Progress Report for April 1 to June 30, 1960, USAEC Report NYO-2689, Olin Mathieson Chemical Corp., July 27, 1960.
75. John B. Seastone, Progress for the Month of August 1960, Olin Mathieson Monthly Progress Report No. 13, August 1960.
76. D. H. Turner, Process Development of Uranium Carbide Fuel Slugs for HNPF, USAEC Report NAA-SR-5346, Atomics International, July 30, 1960.
77. A. Strasser and K. Taylor, Carbide Fuel Development Progress Report for the Period September 15, 1959, to January 31, 1960, USAEC Report

NDA-2145-1, The Carborundum Co., Mar. 11, 1960.

78. F. W. Albaugh, Reactor and Fuels Research and Development Operation Monthly Report for June 1960, USAEC Report HW-65854-A, Hanford Atomic Products Operation, July 15, 1960. (Classified)
79. F. W. Albaugh, Reactor and Fuels Research and Development Operation Monthly Report for August 1960, USAEC Report HW-66644-A, Hanford Atomic Products Operation, Sept. 15, 1960. (Classified)
80. B. E. Hopkinson, Corrosion of Unalloyed Uranium by Water, *Corrosion Technol.*, 6: 337–340 (November 1959).
81. Y. Quere and F. Nakache, Estimation of the Volume of a Fission Spike in Uranium, French Report CEA-1304, March 1960.
82. A. H. Willis and A. E. Bibb, The Dimensional Instability of Fissionable Materials During Reactor Irradiation, USAEC Report KAPL-2083, Knolls Atomic Power Laboratory, June 21, 1960. (Classified)
83. R. Resnick et al., Dimensional Instability of Uranium. IV. Final Progress Report for the Period July 1, 1958, to March 31, 1959, USAEC Report SEP-255, Sylvania Electric Products, Inc., February 1960.
84. J. Blin, Energy of Solution of Rare Gases in Metals, French Report CEA-1293, 1959.
85. T. K. Bierlein et al., Metallographic Observations of Swelling in Uranium: Interim Report, USAEC Report HW-63848, Hanford Atomic Products Operation, June 1, 1960.
86. V. B. Lawson and J. R. MacEwan, Thermal Simulation Experiments with a UO_2 Fuel Rod Assembly, Canadian Report CRFD-915, March 1960.
87. W. B. Cottrell et al., Fission-Product Release from UO_2, USAEC Report ORNL-2935, Oak Ridge National Laboratory, Sept. 13, 1960.
88. H. W. Newkirk, Jr., et al., Electron Microscope Studies of Damage in Irradiated Uranium Dioxide, *J. Nuclear Materials*, 2: 269–273 (September 1960).
89. Argonne National Laboratory, Chemical Engineering Division Summary Report for January, February, and March 1960, USAEC Report ANL-6145.
90. R. C. Liimatainen et al., Analog Computer Study of Metal-Water Reactions Initiated by Nuclear Reactor Transients, USAEC Report ANL-6129, Argonne National Laboratory, May 1960.
91. G. W. Parker et al., Fuel Element Catastrophe Studies: Hazards of Fission Product Release from Irradiated Uranium, USAEC Report CF-60-6-24, Oak Ridge National Laboratory, June 30, 1960.

Section II

MODERATOR MATERIALS

Graphite

Fueled graphite spheres which are potential fuel-element candidates for the Pebble-Bed Reactor are being irradiated,[1] mainly to ascertain the extent of fission-gas release. One sphere[2] (fueled with UO_2 particles, each individually coated with vapor-deposited Al_2O_3) performed well at about 1300°F up to 3 per cent fission burnup of the U^{235}. Activity-release measurements were made for seven inert-gas species ranging in half life from 1.7 sec for Xe^{141} to 5.27 days for Xe^{133}. These measurements indicated that only about 1 ppm of the gaseous radioactivity was escaping from the element, with essentially no dependency on half life; however, more recent measurements[1] indicate that activity release is increasing with burnup (5 per cent as of Oct. 1, 1960) for the longer lived species (78-min Kr^{87} to Xe^{133}). These latter measurements show a half-life dependency varying from releases of about 10 ppm of the Kr^{87} activity to about 1 per cent of the Xe^{133} activity, suggesting that release of the short-life species has not become intolerable. Future research will perhaps validate this hypothesis.

(G. E. Raines)

Beryllium

A complete and extensive collection of information on beryllium is presented in a recent book by British authors.[3] Among the topics included are the production and fabrication, metallurgy, and physical and mechanical properties of the metal, together with discussions of alloys and compounds, nuclear properties (cross sections and radiation effects), and health hazards. Two chapters on beryllium oxides and an appendix on methods for the determination of oxygen in beryllium are also included.

A lucid account[4] of the current achievements in the field of beryllium research is presented by Matthews, who is concerned with the use of the metal in missile and space fields. Although the requirements for missile beryllium are different from those for nuclear beryllium, many of the production and fabrication problems and techniques are applicable to both. Among the subjects discussed are flight structures, electron-bombardment melting, radiation-activation analysis, alloying and casting, corrosion in air, electrical resistivity, mechanical properties, and joining.

Since the expanded fields of application of beryllium make its continued availability of some concern to all users, an up-to-date report[5] on resources and world production will be welcome to many. Brief discussions on reduction, uses, and the physical and mechanical properties of beryllium metal are included.

Beryllium Casting and Alloy Development

Research on beryllium casting[6] has shown a typical relation between mold temperature and grain size, with higher mold temperatures producing larger columnar grains in the casting. Atypically, however, higher pouring temperatures produce smaller as-cast columnar grains. No explanation for this effect can be offered at present. Small additions of germanium, lanthanum, and zirconium to beryllium melts each produced some refinement in the columnar grain size. Germanium appeared particularly promising. The optimum amounts cannot be determined with available data.

One practical approach to improvement of the ductility of cast beryllium is to find ways of producing a finer grain size and of maintaining a fine grain size in subsequently wrought materials. On this premise, more than 100 beryllium-rich alloys were made and evaluated.[7]

All the additions refined the cast grain size, the most promising being silicon, silicon plus titanium, silver, aluminum, and aluminum plus titanium. Except for silicon and aluminum (4 per cent each), the preferred additions were limited to 1 per cent.

Purification and Analysis

The progress of the U. S. Bureau of Mines project on the purification of beryllium was reported[8] recently. Small quantities of highly purified beryllium have been made by fused-salt electrorefining. Efforts to perfect and scale up the process are under way.

The valuable properties of beryllium in nuclear devices and reactors are nullified by high-neutron-absorption impurities. Production steps, from ore to metal, and techniques for refining beryllium to a purity suitable for nuclear reactors are described[9] by a vice president of one of the producing companies.

From Great Britain comes a review[10] of purification processes and a discussion of the mode of occurrence of chlorine in electrolytic flake beryllium. The author found that an irreducible minimum of 200 to 300 ppm chlorine can be reached by crushing and leaching, and he suggests three possible ways in which this chlorine may be present: (1) surface films on beryllium powder, (2) chlorine dissolved in the lattice, and (3) discrete chlorine-containing particles enclosed by the metal.

A list of the papers presented and a summary of a symposium on the analysis of beryllium and estimation of impurities recently appeared in *Chemical Age*.[11]

Fabrication of Beryllium

Beryllium Cladding. In attempts to clad uranium fuel elements with beryllium by coextrusion, the stiffness mismatch between the two metals through the workable temperature range is so great that there is difficulty in attaining geometric uniformity in the extruded rod. This problem is worsened by the low resistance of beryllium to cracking. Nevertheless, it is possible to coextrude uranium and beryllium (without integral end seals) by single-temperature extrusion, provided that (1) the uranium is in the alpha phase, (2) the reduction is low (2 : 1 to 4 : 1), (3) the diameter is small ($\frac{3}{8}$ in.), (4) the clad thickness is heavy (50 mils or greater), and (5) the length is short (6 to 10 in.). Much more success was attained by using a multi-temperature extrusion process and a uranium–2 wt.% zirconium core. With this alloy, only a small amount of core shrinkage was observed on thermal cycling from room temperature to 600°C *in vacuo*. In air, two out of five samples failed, and there was some increase in the diameter of rods that did not fail.[12]

These cladding experiments were continued. Roll-clad strips of beryllium over uranium–10 wt.% molybdenum were produced. The difference in the thermal expansion of the core and cladding caused cracks in the latter, although the cracking was less severe than in extruded rods.[13,14]

Melting of uranium and UC_2 in a graphite crucible at 2100 to 2150°C resulted in a two-phase system of UC particles dispersed in a uranium matrix.[15] With about 58 vol.% UC, the extrusion constant of the alloy about matched the extrusion constant of beryllium. A much finer UC particle size was obtained later by melting small buttons in a water-cooled crucible. The alloys were pulverized and coextruded with beryllium. The magnitude of stiffening of the core depended on both particle content and particle size. The finer dispersions appeared most promising for over-all fabrication purposes, but cracking in the cladding was still a problem.

It was found[16] that a uranium–3.8 wt.% silicon (the reference says lithium, but this is obviously an error) alloy has nearly the same extrusion stiffness as beryllium in the temperature range of 1400 to 1450°F. The feasibility of coextrusion was established, although difficulty was experienced in getting the rods to emerge intact from the press. A 12-in.-long $\frac{3}{8}$-in.-diameter sample of extrusion-clad rod cycled eight times from room temperature to 600°C (1112°F), remaining at temperature 3 hr, did not crack.

Extrusion studies of beryllium-clad epsilon uranium-silicon alloy (previously reported by Nuclear Metals in March 1960) were continued. Rods extruded at temperatures up to 1700°F remained in one piece, with no cracks in the cladding. The cladding thickness was uniform, the seals were integral, and the core shape at the ends was good. These rods were approximately $\frac{5}{8}$ in. in diameter by 36 in. long, with a 20-mil cladding. One rod experienced no failure when subjected to 30 cycles in air by heating to 600°C (1112°F), held 3 hr at that temperature, and cooled at room temperature.[17]

Beryllium Extrusion. The possibility of extrusion of bare beryllium shapes was demonstrated by the extrusion of 10- to 12-ft lengths of a small channel section. It was decided that higher ram speeds were necessary to get reproducibly good and longer (20-ft) extrusions than the available press could deliver. Negotiations were in progress to obtain the use of an adequate press.[18,19]

Beryllium Wire Drawing. Beryllium wire of 0.063-in. diameter was "warm" drawn successfully in 12.5-deg tungsten carbide dies, using MoS_2 with an epoxy resin binder for lubrication. X-ray diffraction studies indicated that the operative slip systems are basal and that the average fiber axis is [2 1 0]. A reasonably efficient stress relief without recrystallization was accomplished by heating the wire to 1290°F for 60 min and air cooling. Complete stress relief with recrystallization was attained by heating to 1480°F with a heat shield, followed by air cooling. This treatment produced more uniform thermal properties. The heating rate appeared to be a critical parameter. The production of draw stock by swaging powder, sintering, and warm swaging the sintered rod appeared promising.[20]

Beryllium Joining. The development of adequate joining methods continues to be an important problem in the fabrication of beryllium components. Final reports[21,22] of an Air Force-sponsored program show that a beryllium–20 at.% silver brazing alloy produced brazed joints with strengths of 60 per cent (30,000 psi) and 80 per cent of the base metal at room temperature and in the temperature range 700 to 1450°F, respectively. Similar strengths were obtained by brazing with pure silver if a continuous interface of unalloyed silver in the joint was avoided—a condition readily achieved by heat-treatment. It was found that a two-phase silver-beryllium alloy with a continuous silver network between the beryllium grains is ductile at room temperature.

Joining of beryllium plates and rods by braze welding, fusion welding, and pressure welding was investigated to develop improved methods, especially for use at or above 1350°F. Room-temperature joint strengths of silver braze welds of about 21,000 psi were retained up to about 1000°F but dropped to 11,000 psi at 1300°F. Pressure welding at temperatures below 1650°F, with weld deformations of less than 0.5 per cent, produced joints with strengths equal to those of the base metal.[22]

A very informative report of experiences at Los Alamos on brazing and soldering of beryllium recently appeared.[23] Excellent results were reported when the beryllium was precoated with magnesium, using a titanium flux, and then brazed with preplaced magnesium in an induction furnace. In general, precoating was recommended prior to brazing or soldering. The beryllium could be electroplated with copper or silver from cyanide or acid solutions, or dip coated in a molten bath of 70 wt.% silver–30 wt.% aluminum at 726 to 822°C for 15 to 60 sec. The bath was covered with a molten flux consisting of 60 wt.% LiF–40 wt.% LiCl. Good adherence was reported also with flame-sprayed coatings of metal powders of either type 1100 aluminum or nickel-chromium alloys and with wire-sprayed bronze. Furnace brazing in an electric muffle furnace was most successful when pure silver, a 45 Ag–15 Cu–16 Zn–24 Cd alloy, or 70 wt.% silver–30 wt.% aluminum was used as the brazing alloy on samples mechanically cleaned or chemically etched. Soft soldering proved to be an effective method of joining beryllium when the design of the joint permitted a press fit. The beryllium could be dip coated for soldering by immersing it in a molten aluminum flux (tin and chlorides) at 250 to 275°C for 20 to 30 sec. Preplating by ultrasonic timing, flame spraying, or silver or copper plating was also used. After the coating procedure, the surfaces were cleaned, and the joints were made with no flux and no protective atmosphere. The necessary safety precautions were observed, of course. The results obtained by soft soldering are presented in Table II-1.

The approximate flow points and the results of wettability and flowability tests on 50 experimental brazing alloys were determined at Oak Ridge.[24] The most promising of these experimental alloys are listed in Table II-2.

In diffusion-bonding experiments with beryllium, it was reported[24] that increased grain coalescence across the grain boundaries became evident with increasing temperature and time at temperature, but only when grain growth occurred. Grain growth starts only when the temperature and pressure are sufficient to disrupt the oxide film surrounding the grains. The use of helium atmospheres decreased the vaporization of both beryllium and impurities.

Table II-1 CHARACTERISTICS OF SOFT-SOLDERED BERYLLIUM JOINTS[23]

Solder composition, wt.%	Surface pretreatment	Bursting pressure, psig	Shear stress in joint, psi
41.6 Pb, 31.6 Sn, 26.8 Zn, no flux	Flame-sprayed silver	1650	1830*
41.6 Pb, 31.6 Sn, 26.8 Zn, no flux	Flame-sprayed silver	2620	2900*
50 Sn–50 In, tin chloride flux	50 Sn–50 In, tin chloride flux	620	1460†
50 Sn–50 In, tin chloride flux	50 Sn–50 In, tin chloride flux	1150	1100†
50 Pb–50 Sn, no flux	50 Sn–50 In, tin chloride flux	1650	1590†

*Shear stress sustained by joint, fractured in beryllium.
†Fracture stress of joint, in shear.

Table II-2 EXPERIMENTAL BRAZING ALLOYS FOR BERYLLIUM[24]

Alloy composition, wt.%	Flow point, °C	Flowability on beryllium T-joints
55 Pd–30 Ti–10 Al–5 Be	1150	Good
46 Pd–46 Ti–6 Al–2 Be	1100	Excellent
43 Pd–43 Ti–9.5 Al–2 Be	1150	Good
49 Pd–49 Ti–2 Be	1000	Excellent
48 Pd–48 Ti–4 Be	1000	Excellent
45 Pd–45 Ti–10 Be	1000	Excellent
80 Au–10 Ni–10 Ta	1000	Poor
48 Au–48 Ti–4 Be	1200	
70 Au–15 Ta–13 Ni–2 Be	1200	
49 Ti–49 Cu–2 Be	1100	Excellent

It was reported[24] that caps were fusion welded to beryllium fuel tubes and that these joints were leaktight when tested with a mass spectrometer. It was noted that porosity was quite pronounced in the welds made on extruded tubing. The optimum welding conditions were a weld speed of 10 in./min, a low-current (approximately 12 amp) preheat for three to four revolutions, and a 30- to 35-amp welding current for two revolutions, followed by a slow current taper to allow postheating of the weld.

A capsule was fabricated and tested out-of-pile by pressurizing to a hoop stress of 2000 psi in the tube wall. Failure occurred in the tube wall after 3.2 hr at 750°C. The diffusion-bonded end closure was not disturbed.[24]

Plugs were also upset welded into tubes by the use of a special welding jig that presses an Armco-iron or mild-steel deformation ring into the specimen, producing extensive radial deformation of the tube and plug during welding. Leaktight joints were produced with an initial deformation temperature of 550°C and an axial pressure of approximately 3000 psi. The temperature was raised to 800°C and held for about 2 min to promote bonding immediately after the deformation at 550°C. The joint was then air cooled under pressure. Such joints, although leaktight, are mechanical rather than metallurgical.[24]

Physical Metallurgy of Beryllium

Phase Diagram of Zirconium-Beryllium System. The zirconium-beryllium system was investigated by the Russians[25] by means of metallographic, thermal, and qualitative X-ray phase analyses, and by hardness measurements. Four intermediate phases, $ZrBe_2$, $ZrBe_6$, $ZrBe_9$, and $ZrBe_{13}$, were found. The first three of these form by peritectic reactions at 1235, 1475, and 1555°C, respectively. The compound $ZrBe_{13}$ melts at 1645°C. A eutectic containing 5 wt.% beryllium which melts at 965°C is formed between zirconium and $ZrBe_2$. The addition of beryllium to zirconium lowers the alpha-beta transformation temperature and results in the formation of a eutectoid at 800°C. The solid solubility of beryllium in alpha zirconium is less than 0.1 wt.%, and in beta zirconium it is less than 0.3 wt.%. The solubility of zirconium in beryllium does not exceed 0.3 wt.%. The phase diagram constructed from this effort is shown in Fig. 7. There are significant differences between this diagram and that published by Lustman and Kerze in *The Metallurgy of Zirconium* (National Nuclear Energy Series, Div. VII, Vol. 4, McGraw-Hill); for example, the latter shows a $ZrBe_{16}$ phase and no $ZrBe_{13}$.

Structure of Beryllium. Studies related to the structure of beryllium were reported by several authors. Prominent among these is S. H. Gelles of Nuclear Metals who described the start of the work carried out in his laboratory in a report[26] to the AEC. An anomalous heat effect in the form of a thermal arrest near 1265°C (the thermal arrest due to the melting point occurs at 1283°C) had been noted at various times in various laboratories. This could have been caused by impurities or by an allotropic transformation. High-temperature X-ray work at Nuclear Metals indicated that the pattern from the hexagonal low-temperature phase disappeared at about 1250°C and a new pattern

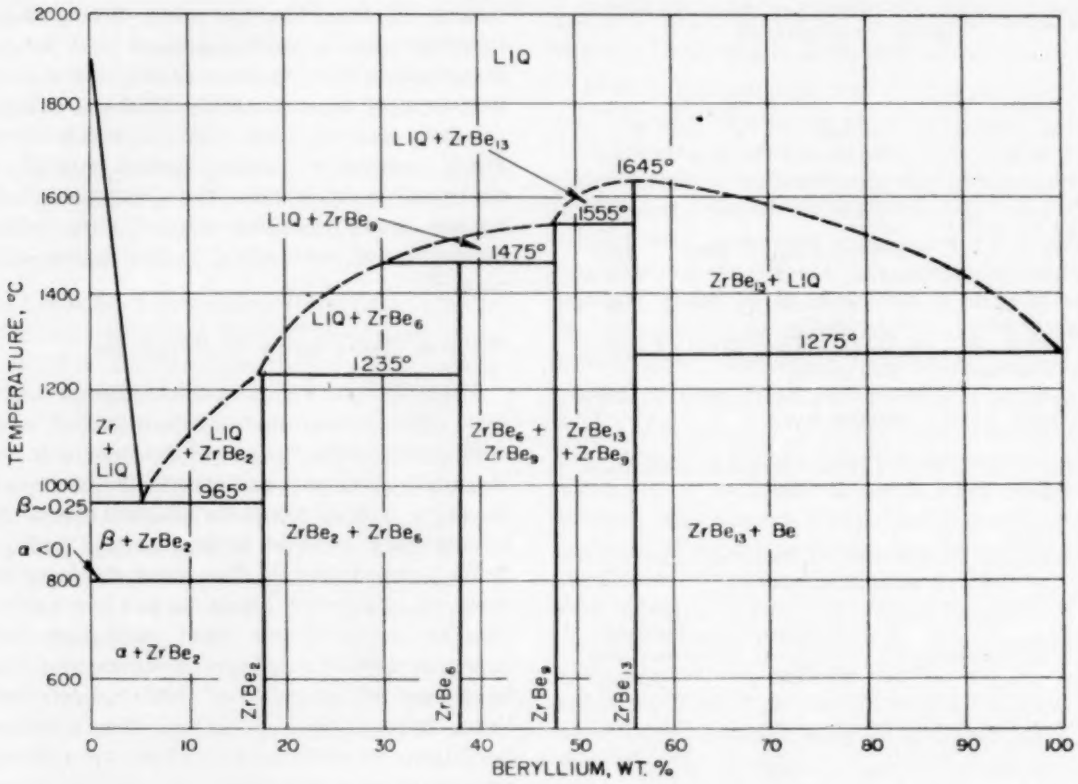

Figure 7 — Beryllium-zirconium phase diagram.[25]

formed (see Fig. 8). The new pattern could be made to disappear and the old one to reappear by cooling.

A program was set up in the hope of stabilizing the beta phase of beryllium, which is body-centered cubic, by alloying and quenching. The choice of possible alloying elements is limited by the very low solubility of most elements in beryllium and its strong compound-forming tendency. Among the elements chosen were iron, cobalt, nickel, copper, palladium, and silver (because of their probable solubility) and vanadium, mercury, zirconium, silicon, zinc, platinum, nickel-palladium, chromium, cerium, and lanthanum. Retention of the beta phase at appreciably lower temperatures has not been possible.[16,17,26]

Tests on beryllium tubing have shown that the amount of preferred orientation in thin-walled filled-billet extrusions increased with increasing extrusion temperatures and reduction ratios, whereas the orientation in heavy-walled filled billets was unaffected by the extrusion ratio. Billets extruded over a mandrel at high reduction ratios show strong preferred orientation. In all except the heavy-walled filled billets, the texture consisted of basal planes normal to the tube and parallel to the extrusion direction. The highest strength tubing was made[24] by extruding filled billets at a high reduction ratio (23 : 1) at a temperature near 1800°F.

The lattice reorientation caused by abrasion on single crystals of beryllium has been studied by electron diffraction. The twinning sometimes found in subsurface regions of abraded single crystals is dependent on the initial crystal orientation with relation to the direction of the applied stress. Development of the characteristic oblique [0 0 1] compression fiber texture was facilitated most by the operative $\{1\,0\,\bar{1}\,2\}$ set of twinning planes.[27]

The Swedish report[28] that beryllium exhibits its highest hardness in directions perpendicular to the basal plane. To reach this conclusion, the metallographic structure, microhardness, and texture were determined on the following materials: material from the beryllium reflector in the MTR R2 (probably hot-pressed powder), a 1- by 10-mm strip of cross-rolled beryllium from Pechiney, a hot-extruded tube of 9.5-mm

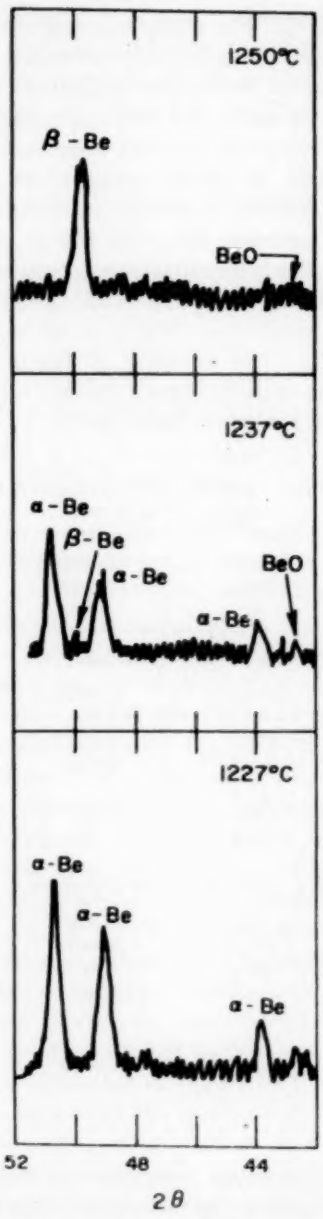

Figure 8—X-ray diffractometer tracings of beryllium at 1227, 1237, and 1250°C.[26]

bore and 1-mm wall thickness (produced by Tube Investment Company) with a 12 : 1 reduction ratio, and electrolytic flake beryllium from Pechiney.

If it is assumed that beryllium is inherently brittle, then ductility can best be developed by manipulation of crystallographic textures. The $(10\bar{1}2)$ type twinning is one of the most predominant modes of deformation of beryllium at temperatures as high as 1950°F, and therefore it is instrumental in texture development. The prior texture of beryllium appears to affect the development at low values of reduction. The degree of preferred orientations developed by rolling beryllium at 1000°C is greater than that obtained by rolling at 450°C and annealing the sheet between each pass at about 800°C. The mechanical properties of sheet formed by compression rolling approach those of hot-upset sheet. Up to the date of the report (July 1960), the material which approached most closely to the texture of randomly oriented wrought beryllium exhibited a ductility of approximately 1 per cent.[29]

As a result of early efforts to produce randomly oriented wrought beryllium sheets, the following tentative conclusions were reached:[30]

1. Single crystals can be rolled readily at 600 and 1060°C.
2. Considerable recrystallization occurs during rolling of single crystals.
3. The turbulent-flow mechanism, as triggered by BeO inclusions, can be made operative in beryllium.
4. Although the turbulent-flow process decreases the degree of preferred orientation, the embrittling effect associated with BeO additions is greater than any ductility increase that might have been realized by the decrease in crystallographic anisotropy.

A number of beryllium-rich binary alloys were made to study their microstructure and tensile properties. The alloying elements investigated included zinc, copper, chromium, yttrium, lithium, cadmium, manganese, and germanium. It was noted that zinc has little or no tendency to form a beryllium-rich solid solution, or to form any intermetallic compounds.[26]

Single-crystal-deformation studies on a square specimen revealed isolated slip traces and twins, which were formed at a stress of approximately 2000 psi, concentrated at the corners. Under a stress of about 5000 psi, all the surfaces became almost completely covered with a series of fine slip traces that were not parallel to those noted at lower stress levels. These new traces indicated the onset of primary slip.[16]

Impurity Precipitation in Beryllium. In a paper[31] that describes some sound approaches toward understanding and eliminating the persistent problem of brittleness in beryllium, support is given to the thesis that precipitation of

metallic impurities takes place in commercially pure beryllium in the temperature range of 200 to 1000°C. Between 600 and 800°C, the precipitation occurs rather quickly. Solution treating the aged metal for 1 hr at 1100°C redissolves the precipitate. In France, the precipitation of trace impurities (especially the transition elements) was studied[32] by radiocrystallography, resistivity measurements, micrography, and an electron microprobe. One precipitate, at least, was found to have an orientation relation with the matrix.

Physical and Mechanical Properties and Testing of Beryllium

Research is in progress on (1) effects of impurities on the electrical resistivity of beryllium, (2) the relation between the electrical and thermal conductivities of beryllium, and (3) an investigation of the electronic structure of beryllium. A definite relation has been indicated between the electrical resistivity and metallic-impurity content of the metal, but the effects of specific impurities have not yet been evaluated. The development of a universal expression relating the electrical and thermal conductivity of various grades of beryllium over the entire temperature range of 0 to 1500°K now appears to be impossible, but it may be possible for temperatures above 1000°K.[33]

Meanwhile, X-ray data for several aged specimens of commercial beryllium have shown an excellent qualitative correspondence between the resistivity and the amount of an unknown impurity phase precipitated. Work is in progress to determine the identity of this phase.[17] Beryllium was solution heat-treated for 1 hr at 1100°C and water quenched. Parts of the sample were then aged (1) at 200°C for one month, (2) at 800°C for one week, and (3) at 1000°C for one week. No change in the electrical resistivity beyond that previously reported[27] was noted after the treatments at 200 and 800°C, but there was an unexplained increase after the treatment at 1000°C, which will be rechecked. No grain growth or change in texture was noted after any of the treatments, and hardness studies were inconclusive.[16]

A Canadian report[34] describes extensive results of a mechanical testing program on beryllium. Sharp yield points were noted in specimens pulled at room temperature and 400°C, but none were evident in specimens pulled at 600 and 800°C. The sharp yield points were interpreted as indicating the presence of interstitial atoms in the beryllium lattice. Annealing treatments of 900°C for 24 hr, followed by cooling at either 15 or 2°C per hour increased the ductility over the whole temperature range and eliminated brittle cleavage fractures at temperatures between 200 and 400°C. It is suggested that the interstitials evaporated from the lattice at the high temperatures. Stress-rupture data from specimens tested in air were somewhat erratic. The results of tests at 620°C (1148°F) on specimens from two different sources are shown in Table II-3.

Table II-3 STRESS-RUPTURE DATA FOR BERYLLIUM ROD[34]

Specimen	Rupture time, hr	Minimum creep rate, %/hr	Stress, psi
Rod from Nuclear Metals, Inc.			
D1	764.6	0.0014	3360
D3	64.4	0.008	4480
D8	593.5	0.0023	3360
D9	159.7	0.0075	3920
D10	7.4		5600
D16	49.1	0.040	5040
D23	28.7		5390
Rod from Pechiney (France)			
D57	60.3	0.006	3990
D58	224.2	0.0017	3570
D59	39.8	0.010	4480
D60	13.0	0.061	5040
D61	12.1		5410
D62	7.5		4830
D63	127.2	0.0025	3780

Tests on cladding integrity and thermal cycling in a vacuum of beryllium-clad fuel cells are reported by Nuclear Metals.[35] The central 6-in. portion of an extruded rod was heated in air at 600°C for 72 hr. The ends of the rod protruded from the furnace. The cladding thickness was about 52 mils. After 48 hr a crack about 1 in. long appeared in the central portion of the heated zone; and at the end of 72 hr the crack was 7 in. long, and the core had swollen excessively. Failure occurred in two out of four rods tested. On another test, a sample 5.990 in. long by 0.50 in. in diameter with a 0.110-in. cladding was sealed in an evacuated quartz tube and cycled 295 times, 30 min in a furnace at 600°C and 15 min outside. Eventually the core shrank

and the cladding cracked, presumably because it lacked ductility to follow the shrinking core.

Acceptance tests of beryllium tubes from several sources are reported by Oak Ridge[24] and by AECL.[34]

Chemical and Thermal Properties of Beryllium

The reaction of beryllium in air at pressures approaching 760 tons was investigated[36] over the temperature range 930 to 1245°C. The reaction follows a linear rate law and is temperature dependent as it follows the Arrhenius equation

$$k = Ae^{-\Delta H/RT}$$

The activation energies are 1.10×10^5 cal/mole in the temperature range of 930 to 1065°C and 1.06×10^4 cal/mole in the temperature range of 1065 to 1295°C. An induction period exists which appears to be a thermally activated process with an activation energy of about 30 kcal/mole.

The kinetics of French flake beryllium in dry oxygen were studied[37] for 300-hr periods at temperatures in the range of 500 to 700°C, using a vacuum microbalance. At temperatures up to and including 650°C, the oxidation is protective and the rate decreases continuously with time, reaching a value of 0.02 to 0.04 $\mu g/(cm^2)(hr)$ after 300 hr. At 750°C the rate first decreases and then increases with time, indicating a breakaway reaction and subsequent nonprotective oxidation. The curves of weight gain versus time show small discontinuities that are ascribed to cracking and healing of the oxide film.

The chemistry of the reaction of French flake beryllium with carbon dioxide and with carbon monoxide also has been investigated, at temperatures in the range of 500 to 750°C, by means of a radioactive-tracer technique. The results lead to the conclusion that the following reactions occur:

$$Be + CO_2 = BeO + CO$$

$$2Be + CO_2 = 2BeO + C$$

$$Be + CO = BeO + C$$

and it is argued that the beryllium carbide which is also present in the oxide layer is formed by the reaction

$$2Be + C = Be_2C$$

and not directly according to

$$4Be + CO_2 = 2BeO + Be_2C$$

or

$$3Be + CO = BeO + Be_2C$$

There was no evidence for the reaction of carbon dioxide with deposited carbon according to the equilibrium:

$$C + CO_2 \rightleftharpoons 2CO$$

nor for the reverse reaction, namely, the decomposition of carbon monoxide to deposit carbon and evolve carbon dioxide. A less detailed investigation suggests that, for oxidation in carbon monoxide–carbon dioxide mixtures, there exists a minimal concentration of carbon monoxide above which carbon monoxide also reacts with beryllium.[38,39]

The corrosion of beryllium by CO_2 was further studied in tests of 350- and 1000-hr duration and at pressures of 1×10^{-3} mm Hg and 760 mm Hg. The attack rate is parabolic, and there is but little difference in the rate constants at 720°C for the low-pressure and the atmospheric-pressure tests. (At the low pressure the observed oxidation rate is approximated by the equation

$$W_{720°C} = 6.78 \times t^{0.24}$$

where W is the weight gain in micrograms per square centimeter and t is the time in hours.) This strongly infers that the reaction of beryllium with CO_2 is independent of pressure and that the rate-controlling mechanism is the diffusion of the oxidizing species through the protective oxide film.[24,40]

The reflection electron-diffraction patterns showed that beryllium carbide is formed, together with beryllium oxide, during the reaction at 700°C of beryllium with static CO_2 gas, and also with static CO gas, and that carbon particles are dispersed within the oxide layer. Thermodynamic calculations indicate that free carbon could also be formed during the reactions.[41]

Stressed specimens of block and sheet beryllium were exposed to salt spray and several other aqueous media. No stress corrosion occurred after any exposure, although some general surface corrosion was observed.[42]

The compatibility of beryllium with stainless steel in NaK environment at 600, 700, and 800°C was determined by tests of 1000-hr duration. A reaction layer, primarily a nickel-beryllium compound, appeared on the stainless steel in contact with the beryllium. The thickness of the layer varied[24] from less than 0.0005 in. (600°C) to 0.010 in. (800°C).

Beryllium samples, exposed to a fast-neutron irradiation at temperatures of 505 to 615°C, decreased in density from 1.5 to 5 per cent. No correspondence to temperature, within the range of the experiment, was observed. The density change was greatest in extruded rod (one specimen), generally less in unidirectionally rolled and cross-rolled sheet, and least in hot-pressed block.[24]

A. R. Gilman reported[26] on a comparison of the results obtained in the analysis of oxygen in beryllium by two chemical methods and a radioactivation technique. The chemical methods, HCl volatilization of beryllium metal as chloride and selective dissolution of beryllium in a bromine-methanol solution, did not agree with each other and gave inconsistent results. The radioactivation method gave lower values, but they were consistent.[26]

Miscellaneous Beryllium Studies

Two techniques used at Oak Ridge[40] for polishing beryllium specimens are described. A Syntron vibratory polisher gives good results, but the use of this method for polishing specimens requires 4 to 16 hr; also, with multimetallic specimens, the beryllium adjacent to the dissimilar metal may be attacked. An attack-polish method on a high-speed handwheel gives excellent results and avoids the interaction between dissimilar metals. However, inclusions such as BeC are lost since an aqueous solution of oxalic acid is used. The Canadians[34] prefer mechanical polishing to electrolytic polishing because the electrolytic methods produce severe pitting at the finely dispersed oxide inclusions.

Two bibliographies on beryllium were received. One from Lockheed[43] lists 135 government reports and articles in the open literature, most of which have been published recently. Informative abstracts of many of the items noted are included. The second bibliography[44] gives 147 references to publications on the fabrication of beryllium. Also included are references to reports on the brazing, casting, cladding, extrusion, and welding of beryllium and some beryllium alloys. The bibliography is limited to the period 1950–1959. (W. Hodge)

Beryllium Compounds

At Atomics International,[45] the thermal conductivity, k, of BeO was measured from 350 to 2000°C as a function of density. BeO specimens of 91 to 95 per cent of the theoretical density had thermal resistivities given by $1/k = (1.999 \times 10^{-2}\ T - 9.21)$(cm-sec)(°K)/cal from 650 to 1680°K. BeO specimens of 99 per cent of the theoretical density had thermal resistivities given by $1/k = (1.906 \times 10^{-2}\ T - 9.56)$(cm-sec)(°K)/cal from 900 to 1850°K.

The thermal expansion of BeO specimens was measured from room temperature to 1000°C in a dilatometer. No appreciable differences were observed when the density was varied from 50 to 95 per cent of the theoretical density. The measured coefficients of thermal expansion varied from 8.61 to 9.02×10^{-6} cm/(cm)(°C).

(J. Koretzky)

Solid Hydrides

An extensive bibliography on hydrides has been completed by Tufts University.[46] It is organized in 18 sections, mostly by periodic-family groupings. A general section contains 316 references, and the remaining 17 sections, which cover both binary and ternary hydrides, comprise 1629 listings.

A review of transition-metal hydrides, with emphasis on the true hydride phases rather than on the dilute solutions of hydrogen in the metals, has been published by Libowitz.[47] The paper discusses phase relations, crystal structures, and P-C-T relations of the hydrides, together with thermodynamic, electrical, and magnetic properties. It includes hydrides of the metals of Groups IV-A and V-A, the lanthanides, and the actinides, plus a brief discussion of alkali and alkaline-earth hydrides.

Zirconium Hydride

Correlations of metallographic structures in the zirconium-hydrogen system with the phase diagram have been presented by Whitwham.[48] He reports a eutectoid composition of 36 ± 2 at.% hydrogen and confirms the existence of an epsi-

lon phase of the hydride, which is related to the delta phase by a pseudomartensitic transformation.

The thermal diffusion of hydrogen in delta-phase zirconium hydride in the temperature range of 1000 to 1300°F has been measured at Atomics International.[49] With temperature gradients of about 100°F/in., the hydrogen concentration of four samples that initially contained 1.84 wt.% increased to an average of 1.90 wt.% at the cold end and decreased to an average of 1.78 wt.% at the hot end. No radial concentration gradients of hydrogen were found, however. The heat of transport of hydrogen was calculated to be 1.3 ± 0.4 kcal/mole. Specific-heat measurements on $ZrH_{1.6}$ have been extended to 500°C.[50] The values range from 0.085 cal/(g)(°C) at 30°C to 0.16 cal/(g)(°C) at 500°C.

The physical and mechanical properties of zirconium hydride of varying compositions have been summarized by General Electric.[51] The density of hydrided zirconium at various percentages of hydrogen is given in Fig. 9. The

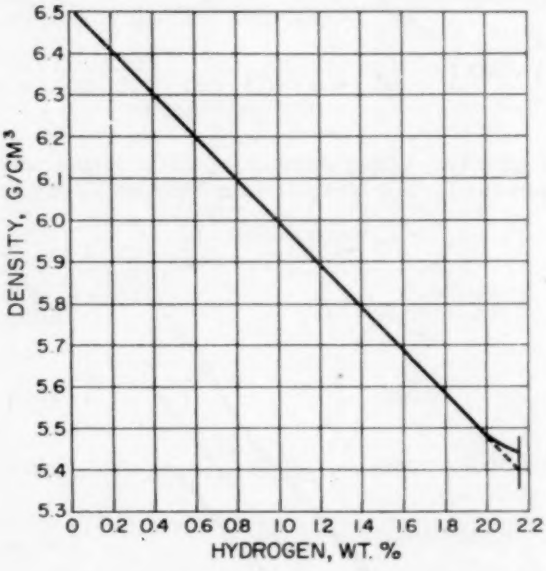

Figure 9 — Density for hydrided zirconium (ZrH_x).[51]

values are dependent on the original density of the zirconium from which the hydride is prepared, and slight variations of density for reactor-grade zirconium have been observed.

The ultimate tensile strength of zirconium hydride is plotted as a function of temperature for various N_H values in Fig. 10. The rapid drop in ultimate strength that occurs above

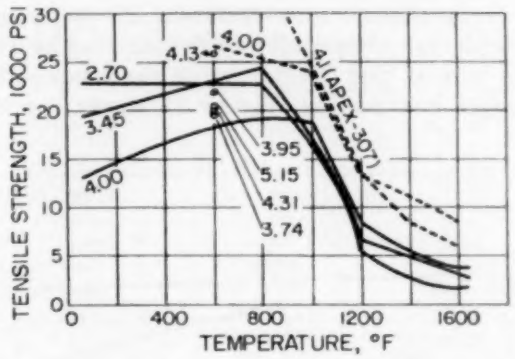

Figure 10 — Ultimate tensile strength of ZrH_x at various temperatures.[51] ——, Battelle Memorial Institute data. – – –, GE-ANP data. Numbers refer to N_H values.

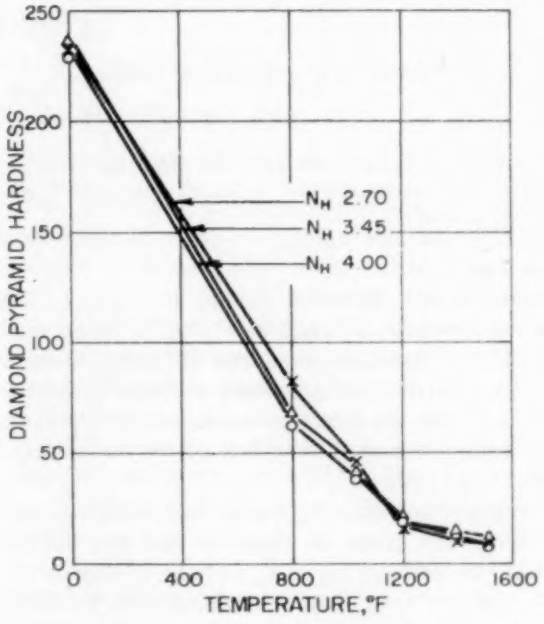

Figure 11 — Hardness of hydrided zirconium at various temperatures.[51]

800°F is probably connected with the phase change of alpha-plus-delta hydride to the beta-plus-delta hydride.

The hardness of zirconium hydride drops off rapidly with an increase in temperature, as shown in Fig. 11. The slight differences noted for the various N_H values could be due to poor reproducibility in experimental results. The large grains present in hydrided zirconium make it difficult to reproduce indentation hardness measurements.

Creep-rupture measurements on zirconium hydride are complicated by the fact that hydrogen loss at high temperatures can change the sample composition. Figure 12 shows results

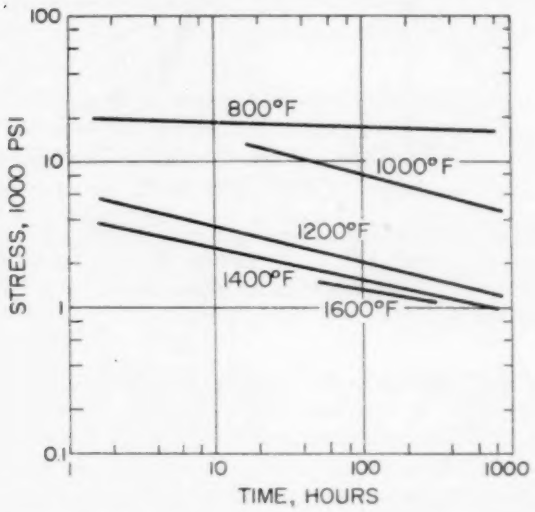

Figure 12—Rupture strength and time of rupture at various temperatures for hydrided zirconium[51] with an N_H of 4.00.

obtained with material having an N_H of 4. The measurements at 1400 and 1600°F were conducted with partial pressures of hydrogen equal to the equilibrium pressure at these temperatures, thus minimizing composition changes. Hydrogen loss at 1200°F and below was considered negligible.

Linear-thermal-expansion data on zirconium hydride are given in Figs. 13 and 14. For the material with an N_H of 4, a phase change is indicated at a temperature of about 1000°F. However, the hydrides with higher concentrations of hydrogen do not undergo this phase transformation, and the curves of Fig. 14 do not have a break.

The instantaneous specific heats of hydrided zirconium are presented in Fig. 15. No measurements were made in the transformation range, which is indicated by the broken lines in the graphs, and values read from this region are not valid.

Thermal-conductivity measurements are characterized by a lack of agreement, as indicated in Fig. 16. These wide variations may be due to migration of hydrogen or loss of hydrogen during the experiments, and they reflect the difficulty in making accurate determinations with this type of material. The drop in conductivity for the hydride with an N_H of 4.89 in the 1000°F range is particularly questionable because material of this composition should not show a transformation in this range.

The electrical resistivity for zirconium hydride of two hydrogen concentrations is given

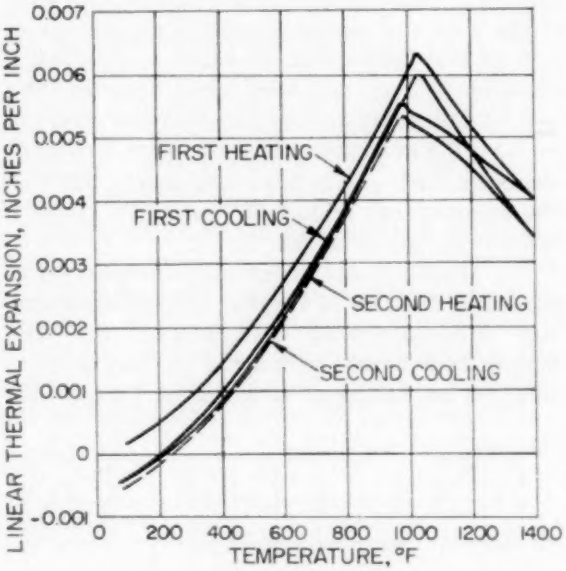

Figure 13—Linear thermal expansion versus temperature for hydrided zirconium[51] with an N_H of 4.00.

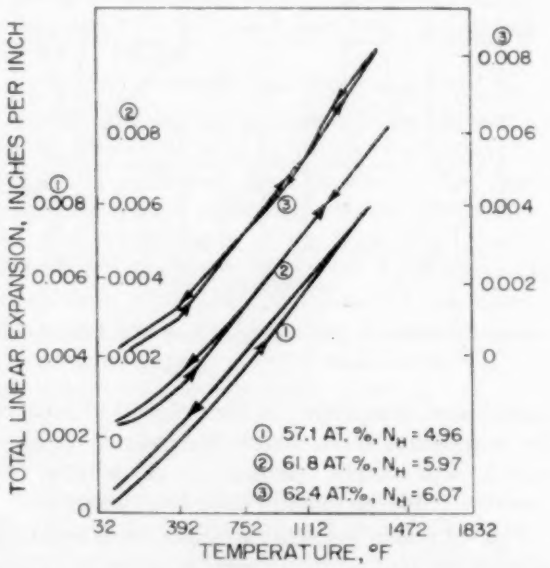

Figure 14—Thermal expansion of hydrided zirconium.[51]

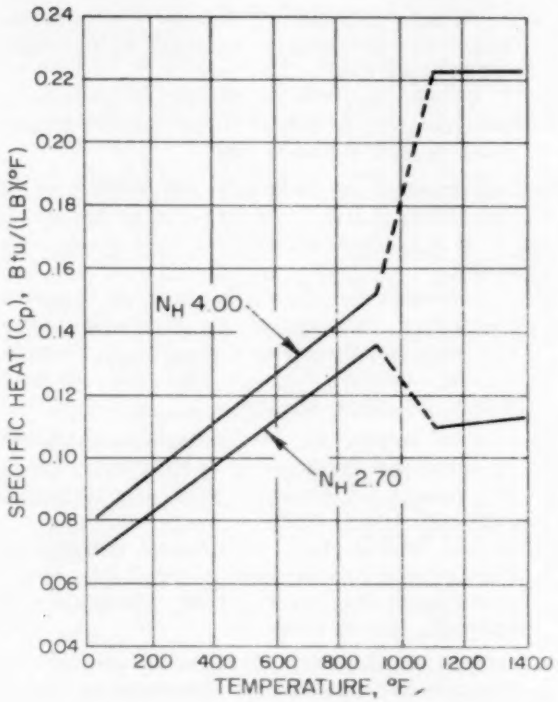

Figure 15 — Instantaneous specific heat versus temperature for hydrided zirconium.[51]

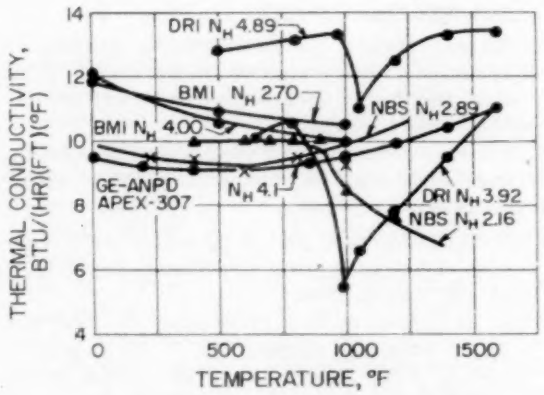

Figure 16 — Thermal conductivity of hydrided zirconium.[51]

in Table II-4. Over the temperature range studied, there is no change in resistivity with composition.

Lithium Hydride

The enthalpy of lithium hydride has been measured by investigators at Oak Ridge.[52] Empirical equations have been fitted to the data.

Table II-4 ELECTRICAL RESISTIVITY FOR HYDRIDED ZIRCONIUM[4]

Temp., °F	Electrical resistivity, μohm-cm	
	N_H = 2.70	N_H = 4.00
100	56	56
200	67	67
300	77	78
400	87	88
500	97	99
600	107	108
700	117	118
800	126	127
900	134	135
1000	142	143

From 100 to 650°C,

$$H_t - H_{30} = -32.17 + 0.914t + (71.30 \times 10^{-5})t^2$$

At 680°C,

Heat of fusion = 694.4 cal/g

From 700 to 900°C,

$$H_t - H_{30} = 291.47 + 1.988t - (6.35 \times 10^{-5})t^2$$

The solubility of titanium hydride and zirconium hydride in molten lithium hydride has been studied at Tufts University.[53] Determinations were made at 680°C with the compositions $TiH_{0.91}$, $TiH_{1.75}$, and $ZrH_{1.88}$. The observed melting and freezing points of the mixtures were identical with the melting point of pure lithium hydride within the experimental error of about 1°C. The results indicate that the degree of metallic interaction is sufficient to offset the ionic character of the compounds and to prevent measurable solubility.

Tantalum Hydride

Electrical measurements have been made on specimens of $TaH_{0.5}$ at Atomics International.[50] The results of Hall coefficient and resistivity determinations are shown in Table II-5.

Hydrided Alloys

Research at Chalk River[54] has shown that it is possible to form thin layers of zirconium hydride on Zircaloy-2 by electrolysis in the temperature range of 20 to 80°C. The effect of the hydride layer on the mechanical properties of the alloy is to be studied. The rate of hydriding was found to be independent of current density for values greater than 100 ma/cm^2. The growth of the hydride layer is diffusion controlled, with

Table II-5 ELECTRICAL PROPERTIES OF TANTALUM HYDRIDE[50]

Temp., °K	Hall coefficient, 10^{-5} cm³/coulomb	Resistivity, μohm-cm
4.2		3.00
77	10.40	5.37
300	11.52	20.81
318	12.48	30.78
335	12.11	45.15

the diffusion coefficient $D = 3.23 \times 10^{-5}$ exp $(-9700/RT)$ cm²/sec.

Studies of fueled moderators have resulted in a patent granted to Weeks and Goeddel,[55] assigned to the AEC, for a method of evenly dispersing uranium in a zirconium hydride moderator to produce a fuel element. Enriched UH_3 and zirconium hydride powders of 200 mesh are mixed in such quantities that the product contains from 0.1 to 3 per cent of U^{235} hydride. The powder mixture is then cold pressed at 100 tsi, and the resulting compact is heated *in vacuo* to 300°C to decompose the UH_3. The escaping hydrogen forms a porous matrix of zirconium hydride containing a uniform dispersion of uranium metal. (H. H. Krause)

References

1. R. W. Dayton and C. R. Tipton, Jr., Progress Relating to Civilian Applications During September 1960, USAEC Report BMI-1469, Battelle Memorial Institute, Oct. 1, 1960. (Classified)
2. Battelle Memorial Institute, Progress on Ceramic Coated Fuel Particles at Battelle, USAEC Report BMI-1468, Sept. 16, 1960.
3. G. E. Darwin and J. H. Buddery, *Metallurgy of the Rarer Metals, Series No. 7, Beryllium*, Academic Press, Inc., New York, 1960.
4. Clayton O. Matthews, Beryllium Research in Missile Development, *J. Metals*, 12(10): 780–785 (October 1960).
5. A. Knoerr, Beryllium—Today and Tomorrow, *Eng. Mining J.*, 161(9): 93–102 (September 1960).
6. P. M. Cohen and R. C. Harris, Beryllium Casting, Phase II, Interim Technical Report No. 6 for Dec. 19, 1959–March 18, 1960, Report NP-8797, Beryllium Corp., July 25, 1960.
7. D. Crooks and H. Sumsion, Grain Refinement in Beryllium by Alloying, Technical Note for Period July 1, 1958–December 31, 1959, Report LMSD-288233, Lockheed Aircraft Corp., January 1960.
8. M. M. Wong et al., Fused Salt Electrorefining of Beryllium, *J. Metals*, 12(10): 786–788 (October 1960).
9. C. W. Schwenzfeier, Jr., Nuclear Purity Beryllium—Its Manufacture, *J. Metals*, 12(10): 793–797 (October 1960).
10. R. G. Bellamy, The Occurrence of Chlorine in Electrodeposited Beryllium, British Report AERE-M-619, February 1960.
11. Determination of Beryllium and Estimation of Impurities, A.E.A. Symposium at Blackpool, *Chem. Age (London)*, 84(2144): 224 (Aug. 13, 1960).
12. J. Greenspan, Beryllium-Clad Uranium Elements Fabrication Development by Multitemperature Extrusion and Dimensional Stability on Thermal Cycling, USAEC Report NMI-1219, Nuclear Metals, Inc., Mar. 18, 1960.
13. Nuclear Metals, Inc., Fundamental and Applied Research and Development in Metallurgy, Progress Report for November 1959, USAEC Report NMI-2081, May 6, 1960.
14. Nuclear Metals, Inc., Fundamental and Applied Research and Development in Metallurgy, Progress Report for January 1960, USAEC Report NMI-2083, May 6, 1960.
15. Nuclear Metals, Inc., Fundamental and Applied Research and Development in Metallurgy, Progress Report for February 1960, USAEC Report NMI-2084, May 20, 1960.
16. Nuclear Metals, Inc., Fundamental and Applied Research and Development in Metallurgy, Progress Report for March 1960, USAEC Report NMI-2085, June 13, 1960.
17. Nuclear Metals, Inc., Fundamental and Applied Research and Development in Metallurgy, Progress Report for April 1960, USAEC Report NMI-2086, June 15, 1960.
18. Northrop Aircraft, Inc., Program for the Development of Extruded Beryllium Shapes, Report NOR-60-92, June 24, 1960.
19. Northrop Aircraft, Inc., Program for the Development of Extruded Beryllium Shapes, Report NOR-60-192, Aug. 3, 1960.
20. A. G. Gross et al., Fabrication of Beryllium Wire, Progress Report No. 4 for April 16–July 1, 1959, Report AD-227967, Brush Beryllium Co., June 28, 1960.
21. J. B. Cohen, Beryllium Joining—RAD Sponsored Program, Report WADC-TR-59-695(Pt.I), Avco Corp., April 1960.
22. E. M. Passmore, Beryllium Joining—WADC Sponsored Program, Report WADC-TR-59-695 (Pt.II), Avco Corp., April 1960.
23. R. W. Keil et al., Brazing and Soldering of Beryllium, *Welding J.*, 39(9): 406s–410s (September 1960).
24. Oak Ridge National Laboratory, Gas-Cooled Reactor Project Quarterly Progress Report for Period Ending June 30, 1960, USAEC Report ORNL-2964, Aug. 22, 1960.
25. V. S. Yemel'yanoy et al., Phase Diagram of the

Zirconium-Beryllium System, *At. Energ.*, 9(1): 33–38 (1960).

26. Nuclear Metals, Inc., Technical Progress Report to the AEC Reactor Division for Period Ending June 30, 1959, USAEC Report NMI-1216, July 21, 1960.
27. V. D. Scott, Twinning Caused by Abrasion on Single Crystals of Beryllium (in English), *Acta Cryst.*, 13: 313–319 (Apr. 10, 1960).
28. I. Fäldt and G. Lagerberg, Structure Investigations of Some Beryllium Materials, Swedish Report AE-32, January 1960.
29. F. M. Yans and P. Pointu, Preliminary Attempts to Produce Randomly Oriented Wrought Beryllium and Their Relation to Texture Development, USAEC Report NMI-1225, Nuclear Metals, Inc., July 6, 1960.
30. F. M. Yans et al., Development of Randomly Oriented Wrought Beryllium Sheet, USAEC Report NMI-9608, Nuclear Metals, Inc., May 17, 1960.
31. S. H. Gelles et al., Recent Advances in Beryllium Metallurgy, *J. Metals*, 12(10): 789–792 (October 1960).
32. P. Pointu et al., Study of the Precipitation of Trace Impurities in Beryllium (in French), *Compt. rend.*, 250: 2365–2367 (Mar. 28, 1960).
33. J. Ho and E. S. Wright, Electrical Resistivity of Beryllium, Report LMSD-288218, Lockheed Aircraft Corp., January 1960.
34. W. D. Bennett, Annual Report on Beryllium Research, 1959, Canadian Report CW-R&DL-1 (AECL-1029), April 1960.
35. Nuclear Metals, Inc., Fundamental and Applied Research and Development in Metallurgy, Progress Report for March 1959, USAEC Report NMI-2076, May 13, 1959.
36. W. Bradshaw and E. S. Wright, High-Temperature Corrosion of Beryllium in Air, Report LMSD-288232, Lockheed Aircraft Corp., January 1960.
37. D. W. Aylmore et al., The High-Temperature Oxidation of Beryllium: Part I—In Dry Oxygen, *J. Nuclear Materials*, 2(2): 169–175 (June 1960).
38. S. J. Gregg et al., The High-Temperature Oxidation of Beryllium: Part II—The Reaction with Carbon Dioxide and Carbon Monoxide, *J. Nuclear Materials*, 2(3): 225–233 (September 1960).
39. S. J. Gregg et al., Oxidation of Beryllium in Carbon Dioxide and Carbon Monoxide, *Nature*, 186: 468–469 (May 7, 1960).
40. Oak Ridge National Laboratory, Metallurgy Division Annual Progress Report for Period Ending July 1, 1960, USAEC Report ORNL-2988, Sept. 30, 1960.
41. V. D. Scott, Formation of Beryllium Carbide During the Corrosion of Beryllium in Carbon Monoxide and Carbon Dioxide Gas, *Nature*, 186: 466–467 (May 7, 1960).
42. C. M. Packer, Stress Corrosion Cracking of Beryllium, Report LMSD-49735, Lockheed Aircraft Corp., May 15, 1959.
43. K. D. Carroll, comp., Beryllium—Survey of the Literature, Report LMSD-288190(Suppl. 1), Lockheed Aircraft Corp., Apr. 1, 1960.
44. Elizabeth A. Cernak, comp., Fabrication of Beryllium: A Bibliography, USAEC Report CNLM-1802-14, Pratt & Whitney Aircraft Div., United Aircraft Corp., Apr. 1, 1960.
45. R. E. Taylor, Thermal Conductivity and Thermal Expansion of BeO at Elevated Temperatures, USAEC Report NAA-SR-4905, Atomics International, July 30, 1960.
46. Tufts University, Hydrides of Metals and Metalloids—A Literature Search, USAEC Report TID-3902, July 1960.
47. G. G. Libowitz, The Nature and Properties of Transition Metal Hydrides, *J. Nuclear Materials*, 2: 1–22 (March 1960).
48. D. Whitwham, Metallographic Study of Zr-H Alloys, *Rev. mét.*, 57: 1–15 (January 1960).
49. A. W. Sommer and W. F. Dennison, Thermal Diffusion of Hydrogen in Nonstoichiometric Zirconium Dihydride, USAEC Report NAA-SR-5066, Atomics International, Oct. 1, 1960.
50. Atomics International, Annual Technical Progress Report on AEC Unclassified Programs, USAEC Report NAA-SR-5350, Aug. 1, 1960.
51. D. S. Parker and C. L. Huffine, Properties of Hydrided Zirconium, USAEC Report APEX-561, General Electric Co., Aircraft Nuclear Propulsion Dept., December 1959.
52. Oak Ridge National Laboratory, Aircraft Nuclear Propulsion Project Semiannual Progress Report for Period Ending April 30, 1960, USAEC Report ORNL-2942, July 28, 1960. (Classified)
53. C. E. Messer and I. S. Levy, Solid-Liquid Equilibria in the Systems LiH-TiH_2 and LiH-ZrH_2, USAEC Report NYO-8029, Tufts University, July 8, 1960.
54. A. Sawatzky, Hydriding Zircaloy-2 by Electrolysis, Canadian Report CRMet-924(AECL-1046), June 1960.
55. I. F. Weeks and W. V. Goeddel, Method of Fabricating a Uranium-Zirconium Hydride Reactor Core, U. S. Patent 2,929,707, Mar. 22, 1960.

Section III

NUCLEAR POISONS

Burnable-Poison and Control Dispersion Materials

Based on experiments involving boron as a burnable poison in stainless steel–UO_2 fuel plates, Oak Ridge workers report[1] that SrB_6 and YB_6 show considerable reaction with type 304B stainless steel after 20 hr at 1150°C in vacuum. Borated glass particles were found to be stable in stainless steel at 1100°F (no boron content was given). In an attempt to eliminate the severe stringering that occurs during rolling, higher strength boron-containing glasses are being investigated. The mechanism of boron loss during hydrogen sintering is reported to be diffusion of boron from the glass to the metal.

The burnup profiles for two irradiated clad SM-1 reactor iron-boron absorber sections are given in Table III-1. Of the eight plates examined, all but one exhibited cladding-frame and core-cladding separations at the high-burnup end. The bonded interfaces were destroyed by irradiation for distances ranging from 1 to 7 in. from the high-burnup end. Calculations were made to determine the boron gradient necessary in a control rod to prevent severe irradiation damage at low average burnups. Owing to self-shielding, 30 per cent of the B^{10} in the surface layers may burn up while the average burnup remains at 4 at.% B^{10}. The design calls for the use of seven compacts of four concentrations ranging from 1 to 3 wt.% B^{10} to be used in fabricating a control rod for 25 at.% B^{10} average burnup.

Table III-1 BURNUP PROFILES FOR TWO IRRADIATED SM-1 REACTOR CORE I ABSORBER SECTIONS[1]

Distance from critical end, in.	Lithium content, wt.%	Average B^{10} burnup, at.%
Central Absorber (ORNL-5)		
0.75	0.44	22.0*
3.5	0.19	9.5
6.5	0.14	7.0
12.5	0.026	1.3
20.5	0.0006	0.03
Shim Absorber 3 (ORNL-2)		
0.75	0.36	18.0†
3.5	0.19	9.5
6.5	0.12	6.0
12.5	0.03	1.5
20.5	0.0012	0.06

*Average of only three plates; plate 18 had tip burnup of 14.5 at.% B^{10}.
†Average of all four plates.

A detailed study of the reaction of Eu_2O_3 and silicon in silicon-bearing steels has been reported,[2] and the major cause of instability of Eu_2O_3 in stainless steel has been attributed to the presence of silicon. Structural properties of the Eu_2O_3 are also thought to affect the stability, but they have not been studied.[1]

Bettis data[3] on irradiation damage in compartmented burnable-poison plates containing B_4C and B_4C-SiC compacts are listed in Table III-2. The diffusion coefficients[4] for the evolution of helium from slightly irradiated enriched boron carbide (40 per cent B^{10}) and depleted boron carbide (10 per cent B^{10}) were determined at 700, 800, and 900°C. The values for the enriched material were 4.5×10^{-11}, 4.5×10^{-10}, and 1×10^{-8} cm²/sec at 700, 800, and 900°C, respectively. At corresponding temperatures, the values for the depleted material were 1.6×10^{-11}, 1×10^{-9}, and 6.3×10^{-9} cm²/sec.

Battelle workers have developed techniques for incorporating boron burnable poisons in UO_2–stainless steel fuel plates with little or no loss during fabrication.[5] Zirconium diboride is the most compatible compound, and no boron loss occurs during vacuum sintering at 2150°F.

Table III-2 IRRADIATION EFFECTS IN BURNABLE-POISON PLATES[3]

Plate No.	Composition	B^{10} burnup: Per cent B^{10}	B^{10} burnup: 10^{20} fissions/cm^3	Helium gas released, %	Density, g/cm^3	Δ density, %
HC 101-2	B_4^NC	27.6*	56.6	0.57		
HC 101-6	B_4^NC	25.6	52.5	0.70		
HC 101-11	B_4^NC	22.6	46.4	0.92	2.22 ± 0.04	11.2
HC 93-2	B_4^NC + 50 vol.% SiC	31.78*	34	0.56		
HC 93-6	B_4^NC + 50 vol.% SiC	34.5	37	0.6		
HC 93-11	B_4^NC + 50 vol.% SiC	33.4	35.7	0.87	2.55 ± 0.02	7.6
HC 105-2	B_4^EC(38 vol.% B^{10})	29.7*	101	4.45		
HC 105-6	B_4^EC(38 vol.% B^{10})	27.6	94	2.70		
HC 105-11	B_4^EC(38 vol.% B^{10})	24.5	83.5	4.60	2.13 ± 0.15	14.8
PB 37-2	B_4^EC(38 vol.% B^{10})	25.7*	88	2.5		
PB 37-6	B_4^EC(38 vol.% B^{10})	27.4*	93.5	3.44		
PB 37-9	B_4^EC(38 vol.% B^{10})	28.7	98	3.13		
PB 37-11	B_4^EC(38 vol.% B^{10})	30.0	102	2.61	1.74 ± 0.10	30.4

*Radiochemical analysis.

Table III-3 BORON ANALYSIS ON ENRICHED SM-2 REACTOR FUEL PLATES[5]

Plate No.*	Type	Section	Boron type	Sample weight, mg	Boron placed in core,† mg	Boron analysis: %	Boron analysis: Mg	Boron change, %	Average boron change,‡ %
EAR-54	SM-1	D	B_4C	6.4117	6.95	0.072	4.63	33.4	−34.5
		E	B_4C	6.1920	6.64	0.070	4.33	34.8	
		F	B_4C	6.3577	6.87	0.070	4.44	35.4	
EAR-59	SM-2 reference	D	ZrB_2	6.6493	11.6	0.165	11.0	5.2	−2.04
		E	ZrB_2	6.6690	11.6	0.172	11.5	0.9	
		F	ZrB_2	6.5728	11.4	0.173	11.4	0	
EAR-62	SM-2	D	Nb-coated ZrB_2	6.5144	11.1	0.189	12.3	10.8	+2.07
		E	Nb-coated ZrB_2	6.4550	11.0	0.166	10.7	2.7	
		F	Nb-coated ZrB_2	6.3896	10.8	0.169	10.8	0	
EAR-69	SM-2 green core	D	ZrB_2	6.5833	11.6	0.169	11.1	4.3	−1.76
		E	ZrB_2	6.5547	11.4	0.171	11.2	1.8	
		F	ZrB_2	6.4187	11.1	0.174	11.2	1.1	
EAR-72	SM-2 high-fired UO_2	D	ZrB_2	6.5773	11.4	0.166	10.9	4.4	−2.88
	SM-2 high-fired UO_2	E	ZrB_2	6.6601	11.6	0.168	11.2	3.5	
	SM-2 high-fired UO_2	F	ZrB_2	6.4978	11.3	0.173	11.2	0.9	
EAR-77	SM-2 alternate	D	NbB_2	6.6452	11.6	0.160	10.7	7.8	−7.10
	SM-2 alternate	E	NbB_2	6.4764	11.2	0.160	10.3	8.0	
	SM-2 alternate	F	NbB_2	6.4413	11.1	0.163	10.5	5.4	

*Samples are 1¼-in.-diameter punched disks.

†Based on a 4½-mil cladding thickness. If a 5-mil thickness were used, the figures would be approximately 3.5 per cent less.

‡Boron change based on total change in the three specimens.

Boron losses during roll cladding are reported to be less than 10 wt.% for both the reference and the alternate materials, and, as shown in Table III-3, the losses are very small compared to losses incurred when B_4C is used. Losses can be completely eliminated by the use of niobium-coated ZrB_2. (G. W. Cunningham)

Control-Rod Alloys

Boron Alloys

Bettis[6] has investigated several iron, stainless-steel, and niobium-base materials containing 1 to 3 wt.% B^{10} for possible applica-

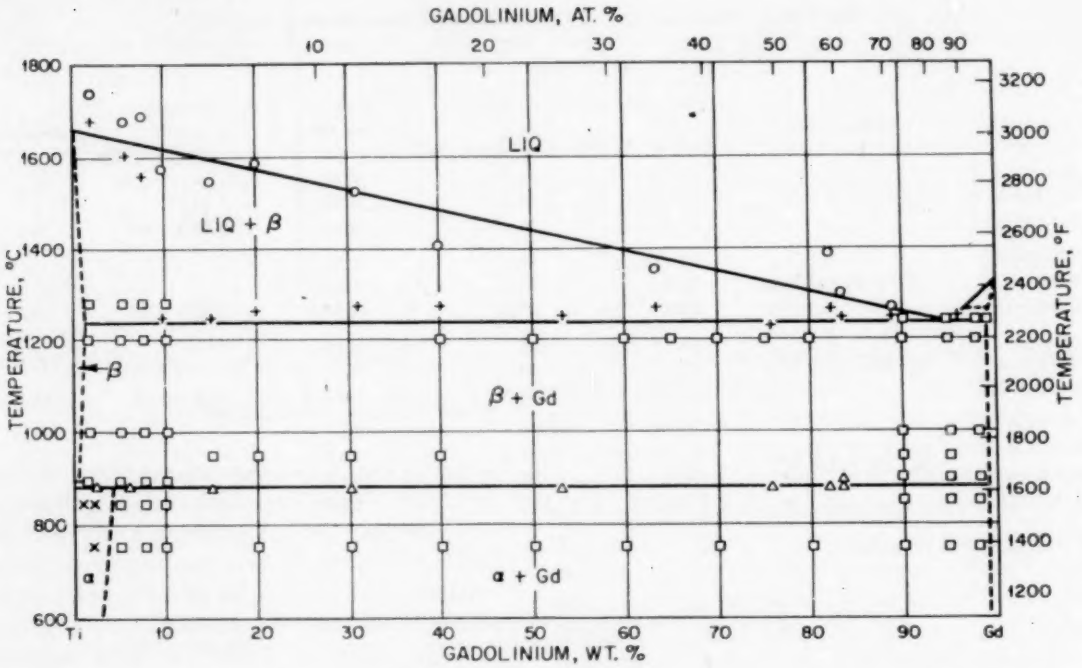

Figure 17 — Titanium-gadolinium phase diagram.[7] Optical method: ○, liquidus; +, solidus. Metallography and X ray: ×, single phase; □, two phase. Δ, $\alpha \rightarrow \beta$ by thermal analysis and resistivity.

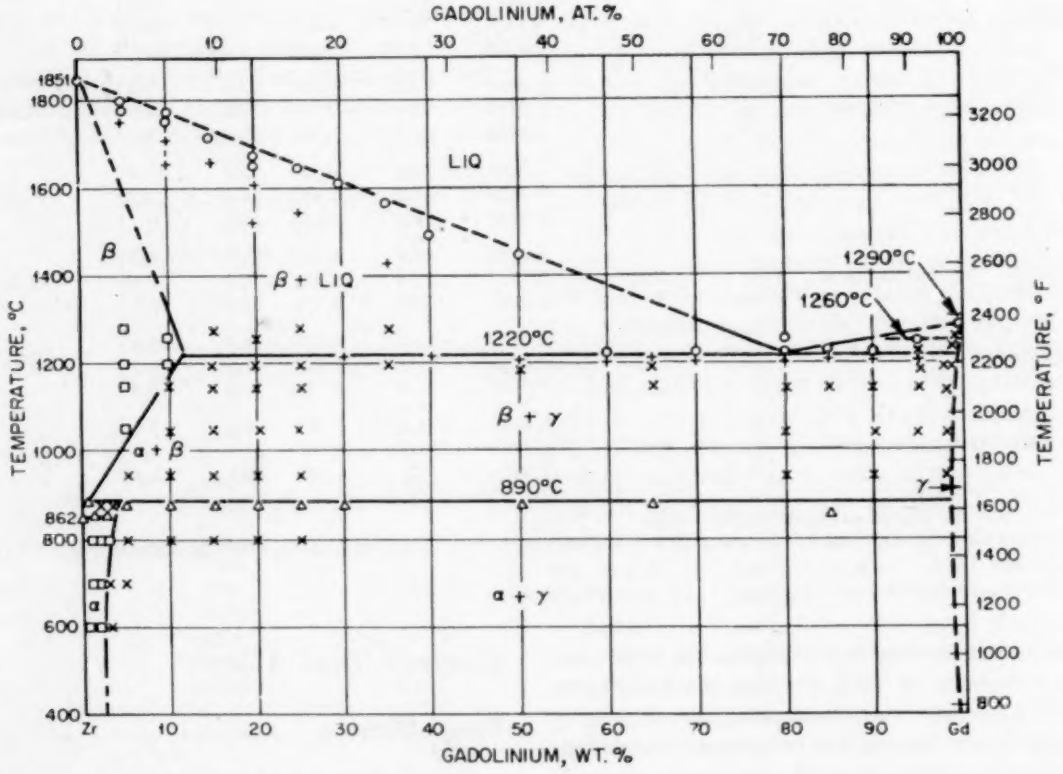

Figure 18 — Zirconium-gadolinium phase diagram.[7] ○, liquidus; +, solidus; Δ, $\alpha \rightleftharpoons \beta$ transformation; □, single phase; ×, two phase.

tions as lumped burnable poisons. On the basis of fabricability, mechanical and physical properties, corrosion resistance, and some irradiation data, the most promising materials appear to be austenitic and ferritic stainless steel containing less than 2 wt.% B^{10}.

Rare-Earth Alloys

The titanium-gadolinium and zirconium-gadolinium systems have been determined by the Bureau of Mines.[7] Phase diagrams appear in Figs. 17 and 18. Hardness of as-cast titanium-gadolinium alloys varied from Rockwell A44 for pure titanium to Rockwell A50 for a titanium–20 wt.% gadolinium alloy and Rockwell A17 for pure gadolinium. An as-cast zirconium–2 wt.% gadolinium alloy exhibited a hardness of Rockwell A36, whereas a zirconium–50 wt.% gadolinium alloy showed a hardness of Rockwell A45.

(V. W. Storhok)

References

1. J. H. Frye, Jr., et al., Metallurgy Division Annual Progress Report for Period Ending July 1, 1960, USAEC Report ORNL-2988, Oak Ridge National Laboratory, Sept. 30, 1960.
2. C. F. Leitten, Jr., The Stability of Europium Oxide in Silicon-Bearing Stainless Steel (thesis), USAEC Report ORNL-2946, Oak Ridge National Laboratory, Sept. 12, 1960.
3. Westinghouse Electric Corp., Bettis Atomic Power Laboratory, Pressurized-Water Reactor (PWR) Project Technical Progress Report for the Period June 24 to August 23, 1960, USAEC Report WAPD-MRP-87.
4. Westinghouse Electric Corp., Bettis Atomic Power Laboratory, Pressurized-Water Reactor (PWR) Project Technical Progress Report for the Period April 24 to June 23, 1960, USAEC Report WAPD-MRP-86.
5. R. W. Dayton and C. R. Tipton, Jr., Progress Relating to Civilian Applications During July 1960, USAEC Report BMI-1455, Battelle Memorial Institute, Aug. 1, 1960.
6. D. Jaffe et al., Development of Boron-Bearing Materials for Application as Lumped Burnable Poisons, USAEC Report WAPD-221, Westinghouse Electric Corp., Bettis Atomic Power Laboratory, May 1960.
7. Mark L. Wright, Quarterly Metallurgical Progress Report No. 7 for the Period April 1 to June 30, 1960, USAEC Report USBM-U-745, Bureau of Mines, Albany Metallurgy Research Center.

Section IV

CLADDING AND STRUCTURAL MATERIALS

Corrosion

Zirconium Corrosion

The hydriding of zirconium and its alloys during exposure to water and steam, under conditions simulating those anticipated in reactor service, continues to receive major attention.

At Hanford,[1,2] hydriding of Zircaloy-2 has been studied in simulated New Production Reactor (NPR) atmospheres and in 400°C, 1500-psi steam. Samples of Zircaloy-2, exposed 102 days at 300 and 350°C in helium gas containing 0.01 per cent H_2 and 0.01 per cent CO, do not indicate significant hydrogen pickup. However, the hydrogen levels obtained at 102 days tend to be higher, in general, than those obtained at 43 days. This suggests a slow hydriding reaction.

The data obtained by Hanford for Zircaloy-2 exposed to 400°C, 1500-psi steam show a somewhat lower hydrogen pickup than those previously reported by Bettis, Battelle, and other laboratories. Corrosion rates, on the other hand, are comparable. The reasons for these differences appear to be related to the test methods employed. For example, at Hanford the autoclaves are operated under refreshed conditions, whereas they are static at other sites. When Hanford operated autoclaves under static conditions, hydrogen-absorption values more nearly approached those reported by Bettis and others. The lower hydrogen-absorption values observed in the Hanford refreshed autoclaves may be due either to a higher oxygen concentration in the steam (3 ppm) or to the absence of hydrogen buildup. Recent information seems to favor the oxygen inhibiting effect.

The oxidation kinetics of zirconium-base materials is being studied at Harwell.[3] In addition to the normal two corrosion stages (an induction period during which oxidation follows a cubic rate law, followed by a second period with a linear rate law), the data show a second corrosion-rate discontinuity in some specimens exposed to 500°C steam. It is interesting to note that the second corrosion-rate transition appears to occur only for those alloys evincing severe hydrogen absorption. This observation, together with the fact that oxygen diffusion is probably too slow to account for the change in kinetics at the time it is found, suggests that it is associated with hydrogen accumulation in the metal.

A program to study the effects of alloying elements and oxidizing environments on the oxidation rates and mechanisms for zirconium alloys is being initiated at the Oak Ridge National Laboratory (ORNL).[4] The first studies will be limited to oxidation in pure oxygen and water. Later, studies will involve uranyl sulfate solutions, steam, and CO_2. The techniques to be used include high-pressure oxidation-rate measurements over a range of temperatures and pressures, coupled with electron microscopy and X-ray diffraction studies of thin films on single crystals.

Zirconium specimens have been prepared at Bettis[5] using powder-metallurgy techniques. After exposure of only one and three days in 750°F steam and 680°F water, respectively, the samples exhibited heavy white corrosion products and high weight gains. The poor corrosion resistance of these materials is believed to be associated with network porosity and the high chlorine content of the zirconium powders.

(W. K. Boyd)

Aluminum Corrosion

A ceramic-fueled plate clad with an aluminum-nickel alloy (M-388) has been examined at Argonne[6] after exposure in the MTR. Irradiation was at 600 psig and 465°F, with local boiling occurring in the area of highest neutron flux. The corrosion rate, based on 122 days of exposure, was approximately 10 mils/year. This is higher by a factor of almost 2 than that obtained in out-of-pile investigations. The high corrosion rate is believed to result, at least in part, from the unfavorable aluminum-surface-area to water-volume ratio in the in-pile studies. Results from out-of-pile studies indicate that, with the aluminum-surface-area to water-volume ratio anticipated in a reactor using this type of fuel element, corrosion rates of the aluminum-nickel alloy would be considerably below the 10 mil/year rate.

In other studies,[7] high corrosion rates were observed for an aluminum-nickel-clad, aluminum-uranium-cored fuel element exposed at 420°F in the MTR loop. The high rates, in this case, were also attributed to an unfavorable aluminum-surface-area to water-volume ratio.

The corrosion behavior of powder-product dispersed-phase (Al_2O_3, $AlPO_4$, SiO_2, B_4C, or SiC) aluminum alloys was studied by Armour for Argonne.[8] The results to date indicate that corrosion-resistant aluminum alloys with superior tensile strengths can be obtained by powder-metallurgy techniques. In 350°C water, these materials exhibit corrosion rates that approach those observed for the wrought dispersion-free alloy. (W. K. Boyd)

Corrosion of Stainless Steels

The oxidation behavior of type 304 stainless steel in argon carrier gas containing CO and/or CO_2 is being studied at ORNL[9] over the temperature range of 1400 to 1800°F. It was determined that both CO and CO_2 oxidize type 304 stainless steels. In addition, CO was found to be carburizing, whereas CO_2 was either neutral or decarburizing, depending on the temperature. The data also indicate that carburization is governed by the $CO:CO_2$ ratio and is therefore controllable.

Both Fe_2O_4 and Cr_2O_3 have been identified in the corrosion film, Cr_2O_3 occurring at the oxide-metal interface, whereas Fe_3O_4 was found at the gas interface. The formation of Fe_3O_4 is unexpected under the test conditions. (W. K. Boyd)

Corrosion of Base-Metal Alloys (Iron, Nickel, Cobalt, and Copper)

Aqueous Corrosion. The good resistance of Inconel to stress-corrosion cracking in hot water containing 1000 ppm chloride was demonstrated in statistically designed autoclave tests at Martin Nuclear[10] as qualification for heat-exchanger structural material. Alloy steels (Croloys) exhibited comparatively poor corrosion resistance. The results of a two-month exposure to 680°F, 3200-psi deionized water on various metals have been released by Hanford,[11] and the materials are categorized in two broad groups as shown below:

Corrosion rate	
5–10 mg/dm^2	10–25 mg/dm^2
406	302
406 (mod.)	410
430	Alfenol
Ferral (mod.)	Ferral
Fe–24 Cr–6 Al	Hastelloys
	Inconels

Testing of Inconel in ammoniated hot (600°F) water at Babcock and Wilcox[12] yielded results similar to the above—a relatively great amount (~30 mg/dm^2) of corrosion was observed during the first exposure cycle (1000 hr), with essentially no additional corrosion upon longer exposure (to 4000 hr). Knolls workers have demonstrated that the corrosion rate of Inconel may be reduced to 1.6 ± 0.8 mg/(dm^2)(month) with 99 per cent confidence by environmental alteration (600°F, deionized, deoxygenated, lithiated water with *p*H 9.5 to 10.5).[13] A potential problem in lithiated hot water is caustic cracking. This is currently under investigation at Knolls. Chromium plating of Inconel for improved abrasion resistance also resulted in good corrosion resistance, even under spasmodic low-*p*H aerated conditions designed to simulate air-insurgence incidents.

The corrosion resistance of three candidate Inconel-brazing alloys for use in pressurized-water reactor systems was investigated.[13] Two of these, nickel-chromium-boron and gold-nickel, may only be considered for noncore applications because of transmutation and decay characteristics; but the third, manganese-nickel, should be amenable to in-core application as well. These alloys were screened in the

standard pressurized-water reactor corrosion test (2000 hr in 600°F, deionized, deoxygenated, lithiated water), in aerated high-*p*H water, and in a conventional salt-spray test. In general, the manganese-nickel alloy exhibited relatively poor corrosion properties and cannot be recommended for use. Either of the noncore brazing alloys is suitable from the standpoint of corrosion resistance, but the gold-nickel alloy is somewhat preferred because of easier brazing and greater joint strength.

Control-rod-drive thrust-bearing materials are being screened for corrosion resistance (600°F reference water) at Knolls.[13] After the 1000-hr exposure, rates for the various materials are as listed below:

Level of corrosion after 1000 hr (600°F water)	
<20 mg/dm^2	$\gg 20$ mg/dm^2
Stellites 6, 6B, 6K, 3, 19	Colmonoy 5, 6
Haynes 25, 90, 8589	FS 26
S Monel	Haynes 40, 41
Timken 16-15-6	Kennametal 3047
Kennametal K163B1	

In tests at Bettis,[12] silicon brass was indicated to be superior to aluminum or manganese bronzes in 300 to 500°F water for service as yoke-sleeve material for small valves in pressurized-water reactor coolant systems. The latter materials showed excessive pitting when in contact with Haynes 25 (stem material). Tests are continuing.

The economic desirability of substitution of carbon steel for stainless steel in certain reactor applications prompted a survey of the potential for mild steel in the Hanford NPR cooling system.[14] The principal problem appears to be to develop primary system decontamination procedures compatible with, and effective on, both carbon steel and the more noble components necessary to the structure. For example, decontamination procedures that are satisfactory for carbon steel are too mild for stainless-steel components, and procedures that are satisfactory for stainless steel are too corrosive for carbon steel.

Gaseous Corrosion. Tests to define corrosion rates of two candidate structural materials for gas-cooled reactor systems, Hastelloy X and Inconel, in both air and 99.5 per cent nitrogen–0.5 per cent oxygen at 1750°F and 300 psi were extended to 5000 hr at Aerojet-General.[15] The results of this work are presented in Table IV-1.

Table IV-1 ATTACK OF NICKEL ALLOYS BY 1750°F GASES

Time, hr	Atmosphere	Hastelloy X		Inconel	
		Penetration, mils	Weight change, mg/cm^2	Penetration, mils	Weight change, mg/cm^2
1000	Nitrogen	1	0.7		
2500	Nitrogen	1.2	1.2	1.7	1.6
5000	Nitrogen	1.5	1.2		1.8
1000	Air	2	0.5	0.9	8.6
2500	Air	2.7		2.3	
5000	Air		−0.2	2.0	−0.5

Low-pressure thermal convection loop tests at 1100°F in 99+ per cent helium with controlled levels of CO_2, CO, O_2, CH_4, H_2O, and H_2 were conducted on Croloy-3M, Croloy-2¼, and T-1 steel at ORNL.[9] In 1000-hr exposures, these steels lost about one-third as much metal in the controlled atmosphere as would be expected in a 1000-hr air exposure. Metal losses were between 5 and 20 mg/cm^2 for all materials. At higher temperatures (1350°F and higher), an atmosphere of helium +0.02 atm ($P_{CO} + 2P_{CO_2}$) showed tendencies toward carburization on several iron- and nickel-base alloys.[16] General Atomic workers concluded from their observations that extreme caution must be exercised when considering the use of materials with recognized carburization potentials in atmospheres containing measurable quantities of CO at elevated temperatures.

Nickel and Monel were the principal metals considered for potential use in a homogeneous UF_6 reactor.[17] Corrosion tests of UF_6 in 1 atm of fluorine or 12 cm mercury supported the use of nickel in such an application at temperatures to 1500°F. Monel was generally unsatisfactory. Alpha alumina, included in this study, was also unsatisfactory. (E. S. Bartlett)

Attack of Niobium and Its Alloys

A significant amount of information concerning the oxidation behavior of refractory metals in general and of niobium in particular was generated at the recent Conference on Niobium, Tantalum, Molybdenum, and Tungsten held in Sheffield, England. Progress has also been made

in the development of protective coatings for niobium.

Kubaschewski and Hopkins[18] discussed the general oxidation behavior of the four refractory metals at the Sheffield conference. Niobium forms an adherent amorphous Nb_2O_5 scale at low temperatures, following first the inverse logarithmic rate law and then the parabolic rate law as the temperature is raised. Between 500 and 700°C, niobium shows a transition from parabolic to linear behavior as the oxide scale thickens and cracks. The minor structural changes in Nb_2O_5 as it transforms through its various allotropic modifications are considered not particularly significant in interpreting the oxidation behavior of niobium.

Other important English papers presented at the Sheffield conference dealt with the oxidation of niobium alloys containing chromium,[19] titanium,[20-22] molybdenum,[20] and tungsten.[21,22] Niobium-chromium alloys containing chromium in the 35 at.% range are severely attacked by nitrogen at 1100°C. These alloys oxidize more rapidly in air than in pure oxygen due to the catalytic action of nitrogen.[19] Titanium and molybdenum binary additions improve the oxidation resistance of niobium by about three orders of magnitude at 700°C and one order of magnitude at 1000°C,[20] in agreement with previous observations.[23] Niobium-titanium-tungsten-base alloys containing quaternary additions of nickel or iron were shown to have exceptional oxidation resistance at 1000 to 1200°C. A niobium–20 at.% titanium–10 at.% tungsten–4 at.% nickel alloy shows a 100-fold improvement in oxidation resistance over unalloyed niobium at 1100°C,[21] whereas niobium–17.5 at.% titanium–17.5 at.% tungsten–5 at.% iron shows a 50-fold improvement at 1200°C.[22] These alloys are slightly more oxidation resistant than the General Electric F-48 and F-50 niobium-base alloys, but they would require protective coatings for prolonged exposure at elevated temperatures.

Recent Norwegian work[24] has confirmed that vanadium, tungsten, and molybdenum ternary additions improve the oxidation resistance of a niobium-titanium base. The effects of the ternary additions vary with temperature over the range of 600 to 1200°C.

Alloys recently developed at Union Carbide[25] show good oxidation resistance at 2200°F (1200°C), the rates being comparable to those for the niobium-titanium-tungsten-base alloys described above. Two of these alloys, niobium–28 wt.% tungsten–7 wt.% titanium (Cb 7) and niobium–20 wt.% tungsten–10 wt.% titanium–3 wt.% vanadium (Cb 16), oxidize only slightly faster than type 316 stainless steel at 2200°F (1200°C). A third alloy, niobium–3 wt.% aluminum–3 wt.% vanadium (Cb 22), also appears attractive on the basis of lower temperature liquid-metal corrosion resistance.

The development of a protective coating for niobium has been described by Thompson Ramo Wooldridge, Inc.[26] This coating consists of chromium-titanium-silicon applied to niobium by vacuum evaporation in the temperature range of 2000 to 2400°F (1090 to 1320°C). Preliminary cyclic oxidation tests have shown that this coating protects niobium from oxidation for 100 hr at 2300°F (1260°C) and for 10 to 20 hr at 2500°F (1370°C).

Studies on the reaction of niobium with CO and CO_2 are continuing at General Atomic.[16] At 1000°F (540°C), niobium and alloys with titanium and zirconium form a thin protective carbide case in CO and suffer no loss of ductility. However, at 1700°F (930°C), severe carburization and oxidation are encountered in 0.02 atm of CO plus CO_2. (W. D. Klopp)

Tantalum Oxidation

Recent data from Battelle[27] indicate significant progress in the development of alloys with oxidation resistance in the temperature range of 1200 to 1400°C. Additions of aluminum, chromium, aluminum-chromium, and aluminum-silicon improved the oxidation resistance of a tantalum-titanium base by a factor of 10 at 1400°C. These alloys oxidize two to three times faster than commercial heater alloys, such as Fecral.

High-temperature protective coatings for tantalum are being evaluated at Sylvania-Corning.[28] Sylcor has demonstrated that both aluminide and beryllide coatings can protect tantalum for at least 10 hr at 2500°F (1370°C) in isothermal and cyclic exposures. (W. D. Klopp)

Corrosion of Miscellaneous Metals

Investigations at the University of California Lawrence Radiation Laboratory on the oxidation of chromium showed parabolic behavior from 1832 to 2372°F, with an associated activation energy of 36.0 kcal/mole. Yttrium at 2192°F

oxidizes linearly, with 30 mils of metal loss resulting from a 2-hr exposure.

In an Argonne study,[29] the high hot-water corrosion rate of magnesium alloy AZ31 (Mg–3 Al–1 Zn–2 Mn), 3 mils/day at 300°F, was found to be reduced to about 0.1 mil/day in 300°F water containing from 1 to 10 ppm fluoride ion (*p*H 6 to 7). (E. S. Bartlett)

Corrosion by Liquid Metals, Fused Salts, and Organics

Los Alamos Molten Plutonium Reactor Experiment No. 1 (LAMPRE-1), under development at Los Alamos Scientific Laboratory, proposes the use of a molten plutonium-iron fuel alloy contained in a tantalum vessel cooled by flowing sodium. A major problem in this development has been the unpredictable resistance of tantalum to intergranular corrosion by the molten fuel in the 600 to 800°C range. Improvements in the purity of tantalum, although beneficial in reducing corrosion, have not completely solved the problem. A recent report[30] from Los Alamos presents preliminary data relative to suppressing corrosion through additives in the fuel mixture. Additions of carbon have yielded encouraging results; for example, fuel mixtures in which cast iron is the alloying agent are found to be significantly less corrosive than mixtures based on pure iron. There are also prospects for the use of ternary fuel systems which have reduced corrosivity. Preliminary corrosion experiments with a plutonium-cerium-cobalt alloy have demonstrated a distinct trend in this regard.

Two recent reports[31,32] issued by Atomics International present a variety of information relative to various sodium and corrosion problems. The first report[31] deals solely with carbon transfer in sodium–type 304 stainless-steel systems and presents carbon equilibrium data, with temperature and carbon contents of the steel and the sodium as parameters. For example, in the 1000 to 1600°F range, the equilibrium carbon content of the steel in carbon-saturated sodium ranges from about 2.7 per cent to about 4.3 per cent. It is suggested that the equilibrium relations established, plus the sensitivity of hardness of the steel to carbon content, present a technique for measuring indirectly the carbon content of sodium baths through observations of the hardnesses of sodium-exposed steel samples.

The second report[32] presents summaries of investigations conducted during the fiscal year 1960. General results of some of the corrosion studies are as follows:

1. Modifications to a basic 2¼ wt.% chromium–molybdenum ferritic steel are being investigated to improve the material for service in long-life sodium coolant systems operating at 1050°F peak temperature. During the year, 11 steels modified by additions of titanium, niobium, and vanadium were evaluated for mechanical strength and for corrosion resistance in 1200°F low-oxygen flowing sodium for periods up to 2000 hr. In nearly all cases the alloys exhibited a definite superiority over the base material in both instances.

2. Oxidation rates were determined for zirconium and zirconium alloys (containing minor additions of agents such as aluminum, tin, and molybdenum) in sodium at 630°C (cold-trap temperature of 172°C). The experiments constitute a part of a basic program to pinpoint the chemistry of zirconium attack by sodium. The rate data obtained fit the relation $\Delta W = kt^n$ (ΔW = change in weight, t = time, and k and n = constants), where n ranged from 0.37 to 0.44

Table IV-2 AVERAGE WEIGHT CHANGES, OMRE IN-PILE CORROSION COUPONS[32]

Material	Average weight change, mg/cm²	
	Dummy element No. 2*†	Dummy element No. 1*‡§
Type 1018 carbon steel	−1.76(4)	NT
Type 4130 alloy steel	−1.48(6)	−0.53
Type 410 S.S., 12 Cr	+0.18(6)	+0.85
Type 304 S.S., annealed	+0.22(6)	+0.01
Type 304 S.S., sensitized	+0.22(6)	+0.01
1100 aluminum	+0.31(5)	−0.34
Magnesium	−24.0(6)	−17.80
Magnesium, light anodized	All specimens corroded away (3)	NT
Magnesium, heavy anodized	All specimens corroded away (3)	NT

*Both dummy elements were inserted in the core at the start of operation of the OMRE. Dummy element No. 1 was removed after eight months in-pile, and element No. 2 was removed after 28 months in-pile.

†Parenthetical figures indicate number of coupons.

‡NT = not tested. Bulk coolant temperature, nominally 600°F.

§Only one coupon of each material in dummy element No. 1.

mg/(cm^2)(hr) and k ranged from 0.029 to 0.060 mg/(cm^2)(hr). For comparison, previously established constants for exposure of zirconium in oxygen at 600°C are $k = 0.37$ and $n = 0.34$.

3. Weight-change data were obtained for corrosion specimens exposed in the Organic-Moderated Reactor Experiment (OMRE) to a polyphenyl moderator coolant for a period of 28 months. Table IV-2 presents these data, in addition to corresponding data for specimens previously exposed for eight months. A comparison indicates that the longer exposure was not particularly significant from the corrosion viewpoint.

Molten-fluoride-salt forced-convection-loop experiments are being performed at Oak Ridge[4] in the Molten Salt Reactor Program (MSRP). Table IV-3 summarizes data now available for long-time exposures of Inconel and INOR-8, the materials of prime interest. As past experiments in this research have indicated, both materials exhibit outstanding resistance to corrosion, with INOR-8 definitely having the edge. The modest attack apparent in Loop 9354-1 is attributed to minor system impurities.

Brazing materials for INOR-8 and Inconel are also being investigated extensively at Oak Ridge. Long-term thermal-convection-loop experiments with a 62 mole % LiF–37 mole % BeF_2–1 mole % UF_4 mixture circulating at a peak temperature of 1300°F produced no attack on the following brazes with INOR-8 as the base material: Coast Metals 82 and 53, General Electric 81, 82 Au–18 Ni, and copper. With Inconel as the base material, best results were observed for the latter two brazes.

In view of the advantage gained in MSRP if unclad graphite can be used as the moderator, Oak Ridge is studying the permeation of graphite by fluoride-salt mixtures.[4] Several graphites have exhibited permeabilities (under 150 psi, the screening-test pressure) lower than 0.5 per cent, the reference specification for laboratory tests. The effects of irradiation on this permeation characteristic are being investigated in capsule experiments at MTR. The capsules involved are in the hot-cell stage; preliminary results[33] indicate that several of the graphite pieces failed, presumably from undesirable thermal-cycling effects during the exposure. However, one intact sample exhibits a

Table IV-3 OPERATING CONDITIONS AND RESULTS OF MSRP FORCED-CONVECTION TESTS[4]

Loop	Salt No.*	Maximum salt-metal interface temp., °F	ΔT, °F	Time operated, hr	Reynolds No.	Flow rate, gal/min	Metallographic results
				Inconel			
9344-2	12	1200	100	8,735	8200	2.5	Moderate intergranular voids ranging from 2 to 3 mils in first heater leg and 4 to 8 mils in the second heater leg
9377-3	131	1300	200	8,746	3400	2	Moderate intergranular voids ranging from 2 to 8 mils in first heater leg and 6 to 14 mils in the second heater leg
9377-4	130	1300	200	9,574	2600	1.8	Heavy intergranular voids ranging from ½ to 11 mils in first heater leg and 7 to 15 mils in the second heater leg
				INOR-8			
9354-1	126	1300	200	14,563	2000	1.8	Heavy surface roughening and pitting to maximum depth of 1½ mils along both heater legs
9354-4	130	1300	200	15,150	3000	2.5	No attack
MSRP-8	124	1300	200	9,633	4000	2	No attack
MSRP-9	134	1300	200	9,687	2300	1.8	No attack

*Salt compositions: No. 12, NaF-LiF-KF (11.5-46.5-42 mole %); No. 124, NaF-LiF-ThF_4 (58-35-7 mole %); No. 126, LiF-BeF_2-UF_4 (53-46-1 mole %); No. 130, LiF-BeF_2-UF_4 (62-37-1 mole %); No. 131, LiF-BeF_2-UF_4 (60-36-4 mole %); No. 134, LiF-BeF_2-UF_4-ThF_4 (62-36.5-0.5-1 mole %).

permeation about the same as that found in the laboratory.

An article appearing in the August 1960 issue of *Nuclear Science and Engineering*[34] presents several aspects of the molten uranium-bismuth corrosion picture as established by research at Brookhaven National Laboratory. The inhibiting effect of zirconium and magnesium on corrosion of steels by this liquid is reviewed, as well as some of the basic chemistry associated with the underlying factors responsible for the inhibition effect. Other parameters that enter the corrosion picture are discussed, including temperature levels, the carbon content of the steel, and carbon and chromium segregation in welds. (J. H. Stang)

Selected Mechanical Properties of Cladding and Structural Materials

Zirconium Alloys

The need for higher operating temperatures of water-cooled reactors has fostered the use of zirconium alloys, chiefly Zircaloy-2 because of its strength and corrosion resistance in water or steam at elevated temperatures. The deletion of nickel from Zircaloy-2 has minimized the formation of zirconium hydride during exposure to high-temperature water or steam. Since the discovery of this improved material, called Zircaloy-4, much time has been devoted to comparing its properties with those of Zircaloy-2. For example, the Canadians[35] have made such comparisons in an evaluation of the design stresses for CANDU pressure tubes. The tensile, creep, and impact properties are compared at room and elevated temperatures. Only slight differences between Zircaloy-2 and Zircaloy-4 were found in these properties. Additions of 35 to 560 ppm silicon to Zircaloy-4 made by Westinghouse[36] have been found to have a significant effect on the room temperature and 600°F tensile properties. Zircaloy-2 has been further examined by Hanford[37] by determining the tensile strengths of samples cut from KER and Plutonium Recycle Test Reactor (PRTR) type Zircaloy-2 tubes. These samples and some rolled-sheet samples were tested at 572°F to compare the strengths of 40 per cent worked material as functions of specimen selection and fabrication. Longitudinal tensile samples were prepared from both the sheet and tube whose tensile strengths were compared with the hoop stress of a tubular specimen.

Development of other zirconium-base alloys to meet the demands of higher operating temperatures for reactors and for greater reactor efficiency has resulted in several promising new alloys. A description[38] of the characteristics of one of these, a zirconium-copper-molybdenum

Table IV-4 TENSILE PROPERTIES OF ZIRCONIUM–1.25 WT.% ALUMINUM–1.0 WT.% TIN–1 WT.% MOLYBDENUM ALLOY[32]

Temp., °F	Ultimate tensile strength, psi	Yield strength (0.2% offset), psi	Elongation in 2 in., %	Reduction of area, %
Vacuum Anneal at 1450°F for 1 Hr				
72	103,000	98,000	5	4.4
1050	59,000	37,500	27	66.5
1200	49,000	34,000		74
Strip (Average of Two Specimens Annealed at 1450°F for 1 Hr)				
72	112,000	84,800	13	
300	96,000	70,500	16	
500	86,000	60,500	15	
700	80,000	56,800	13	
900	73,000	51,500	17.5	
1050	58,000	40,800	31	
1200	39,000	23,000	47	
1350	20,000	4,200	89	

Table IV-5 EFFECT OF COLD WORK AND ANNEALING ON THE ROOM-TEMPERATURE PROPERTIES OF ZIRCONIUM–1.25 WT.% ALUMINUM–1.0 WT.% TIN–1 WT.% MOLYBDENUM ALLOY*[32]

Condition	Ultimate tensile strength, psi	Yield strength (0.2% offset), psi	Elongation, %	Hardness, R_C
As-received vacuum annealed	112,000	84,800	13	23.5
30 per cent cold worked	138,000	117,600	6.5	26.5
30 per cent cold worked, annealed	115,000	84,800	15	23
50 per cent cold worked	148,000	127,600	6.5	27.5
50 per cent cold worked, annealed	111,000	86,000	16	27.5

*Heat-treatment: 1450°F for 2 hr, furnace cooled.

alloy developed in England, shows that it has better corrosion resistance than the Zircaloys, 15 per cent higher tensile strength than Zircaloy-2, and greater creep strength at 600°F. Work at Atomics International[32] includes modification of a zirconium–1.5 wt.% aluminum–1.5 wt.% tin–1.5 wt.% molybdenum alloy to a zirconium–1.25 wt.% aluminum–1.0 wt.% tin–1 wt.% molybdenum alloy. The change in composition was made to aid fabricability. The tensile properties of this alloy at room and elevated temperatures are shown in Tables IV-4 and IV-5.

(F. R. Shober)

Stainless Steel

ORNL[9] has investigated the effects of environment and manufacturing variables on the mechanical properties of AISI type 304 stainless steel at 1500°F. ORNL has found that the rupture times for comparable stressed tubes of type 304 stainless steel vary as much as a factor of 3, depending upon the supplier. The effect of test atmospheres of air, argon, and carbon monoxide on the rupture properties of type 304 stainless steel is shown in Table IV-6.

Table IV-6 RUPTURE PROPERTIES OF AISI TYPE 304 STAINLESS STEEL IN AIR, ARGON, AND CARBON MONOXIDE[9]

Specimen treatment prior to testing	Test environment	Test temp., °F	Tangential stress, psi	Time to rupture, hr
As received	Air	1500	1600	9146
	Argon	1500	6500	197
	Argon	1500	5000	795
	Argon	1500	4300	1057
	Argon	1500	3800	1443
Annealed at 2150°F for 2 hr	Argon	1500	3500	387
	Argon	1500	4000	176
Annealed at 1950°F for ½ hr	CO	1500	5500	615
	CO	1500	5500	505
Annealed at 2150°F for 2 hr	CO	1600	4000	28
	Argon	1600	3000	70

Workers at Atomics International[39] have found that ferritic chromium-molybdenum steels offer certain advantages over austenitic stainless steels in cost, higher thermal conductivity, lower coefficient of expansion, and better resistance to stress corrosion in hot water and steam.

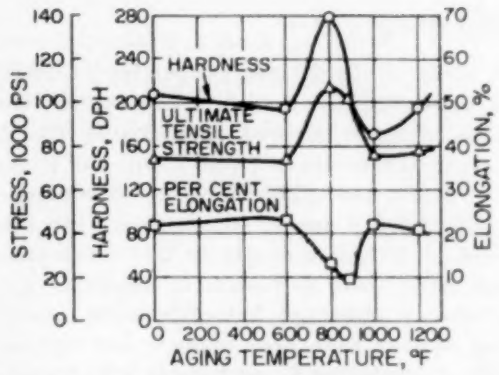

Figure 19—Ultimate tensile strength, hardness, and per cent elongation versus aging temperature for type 430T stainless steel.[16]

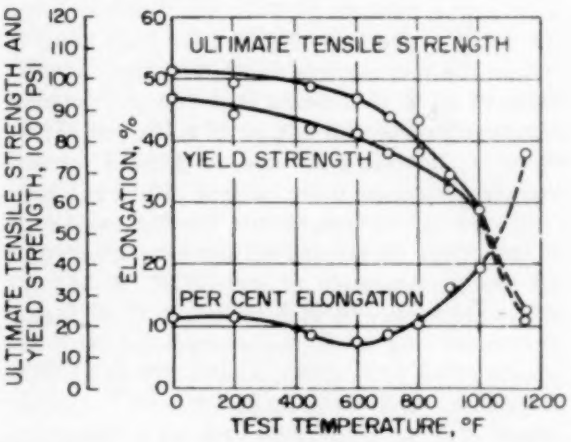

Figure 20—Ultimate tensile strength, yield strength, and per cent elongation versus temperature for type 430T stainless steel annealed for 1000 hr at 885°F.[16]

A conventional iron–2.25 wt.% chromium–1 wt.% molybdenum alloy with experimental additions of 0.4 wt.% niobium and 0.4 wt.% titanium showed that short-time tensile, stress-rupture, and creep properties at 1100°F were comparable to those of type 304 stainless steel. Impact resistance, as measured by the Charpy V-notch test, is good above the transition temperature of 150°F but poor below it.

General Atomic[16] has considered type 430T stainless steel as a potential cladding for graphite. It has a low coefficient of expansion and a resistance to carburization up to 1500°F. However, it exhibits a tendency to embrittle at 885°F after 1000-hr aging treatments. This embrittling effect is shown by the room-temperature tensile properties in Fig. 19. The elevated-temperature properties of this alloy after aging 1000 hr at 885°F are shown in Fig. 20.

(F. R. Shober)

Nickel Alloys

A study of the fatigue properties of Inconel was conducted by Knolls.[40] The cyclic strain fatigue strength showed an increase with increasing temperature from 75 to 400°F, with the greater percentage increase occurring in the 200 to 400°F range. The tendency for an increase in fatigue strength in this temperature range appeared to be related to the strain-aging phenomenon observed in tensile tests. Limited creep studies have been made at Aerojet-General[15] on Hastelloy X and Inconel 702 at 1750°F and 1000 psi. The secondary creep rate of Inconel 702 was found to be about five times that of Hastelloy X. Extended exposures of Hastelloy X to a gas mixture of 95.5 vol.% nitrogen and 0.5 vol.% oxygen at 1750°F have been found to reduce the room-temperature ductility. Aerojet workers have also found that 300-psi external pressure exerted for 500 hr is sufficient to collapse a Hastelloy-X tube at 1750°F around loosely packed enclosed pellets. Work has been continued at General Atomic[16] on the evaluation of the effect of air and helium atmospheres on the creep properties of Inco-713C, W-545 (14 wt.% chromium–26 wt.% nickel–1.75 wt.% molybdenum–1.85 wt.% manganese–3.3 wt.% titanium–51.5 wt.% iron), and D-979 (14.5 wt.% chromium–42.5 wt.% nickel–3.7 wt.% molybdenum–3.5 wt.% tungsten–2.9 wt.% titanium–1.0 wt.% aluminum–31.9 wt.% iron) at 1200°F.

Fatigue studies conducted at Battelle for Oak Ridge[41] have been correlated with results from tests at Oak Ridge. These data are shown in Fig. 21. Additional creep-rupture data, shown in Table IV-7, were obtained by General Electric[42] for Inconel X at 1625, 1675, and 1725°F.

(F. R. Shober)

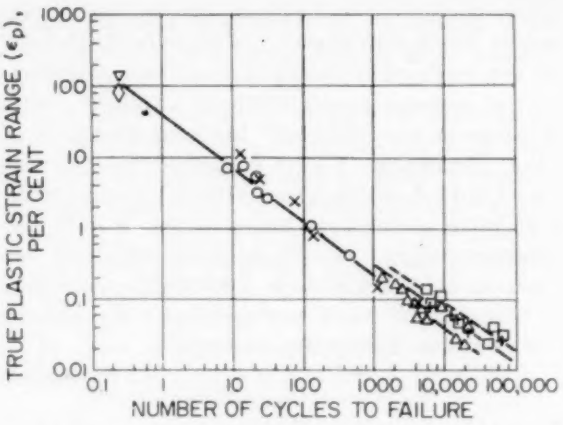

Figure 21—Strain-fatigue properties of Inconel rods at 1300 and 1500°F.[41] ○, 1500°F, 70 cycles per hour, cyclic creep; △, 1500°F, 360 cycles per hour, conventional fatigue; □, 1500°F, 3600 cycles per hour, conventional fatigue; ×, 1300°F, 70 cycles per hour, cyclic creep; +, 1300°F, 3600 cycles per hour, conventional fatigue; ▽, 1500°F, tensile ductility; ◇, 1300°F, tensile ductility.

Table IV-7 HOURS TO RUPTURE OF INCONEL X UNDER CONDITIONS SHOWN[42]

		Hours to rupture at indicated stress, psi					
		3000		6000		9000	
Temp., °F	Heat	Sample 1	Sample 2	Sample 1	Sample 2	Sample 1	Sample 2
1625	1	X*	X§			308.0	339.6
	2	X†	X¶			23.2	225.2
	3	O‡	X**			41.1	15.3
1675	1			265.5	214.8		
	2			217.8	195.2		
	3			25.5	25.9		
1725	1	871.8	532.7			2.8	2.2
	2	587.3	601.7			6.3	2.5
	3	378.8	364.0			1.8	2.7

[Note: X indicates test in progress; O indicates test terminated prior to rupture.]

*After 1414 hr, elongation is 0.089 per cent.

†After 396 hr, elongation is 0.132 per cent.

‡After 2527 hr, elongation was 0.787 per cent when furnace overshot and terminated this test.

§After 3652 hr, elongation is 0.615 per cent.

¶After 475 hr, elongation is 0.188 per cent.

**After 1294 hr, elongation is 0.337 per cent.

Niobium Alloys

Niobium-alloy development being conducted at Westinghouse Research[43] has been concerned with the effects of additions of chromium, zirconium, tungsten, and molybdenum on the mechanical properties of the resulting alloys at room temperature, 2000, 2200, and 2400°F. The results of tensile tests at these temperatures are shown in Table IV-8.

An investigation of the effects of oxygen, nitrogen, and hydrogen on the room-temperature bend ductility of niobium has been concluded by workers at Oak Ridge.[9] In summary, it appears that 3000 ppm oxygen, 1200 ppm nitrogen, and 1500 ppm hydrogen, respectively, will produce brittle fracture upon bending. (F. R. Shober)

Miscellaneous Metals and Alloys

Perlmutter has reviewed[44] the mechanical properties of current refractory alloys. On the

Table IV-8 TENSILE PROPERTIES OF NIOBIUM ALLOYS AT ROOM AND ELEVATED TEMPERATURES[43]

(Fully Recrystallized Hot-Rolled 0.050-In. Sheet)

Alloy composition (balance Nb), wt.%	Test temp.,* °F	Yield strength (0.2% offset), psi	Ultimate tensile strength, psi	Elongation, %		Reduction of area, %
				Uniform	Total	
1.57 Cr†	RT	50,100	76,100	23.9	34.1	73.6
	2000	24,500	25,940	0.5	37.9	100
	2200	15,000	16,000	8.2	55.4	100
1.88 Al†	RT	67,500	75,700		2.5	6.6
	2000	17,600	19,200	3.3	44.1	100
	2200	11,400	12,000	2.4	77.2	100
10 Zr	2000	36,800	44,000	3.6	29	38.3
20 Zr	2000	48,000	53,000	1.8	19.9	22.2
20 Mo	2000	36,800	43,700	1.7	5.9	53.6
19.9W	2000	26,500	34,800	4.6	17.7	100
5 V–7.5 W	RT	89,500	125,800	0	21.5	17.1
	2000	41,000	43,000	0.7	30.7	57.9
5 V–5 W–1 Zr	RT	84,600	104,500	25.4	32.4	455
	2000	46,500	50,000	1.4	18.6	425
5 V–5 Zr	2000	45,600	49,600	1.8	5.6	28.1
10 Mo–10 Hf‡	RT	94,000	109,400	16.7	38.9	72
10 Mo–10 Hf§	2000	40,000	52,700	3.9	19.5	64.9
5 V–5 Mo–1 Zr‡	RT	83,000	101,300	19.8	34.9	70.4
5 V–5 Mo–1 Zr§	2000	42,400	47,400	3.0	41.8	51.1
5 V–5 Mo–1 Zr§	2200	34,200	35,440	1.7	35.1	86.2
5 V–5 Mo–1 Zr‡	2400	18,400	20,000	1.9	62.2	94.4

* RT = room temperature.
† These are actual analyses; all others are nominal compositions.
‡ Extruded, forged, and stress relieved.
§ Extruded and stress relieved.

basis of elevated-temperature strength, the order of superiority is tungsten, molybdenum, tantalum, and niobium-base alloys; however, on the basis of strength-weight ratio, the order is molybdenum, tungsten, niobium, and tantalum-base alloys.

Among the light-metal alloys, magnesium-base alloys are being used as canning material in the Calder Hall and Chapel Cross reactors. A study of the creep ductility and high-temperature fatigue behavior of Magnox A.12 has been made in Great Britain.[45,46] The fatigue strength reached its lowest value at 752 and 842°F. The creep properties of extruded magnesium-manganese and magnesium-zirconium-manganese alloys were investigated at 842 and 932°F. The best alloy in creep at 932°F was a magnesium–0.3 wt.% manganese–0.7 wt.% zirconium alloy. A powder-metallurgy technique was used at Argonne[8] to investigate the effect of a hard stable dispersant on the strength of a corrosion-resistant aluminum alloy. Tensile strengths of extruded rods formed by powder metallurgy were, in some instances, three times that of extruded dispersion-free powdered product. Corrosion resistance of such materials is equivalent to that of a wrought dispersion-free alloy.

(F. R. Shober)

Selected Metallurgical Aspects of Cladding and Structural Materials

Aluminum

A data manual[47] on aluminum has been published by the United Kingdom Atomic Energy Authority (UKAEA). The manual contains such data as mechanical and physical properties plus selected phase diagrams, all slanted toward nuclear applications.

Iron-Base Alloys

The Russians[48] report the following concerning the iron-chromium-titanium constitutional diagram. A eutectic crystallization was observed in the titanium-iron region at the titanium-iron-chromium cross section of the alloy. A wide range of alloys was distributed in the right side with higher chromium content. The solubility of titanium in alpha solid solution increases in the titanium-iron side at 1000°C and decreases at 550°C. Maximum hardness was found in the tempered chi-phase alloy.

Nickel-Base Alloys

The nickel-rich portions of the nickel-molybdenum-aluminum and the nickel-molybdenum-silicon systems were investigated by General Electric Research Laboratory.[49] A ternary alloy designated by ψ was found at 1175°C in the vicinity of 58 at.% nickel–7.5 at.% molybdenum–34.5 at.% aluminum; it was confirmed by the presence of a new set of X-ray diffraction lines. None of the binary compounds Ni_3Al, NiAl, or NiMo show appreciable solubility in this ternary section. In the nickel-molybdenum-silicon system, a ternary alloy was found at 1100°C at composition 50 at.% nickel–32 at.% molybdenum–18 at.% silicon.

Niobium-Base Alloys

Westinghouse[50] reports on recrystallization temperatures of additional niobium-base alloys. These are given in Table IV-9. At the same time the phases shown in Table IV-10 of the niobium-aluminum and niobium-hafnium system were identified.

German investigators[51] have examined a number of niobium-tantalum alloys covering the whole range of compositions. The hardness, strengths, specific electrical conductivity, electrochemical behavior, and corrosion resistances are reported. No maximum in the mechanical properties was noted.

A British study[52] indicates that two intermediate phases occur in the niobium-rhenium system, one with the sigma structure and the other with an alpha-manganese type. The sigma phase is formed peritectically at 57 at.% rhenium and exists over a small range of composition and temperature. The chi phase melts congruently at 2800°C and has a homogeneity range of 62 to 87 per cent rhenium, which falls only slightly with decreasing temperature. Niobium dissolves up to 56 at.% rhenium at the eutectic temperature, falling to 43 at.% at 1000°C. The solubility of niobium in solid rhenium is low.

The mechanism for gas carburization of metallic niobium developed by Lockheed Aircraft[53] is as follows: The gas carburization at the gas-solid interface proceeds through the formation of a chemical complex between the hydrocarbon gas and the surface. This action is followed by the stripping off of hydrogen to yield a chemically bound carbon atom that can then diffuse into the interior. This reactive diffusion of the carbon into the interior yields a hemicarbide

Table IV-9 RECRYSTALLIZATION-TEMPERATURE RANGE OF BINARY NIOBIUM ALLOYS[50]

Composition (balance Nb), wt.%	Recrystallization-temperature range,* °C	
	Beginning	Completion
Levitation Melted in Vacuum		
	850–900	~1100
0.25 W	<1000	~1200
0.5 W	<1000	~1200
1.0 W	~1000	~1200
2.0 W	~1000	~1200
5.0 W	~1000	1200–1300
0.25 Fe	~1000	~1200
0.50 Fe	<1000	~1200
0.25 Co	<1000	~1200
5.0 Re	~1000	~1300
Levitation Melted in Helium		
0.5 Ti	~1100	~1300
2.0 Ti	<1100	1200–1300
1.0 Zr	1100–1200	~1400
1.5 Zr	~1100	1400–1500
1 Hf	~1100	1400–1500

* 75 per cent reduction, 1-hr anneal.

Table IV-10 NIOBIUM ALLOY PHASE STUDY[50]

Composition (balance Nb), at.%	Phase present
6 Al	Nb primary solid solution
8 Al	Nb + Nb_3Al (β)
25 Al	Nb_3Al + trace of another phase (δ)
30 Al	Nb_3Al + δ
40 Al	Nb_3Al + increasing δ
50 Al	Nb_3Al (residual) + δ
40 Hf	Nb solid solution
50 Hf	Nb + hcp Hf phase
60 Hf	Nb + hcp Hf phase
70 Hf	Nb + hcp Hf phase

phase (Nb_2C) which enters the core by intergranular penetration. A monocarbide phase (NbC) follows, and it penetrates the hemicarbide phase along a sharp boundary. The penetrations by the hemicarbide and monocarbide phases proceed simultaneously. The monocarbide phase is extremely brittle, does not adhere well, and would probably not have many engineering applications in the state produced. The hemicarbide phase can be formed as an essentially pure adherent film on the metallic core; nothing is known about the engineering properties of this film.

Tantalum and Its Alloys

A thorough survey of the effect of gas in tantalum and niobium has been prepared by Nuclear Metals.[54] The information contained in the survey is divided into five categories: (1) structure and phase diagrams, (2) thermodynamic data, (3) disposition of gases in the metal and the effect of dissolved gases on physical properties, (4) gas removal by vacuum annealing, and (5) selected oxidation-reduction reactions.

Tentative phase diagrams for the systems tantalum-ruthenium, tantalum-osmium, tungsten-ruthenium, tantalum-rhenium, niobium-rhenium, molybdenum-hafnium, tungsten-osmium, and rhenium-hafnium and a 2500°C (2-hr anneal) isotherm of the tantalum-tungsten-ruthenium system have been presented by Nuclear Metals.[55] Work is continuing to complete these diagrams.

A book edited in England by Miller[56] is a compilation of available unclassified chemical and metallurgical information on both tantalum and niobium. The book contains extensive information on unalloyed tantalum and niobium, but it does not deal much with alloys since most of the alloying work is either of recent origin or classified.

Titanium Alloys

A report on the titanium-yttrium system by Bare and Carlson[57] shows two horizontals, one at 1330°C and the other at 1480°C. The 1330°C horizontal is the result of a eutectic reaction, the eutectic having a composition of 13 wt.% titanium. The 1480°C horizontal is postulated to be the result of a peritectic reaction at 0.2 wt.% titanium. Maximum terminal solubility at the titanium end of the system is placed between 0.6 and 1.3 wt.% yttrium; and, at the yttrium end, it is less than 1 wt.% titanium.

After a solution treatment at 600°C, titanium–10 wt.% vanadium–10 wt.% zirconium alloys exhibit a yield strength of 73,800 psi. This is increased to 142,900 psi by aging 4 hr at 450°C, as reported by the Bureau of Mines.[58]

Zirconium and Its Alloys

Hanford[2] found that abnormal grain growth occurred in 50 per cent cold-worked zirconium after a vacuum anneal for 1000 min at 800°C. During this type of growth, a few grains grew preferentially, consuming the grains of the surrounding matrix. Grains were 100 times larger in diameter than the original 0.01-mm grains. They were from 30 to 40 mils across. Annealing for the same period of time in helium resulted in only a slight indication of abnormal growth, and annealing in air under the same conditions effectively inhibited the abnormal growth.

A heat-treatable zirconium–2 wt.% niobium–2 wt.% tin alloy was studied by Hanford.[39] A Jominy type end-quench test resulted in a maximum hardness of Rockwell G94 near the quench end of the specimen, which was heated to 975°C prior to quenching. A hardness of Rockwell G91 was attained in specimens quenched from 950°C and Rockwell G85 in specimens quenched from 850°C. The heat treatability of this alloy is attributed to the formation of martensite upon quenching from temperatures greater than 950°C.

Research on hardened zirconium alloys containing 15 wt.% niobium and 10 wt.% molybdenum shows that the dependence of certain physical properties on temperature is not monotonic. The results obtained by the Russians[59] from the calculation of the activation energy for the formation of the omega phase show that omega-phase formation is a characteristic feature of beta-phase decay in zirconium alloys.

General

A recent literature survey made by Battelle[60] lists the potential of all refractory metals, emphasizing the stainless steels, nickel, chromium, and niobium-base alloys for reactor application in air at elevated temperature. This survey is a source of information on all the elevated-temperature properties, in addition to

a forecast of the potential usefulness of the above-mentioned materials.

(J. A. DeMastry)

Diffusion Studies

Self-diffusion in the beta phase (body-centered cubic) of pure zirconium is being studied at Chalk River.[61] Temperatures from 1200 to 1500°C for times ranging from 45 min to $2\frac{1}{2}$ hr have been utilized. A preliminary analysis of the results gives the diffusion coefficient as $D = 2 \times 10^{-4} \exp(-28{,}500/RT)$ cm²/sec. In order to extend the self-diffusion measurements to the alpha phase, efforts are being made to produce suitable alpha-zirconium single crystals. In another study,[62] the self-diffusion coefficient of niobium has been measured over the temperature range of 1585 to 2120°C, using the radioactive isotope Nb^{95} as the tracer. The data obtained for the temperature dependence of the self-diffusion coefficient are best fitted by the equation $D = (12.4 \pm 0.8) \exp[(-105{,}000 \pm 3000)/RT]$ cm²/sec.

In recent reports, information pertaining to diffusion and solubility of some gases and carbon in various metals has been presented. Diffusion data for oxygen, nitrogen, carbon, and hydrogen in niobium and tantalum are presented in a survey made for the Defense Metals Information Center by Battelle personnel.[63] Also reported in this survey are data on the solubility limits of carbon, nitrogen, oxygen, and hydrogen in tungsten, tantalum, molybdenum, niobium, vanadium, and chromium at 600 to 1200°C. Mathematical relations and expressions concerning the diffusion systems are discussed. In a study by Rudd et al.,[64] the flux of hydrogen gas through Hastelloy B has been determined as a function of membrane thickness, pressure differential, and temperature. The study was made at temperatures from 640 to 820°C, pressures of 1.1, 1.5, and 2 atm, and membrane thicknesses of 0.0950 and 0.1307 in. The experimental data were fitted (reference 64*a*) to the following equation:

$$J = \frac{1810 P^{1/2}}{X} \exp(-8422/T)$$

where J = flux, cm³ at STP/(cm²)(hr)
P = pressure, atm
X = membrane thickness, mm
T = temperature, °K

The temperature dependence was found to follow the Arrhenius relation, and a diffusion-controlled process is proposed for these conditions. However, some effect of membrane thickness was noted, and further study would be required to confirm the rate-controlling process under various conditions.

The permeability of cladding materials to inert gases is being studied by Materials Research Corp., and results are reported for the system aluminum-helium.[65] Neutron-irradiated aluminum released part of its helium during annealing at 595°C for 94 hr. It was found that the formation of bubbles also occurred, primarily at subgrain boundaries. In a French report,[66] an apparatus is described for measurement of diffusion of gaseous fission products, and of gases in general, across thin metallic walls at high temperatures.

The diffusion between uranium and various other metals has received its usual attention, and recent work is presented in a number of reports. Several studies concerning diffusion of uranium with some other metals have been discussed in French reports. The systems uranium-titanium, uranium-zirconium, and uranium-molybdenum were studied by means of electron-probe microanalysis.[67,68] Also, an investigation[69] of the diffusion of aluminum during the transformation of UAl_3 to UAl_4 has demonstrated that the kinetics of the transformation, which presumably takes place by the diffusion of aluminum through the UAl_4, is strongly influenced by the presence of elements such as silicon in relatively small quantities. In other French work, the diffusion of iron, nickel, chromium, and silicon in dilute solution in uranium was studied.[70] It is reported that comparison of the diffusion constants obtained with those determined in previous investigations showed that the diffusion constant decreases when the atomic radius of the solute increases. The effect of pressure on the intermetallic compound formed by diffusion between uranium and copper has been studied by Adda and coworkers in France.[71] Significant variations were demonstrated in the chemical composition and crystalline parameters of the intermetallic compound formed without external pressure. It was found that these variations were suppressed by the application of hydrostatic or uniaxial pressure greater than 500 kg/cm² during the diffusion treatment. A more comprehensive study in this field is discussed in the subsection on Diffusion Bonding,

Sec. V of this issue. In a study at MIT,[72] interdiffusion and intrinsic diffusion coefficients were determined for the uranium-niobium system from diffusion couples analyzed with an electron-probe microanalyzer. A previously unreported intermediate phase, designated as the delta phase, was found to exist along the niobium-rich side of the miscibility gap. In addition, a literature survey made by the Israel Atomic Energy Commission produced a bibliography of 54 references on diffusion in the couples uranium-aluminum, uranium-nickel, nickel-aluminum, and uranium-nickel-aluminum.[73]

Studies have been initiated to determine the diffusion coefficients of strontium and zirconium in fused UO_2 and in zirconium by the use of radioactive tracers.[4] The program is being conducted by Oak Ridge in a new laboratory to be used in connection with the investigation of various solid-state diffusion phenomena. The variables being considered include fabrication techniques, grain-size effects, stoichiometry, and mechanisms of mass transport. In another study there, the self-diffusion on aluminum is to be measured.

The diffusion of copper in Zircaloy is being investigated by Nuclear Metals in connection with the heat-treatment of Zircaloy tubes contained in copper extrusion jackets.[74] The heat-treatment being considered is ½ hr at 800°C. Analysis of successive layers for copper shows that appreciable copper is present at a depth corresponding to normal Zircaloy removal in etching; 200 ppm copper was found 2.5 mils below the surface. Preliminary qualitative measurements by means of X-ray fluoroscopy were found to be unreliable, since the copper concentration 1 mil below the surface of the Zircaloy had been indicated by this technique to be comparable to that for the base Zircaloy (33 ppm). In a study of possible barrier layers of chromium, molybdenum, or graphite, to enable diffusion heat-treatment in the copper extrusion jacket, only chromium appeared to offer promise. However, the applied chromium plate broke into pieces during extrusion and was therefore generally ineffective. (D. C. Carmichael)

Radiation Effects in Nonfuel Materials

Defects: Structure and Properties

Metals. Barnes and Mazey[75] have used the electron microscope to study point-defect clusters produced in copper and aluminum foils bombarded with 1.4×10^{17} alpha particles/cm^2 at 200°C. The foils were bombarded in stacks. In copper, both the foils through which the alpha particles passed and the foils in which the alpha particles stopped appeared similar, showing dislocation loops ($r \approx 200$ A) and a background of more numerous and smaller dots ($r \approx 20$ A). The behavior at grain boundaries suggests that these two types of clusters were due to different point defects. At 350°C, where a dislocation would normally anneal out, in the foils where the alpha particles came to rest (containing $\approx 10^{15}$ atoms of helium per square centimeter), the dislocations grew to form a tangle, and eventually small helium bubbles ($r \approx 40$ A) appeared in the same concentration as the original small dots. The results indicate that the dislocation loops are due to the clustering of interstitial atoms, and the small dots are spherical voids formed from vacancies. It is also inferred that the helium atoms are in interstitial positions during the bombardment and form bubbles by nucleating upon the voids, which increase in size as the dislocations grow (by climb), adding more interstitials to their cluster. Detailed investigation of the grain boundaries also distinguishes those in which vacancies are generated from those in which they are merely conducted.[76]

Dislocation densities in copper and aluminum which had been deformed at room temperature were determined by Hordon and Averbach[77] by means of a double-crystal rocking-curve broadening technique. The use of several characteristic radiations allowed the broadening to be resolved into components that depended separately on average lattice tilting, localized bending, dislocation strain, and subgrain size. Dislocation densities of about 10^8/cm^2 and subgrain size of about 10^{-4} cm were obtained for annealed crystals. With plastic shear strains in the range of 0.3 to 0.5, dislocation density increased rapidly to about 10^{10} or 10^{11}/cm^2. The corresponding subgrain size decreased to about 10^{-5} cm. This is interpreted as indicating the formation of randomized dislocation arrays at large strains. For several strained crystals, evidence was also found for a small number of piled-up arrays, with four to six dislocations in each pile-up.

Meechan et al.[78] have extended their point-defect-recovery model for copper. Recovery in five different stages is discussed and identified. Much of their own experimental verification is

done in electron-irradiated samples. Specific modifications are two kinds of interstitial configurations, more use of crowdions, and a trivacancy complex that is relatively stable at room temperature but migrates or dissociates at about 100°C.

The lattice parameter of copper decreased after an exposure of 9×10^{18} nvt, with no further change at 1.5×10^{20} nvt.[11] Line broadening decreased continuously with exposure. The peak shifts with exposure observed for copper agree with theoretical calculations for stacking-fault formation. The lattice parameter for iron at first increased with an exposure of 4.6×10^{18} nvt and then decreased with an exposure of 1.5×10^{20} nvt. Changes in parameter are similar to those for irradiated molybdenum, which belongs to the same crystallographic system. The line shape for iron showed a marked sharpening with exposure to 4.6×10^{18} nvt, and only a small subsequent broadening with exposure to 1.5×10^{20} nvt.

Deuterium diffusion in deuterium-irradiated copper between −46° and +20°C was studied[79] by observing the neutrons from the $D(d,n)He^3$ reaction which occurs in metals irradiated with low-energy deuterons. Grain-boundary diffusion is the principal cause for movement of deuterium in polycrystalline copper in this temperature range. Chemical purity has a significant effect on diffusion rate, a decrease in purity causing a decrease in diffusion rate. Copper polycrystals 99.999 per cent pure have an activation energy for deuteron diffusion of 0.12 ± 0.02 ev/atom. A surface resistance effect, proportional to the deuteron beam current but independent of the crystallinity, was found to be of major importance in determining the rate of escape of deuterium. A model for the diffusion process is discussed.

A distortion found in the lattice structure of tantalum bombarded with 350-kev deuterons at 45°C has been attributed to the formation of an interstitial solid solution of deuterium[80] during the D-D reaction. The specimens were heated to 770°C; the pressure reached a maximum at 612°C. This maximum is associated with an increase in the diffusion rate of deuterium. From the observed rates at three temperatures, an activation energy of 0.24 ev is calculated for the diffusion of deuterium in tantalum. The buildup of deuterium in the lattice is monitored by observing the neutrons produced in the D-D reaction.

Peiffer and Stevenson[81] report electrical resistivities associated with point and line defects in aluminum. Their conclusions are drawn from resistivity increases suffered during cold work and are compared with a recently developed theory. Differences in results are explained in terms of different initial conditions between the cold-worked material used here and the annealed aluminum of the previous work.

Grenall,[82] by studying neutron-damaged gold film with the electron microscope, has supported Brinkman's theory of displacement spikes. Vacuum-deposited films (discontinuous films of discrete particles) developed small black spots after an irradiation of 4.2×10^{17} fast neutrons/cm^2. The observed mean density of displacement spikes was 3×10^{16}/cm^3, which agrees well with the calculated value of 9×10^{16}/cm^3. The average diameter was 65 ± 7 A, which is also in good agreement with the theory.

Simmons and Balluffi[83] have extended their measurements of the equilibrium concentration of vacancies near the melting point to silver. The concentration of added sites at the melting point ($\Delta N/N$) is reported as $1.7 \pm 0.5 \times 10^{-4}$, which is 1/5.5 of the corresponding value for aluminum. Monovacancy concentration is greater than 90 per cent, with an energy of formation equal to 1.09 ± 0.10 ev, which is slightly larger than half the activation energy for self-diffusion. Lattice-vacancy-formation energy was found to be 1.10 ± 0.04 ev in quenching experiments of 99.999 per cent pure silver.[84] Combining the two sets of measurements yields a resistivity increase of 1.3 ± 0.7 μohm-cm/at.%.

Molybdenum has been studied by Gray and Cummings[85] after irradiation at 35 ± 5°C to fast-neutron exposures between 6.5×10^{16} and 1.2×10^{20} nvt. The lattice-parameter versus neutron-exposure curve shows a maximum near 5.0×10^{19} nvt. X-ray line width and microhardness also increase with exposure. Conclusions drawn from the experiments are that (1) interstitial atoms are mobile at 35°C, (2) during the initial stages of irradiation a large number of interstitials are trapped at substitutional impurity atoms, and (3) interstitial cluster formation and growth predominate during the remainder of the irradiation. A mechanism for such clustering and growth is discussed.

Trying to check theoretical suggestions as to the effect of neutron bombardment on the embrittlement of body-centered cubic (bcc) metals,

Johnson[86] observed effects in molybdenum which were different from those previously observed in EN2 steel. The suggestion is now that the mechanism of the radiation embrittlement can be more complex than originally observed. It seems likely that point defects created during irradiation of molybdenum cause dislocation climb; whereas, in EN2 steel, climb is inhibited by a precipitate of cementite on the dislocations.

Defects in Metal Alloys. A rather comprehensive report on order-disorder phenomena in alpha brass has been presented.[87–89] Annealing experiments showing stored-energy release, resistivity changes, density, lattice parameter, and hardness are discussed for slow heating and cooling, as well as for quenching experiments. Plastic deformation results in stored-energy release in alpha brass which is quite different from that observed in pure metals, being much larger and showing at least three distinct stages of release.

Schindler and Salkovitz[90] have tested the similarity between thermally induced ordering and irradiation-induced ordering by observing the magnetic properties of iron-nickel specimens irradiated with neutrons while in the presence of a saturating magnetic field. Square hysteresis loops were observed in all samples. These results support the proposal that the neutron bombardment created directional short-range ordering and, consequently, uniaxial anisotropy. By annealing in a magnetic field, Pauleve and Dautreppe[91] have studied the evolution of the orientation superstructure created by neutron irradiation in a magnetic field of the iron-nickel (50 per cent–50 per cent) alloy. Some effects of radiation on the magnetic properties of ferrite have also been observed.[92]

Magnetic properties of neutron-irradiated (>1 Mev) iron and nickel have been studied in specimens annealed for long times near their melting point in a pure hydrogen atmosphere.[93,94] The total flux was 2×10^{18} neutrons/cm^2 for nickel. No changes were observed in nickel which could be due to its poor magnetic properties. However, iron displayed a definite reduction of the maximum permeability and an increase in coercive force. Since these properties depend on defects which have the size of the Bloch wall thickness (of the order 10^3 A), it is suggested that this experiment presents the first evidence that some large defects are produced by fast neutrons at room temperature.

Defects in Other Materials. Bollmann[95] has studied defects produced by neutron irradiation of graphite using transmission electron microscopy. Tentative interpretation of the observations is presented, and the difficulties in making precise identifications are listed.

Electron microscope examination of thin films of ZrO_2, platinum, germanium, aluminum, and SiO_2 evaporated on carbon, irradiated in contact with UO_2 to 1 to 2×10^{16} nvt, showed fission tracks on the surface of contact.[2] In the case of ZrO_2 the tracks were bordered with nodules, whereas for aluminum the tracks appeared as trenches from which the original material had been removed. The tracks on platinum appear as perforated ridges. The morphology suggests that plastic deformation and vaporization had occurred.

The nature and number of defects in fast-neutron-irradiated silicon single crystals have been inferred by Mayer and Lecomte[96] from internal energy and elastic-constant measurements. The doses ranged to 3.7×10^{19} neutrons/cm^2. Effects of heat-treatment on these properties were also studied.

Experiments on single crystals of alpha Al_2O_3 at room temperature indicate no new electron-spin resonances due to exposure to gamma rays or reactor irradiation.[97] Fused silica irradiated with ultraviolet would give the same absorption lines that have been associated with electron and hole defects resulting from X-ray, gamma-ray, and neutron irradiation. However, quenching the fused silica will also produce the same resonances.

Al_2O_3 and $ZrSiO_4$ show little change in properties when exposed to 10^{18} to 10^{19} nvt of thermal neutrons.[98] When, however, a source of fission fragments is provided in the form of a UO_2 dispersant, the grain boundaries and the peaks of the X-ray diffraction profile disappear on irradiation. The crystal structure of U_3O_8 is also destroyed when irradiated in-pile. Al_2O_3 was observed to increase about 30 per cent in volume concurrent with the destruction of its crystal lattice. Calculations indicate that only a small proportion of the atoms are displaced by the fission fragments through elastic collisions or other applicable mechanisms. It is suggested that the fission fragments act indirectly, through anisotropic effects that distort the lattice and render it unstable. There are apparently a number of materials that exhibit this property; this places a serious limitation on the

materials suitable for use within the range of fission-fragment recoil. In contrast to this behavior, a number of ceramic materials having a cubic crystal structure exhibit excellent stability in-pile. These materials include UO_2 and UO_2-ZrO_2.

Quartz or vitreous silica have been bombarded by the positive ions H_2^+, D_2^+, He^+, Ne^+, A^+, Kr^+, and Xe^+ with energies between 7.5 and 59 kev, producing a surface layer of altered refractive index.[99] The depth and refractive index of this layer are found from reflection-coefficient measurements. The changes produced by the ion bombardment are attributed to lattice displacements and are shown to be consistent with the changes produced in these materials by fast-neutron irradiation. Thermal spikes produced by knock-on atoms in quartz and vitreous silica are shown experimentally to be unimportant for knock-on energies around 45 kev.

Weeks and Nelson[100] have completed theoretical calculation on irradiation effects produced in the short-range order in quartz and fused silica. The effect is displayed as a paramagnetic defect by means of electron-spin resonance. The defect is labeled E', which is thought to be an electron trapped in an oxygen vacancy. The theory and the experimental data show excellent agreement.

Changes in the elastic constants of 0.9 to 1.7 per cent for neutron-irradiated (2×10^{19} neutrons/cm^2) quartz were measured by means of the Bergman-Schaeffer method.[101] These changes are considerably different from the changes produced by the thermal cycling. A decrease in density of 0.18 per cent was also observed. (T. G. Knorr)

Theories of Radiation Effects

Thompson[102] points out the inadequacy of present theories on neutron damage because they neglect the effect of lattices which can focus the neutron momentum along the lines of close packing. This reduces the damage that would result from random collisions. The effect is expected if the lattice spacing is less than four times the atomic radius and the mean free path of the recoil atom is small with respect to the lattice spacing. Thus the effect will be small in the light elements (alkali metals, beryllium, and graphite), may be important in the transition metals (cobalt, iron, and manganese), but is important in "full" metals (silver, gold, and copper) and heavy elements (especially alpha uranium).

Holmes and Leibfried have made a detailed investigation of the slowing down in a solid of a primary displaced atom of high energy.[103] The total distance traveled and the vector distance to the end of the path are discussed in terms of certain averages for hard-core potentials.

Damask and Dienes[104] have reported solutions to the general equations for the annealing of vacancies in metals containing impurities to which the vacancies can be attached. For many interesting cases the decay curve is exponential, and the decay constant is related to, but not equal to, the rate constant for vacancy migration. Experiments must be performed only in the purest samples since impurity contents of 10 ppm can seriously affect the results.

The configuration of atoms surrounding a vacancy has been calculated by Girifalco and Weizer[105] for lead, nickel, copper, calcium, barium, sodium, and iron. Only radial relaxations were considered while using a pairwise central-force model in which the energy of interaction was assumed to have the form of a Morse function. The first and second nearest neighbor relaxations are reported, as well as the energies of relaxation.

Born's theory of crystal lattices has been used to calculate the following quantities for copper:[106] energy of formation of an interstitial = 3 ev, energy of formation of a vacancy = 1 ev, and volume expansion by a Frenkel pair $\Delta V = 1.3$ atomic volumes. These results should be valid in regions of large distortion occurring in the environment of an interstitial atom. The representation also satisfies all stability requirements.

The production of displaced atoms by processes resulting from thermal-neutron capture is discussed.[107] The results of an approximate calculation are presented which indicate that, in several elements, the number of displaced atoms produced by the recoil following capture gamma-ray emission may form an appreciable fraction of the total number of displaced atoms produced in a reactor experiment. The unique features of the radiation damage produced by thermal neutrons are noted, and some considerations attendant upon isolating and using such reactions in damage experiments are discussed.

Another calculation has been made for the number of atoms displaced and replaced in a crystal under neutron bombardment.[108] The assumptions used are that all atoms have equal

mass and that only elastic collisions with stationary atoms occur. Experiments show that the theory predicts too few displacements. Planeix[109] also discusses atomic displacements produced by irradiation of metals.

Manley[110] has developed a theory for diffusion which allows a calculation of the activation energy directly from the atomic force constants without resorting to normal mode analysis. Remnev[111] has calculated the stresses arising from the damage produced by fast-neutron bombardment of metals. (T. G. Knorr)

Surveys on Radiation-Induced Defects

The papers presented at the AEC conference on radiation effects in structural material have been compiled in a recently published report.[112] There are a number of papers on the changes in mechanical and other properties due to irradiation effects in various steels and structural material. The Proceedings of the Conference on Lattice Defects in Noble Metals have also been published.[113]

Nucleonics presented a special report on radiation effects,[114] where the field stands, and where it should go. Particularly of interest are the papers by D. S. Billington (Relaxing Reliance on Empirical Data), D. O. Leeser (Radiation Effects on Reactor Metals), and E. L. Burkhard (Combined Environmental Effect).

Cottrell[115] has presented a report on the effects of nuclear radiation on engineering materials. Some of the topics covered include damage in graphite, importance of stored energy, and effects of displaced atoms in hardening and embrittlement. Germagnoli and Granata[116] reviewed the experimental results on the production and analysis of behavior of vacancies in pure metals.

A number of surveys on neutron damage in materials have appeared.[117–120] Goldstein[121] has also written a book of general interest. The particular chapters on radiation-damage effects in materials should be noted. (T. G. Knorr)

Effects of Radiation on Mechanical Properties of Nonfuel Materials

The Naval Research Laboratory[122] has studied the effect of irradiation up to 1×10^{19} neutrons (>1 Mev)/cm^2 on the impact resistance of some low-alloy steels. Three samples of heavy-section submerged-arc welds (two of A-302B plate and one of A-212B plate), one sample of SA-336 heavy-section forging material, and four samples of plate materials (one each of A-302B and A-212B, and two of A-201) were analyzed after irradiation in the Brookhaven Graphite Research Reactor, Low-Intensity Test Reactor, and Materials Testing Reactor. Exposures of 5×10^{18} neutrons (>1 Mev)/cm^2 at temperatures under 200°F resulted in 40 to 100°F increases in transition temperature. Increasing the irradiation temperature to 575°F significantly decreased the amount of damage. Transition-temperature increases on the order of 250°F were developed by irradiation of 1×10^{19} neutrons (>1 Mev)/cm^2 under 200°F. Postirradiation heat-treatment produced recovery of properties after annealing at 650°F. Comparison of Charpy V and drop-weight nil-ductility shifts indicated good agreement between the two test methods.

In work at Argonne[123] on subsize tensile specimens of A-nickel and type 347 stainless steel, it was found that property changes induced by irradiation up to 4×10^{20} neutrons (>0.5 Mev)/cm^2 were qualitatively similar to those produced by cold working. However, no basis for direct correlation of changes was found. Table IV-11 indicates the effect of irradiation on properties. It was determined that the irradiation left the alloys more ductile than did cold work to a comparable ultimate strength. Radiation hardening was completely eliminated by a 1-hr anneal at 500°C, whereas temperatures of 600 to 800°C were required to anneal out cold-work hardening.

The effect of neutron irradiation on the tensile properties of Zircaloy-2 has been investigated at Chalk River.[124] Specimens of (1) annealed 13.1 per cent cold-worked and (2) 25.5 per cent cold-worked and tempered Zircaloy-2 were irradiated at 220 and 280°C with respective fast-neutron fluxes of 3.6×10^{19} and 2.7×10^{20} neutrons/cm^2. Postirradiation tensile tests performed at room temperature and 280°C showed that considerable hardening occurred in all the irradiated material. This change was characterized by an increase in the proportional limit, yield strength, and ultimate tensile strength, and a decrease in the total and uniform per cent elongations. The per cent changes in mechanical properties were greater in the annealed than in the cold-worked material. The tensile properties of irradiated 13.1 per cent cold-worked material were almost identical to those for the irradiated 25 per cent cold-worked

materials suitable for use within the range of fission-fragment recoil. In contrast to this behavior, a number of ceramic materials having a cubic crystal structure exhibit excellent stability in-pile. These materials include UO_2 and UO_2-ZrO_2.

Quartz or vitreous silica have been bombarded by the positive ions H_2^+, D_2^+, He^+, Ne^+, A^+, Kr^+, and Xe^+ with energies between 7.5 and 59 kev, producing a surface layer of altered refractive index.[99] The depth and refractive index of this layer are found from reflection-coefficient measurements. The changes produced by the ion bombardment are attributed to lattice displacements and are shown to be consistent with the changes produced in these materials by fast-neutron irradiation. Thermal spikes produced by knock-on atoms in quartz and vitreous silica are shown experimentally to be unimportant for knock-on energies around 45 kev.

Weeks and Nelson[100] have completed theoretical calculation on irradiation effects produced in the short-range order in quartz and fused silica. The effect is displayed as a paramagnetic defect by means of electron-spin resonance. The defect is labeled E', which is thought to be an electron trapped in an oxygen vacancy. The theory and the experimental data show excellent agreement.

Changes in the elastic constants of 0.9 to 1.7 per cent for neutron-irradiated (2×10^{19} neutrons/cm^2) quartz were measured by means of the Bergman-Schaeffer method.[101] These changes are considerably different from the changes produced by the thermal cycling. A decrease in density of 0.18 per cent was also observed. (T. G. Knorr)

Theories of Radiation Effects

Thompson[102] points out the inadequacy of present theories on neutron damage because they neglect the effect of lattices which can focus the neutron momentum along the lines of close packing. This reduces the damage that would result from random collisions. The effect is expected if the lattice spacing is less than four times the atomic radius and the mean free path of the recoil atom is small with respect to the lattice spacing. Thus the effect will be small in the light elements (alkali metals, beryllium, and graphite), may be important in the transition metals (cobalt, iron, and manganese), but is important in "full" metals (silver, gold, and copper) and heavy elements (especially alpha uranium).

Holmes and Leibfried have made a detailed investigation of the slowing down in a solid of a primary displaced atom of high energy.[103] The total distance traveled and the vector distance to the end of the path are discussed in terms of certain averages for hard-core potentials.

Damask and Dienes[104] have reported solutions to the general equations for the annealing of vacancies in metals containing impurities to which the vacancies can be attached. For many interesting cases the decay curve is exponential, and the decay constant is related to, but not equal to, the rate constant for vacancy migration. Experiments must be performed only in the purest samples since impurity contents of 10 ppm can seriously affect the results.

The configuration of atoms surrounding a vacancy has been calculated by Girifalco and Weizer[105] for lead, nickel, copper, calcium, barium, sodium, and iron. Only radial relaxations were considered while using a pairwise central-force model in which the energy of interaction was assumed to have the form of a Morse function. The first and second nearest neighbor relaxations are reported, as well as the energies of relaxation.

Born's theory of crystal lattices has been used to calculate the following quantities for copper:[106] energy of formation of an interstitial = 3 ev, energy of formation of a vacancy = 1 ev, and volume expansion by a Frenkel pair $\Delta V = 1.3$ atomic volumes. These results should be valid in regions of large distortion occurring in the environment of an interstitial atom. The representation also satisfies all stability requirements.

The production of displaced atoms by processes resulting from thermal-neutron capture is discussed.[107] The results of an approximate calculation are presented which indicate that, in several elements, the number of displaced atoms produced by the recoil following capture gamma-ray emission may form an appreciable fraction of the total number of displaced atoms produced in a reactor experiment. The unique features of the radiation damage produced by thermal neutrons are noted, and some considerations attendant upon isolating and using such reactions in damage experiments are discussed.

Another calculation has been made for the number of atoms displaced and replaced in a crystal under neutron bombardment.[108] The assumptions used are that all atoms have equal

mass and that only elastic collisions with stationary atoms occur. Experiments show that the theory predicts too few displacements. Planeix[109] also discusses atomic displacements produced by irradiation of metals.

Manley[110] has developed a theory for diffusion which allows a calculation of the activation energy directly from the atomic force constants without resorting to normal mode analysis. Remnev[111] has calculated the stresses arising from the damage produced by fast-neutron bombardment of metals. (T. G. Knorr)

Surveys on Radiation-Induced Defects

The papers presented at the AEC conference on radiation effects in structural material have been compiled in a recently published report.[112] There are a number of papers on the changes in mechanical and other properties due to irradiation effects in various steels and structural material. The Proceedings of the Conference on Lattice Defects in Noble Metals have also been published.[113]

Nucleonics presented a special report on radiation effects,[114] where the field stands, and where it should go. Particularly of interest are the papers by D. S. Billington (Relaxing Reliance on Empirical Data), D. O. Leeser (Radiation Effects on Reactor Metals), and E. L. Burkhard (Combined Environmental Effect).

Cottrell[115] has presented a report on the effects of nuclear radiation on engineering materials. Some of the topics covered include damage in graphite, importance of stored energy, and effects of displaced atoms in hardening and embrittlement. Germagnoli and Granata[116] reviewed the experimental results on the production and analysis of behavior of vacancies in pure metals.

A number of surveys on neutron damage in materials have appeared.[117–120] Goldstein[121] has also written a book of general interest. The particular chapters on radiation-damage effects in materials should be noted. (T. G. Knorr)

Effects of Radiation on Mechanical Properties of Nonfuel Materials

The Naval Research Laboratory[122] has studied the effect of irradiation up to 1×10^{19} neutrons (>1 Mev)/cm^2 on the impact resistance of some low-alloy steels. Three samples of heavy-section submerged-arc welds (two of A-302B plate and one of A-212B plate), one sample of SA-336 heavy-section forging material, and four samples of plate materials (one each of A-302B and A-212B, and two of A-201) were analyzed after irradiation in the Brookhaven Graphite Research Reactor, Low-Intensity Test Reactor, and Materials Testing Reactor. Exposures of 5×10^{18} neutrons (>1 Mev)/cm^2 at temperatures under 200°F resulted in 40 to 100°F increases in transition temperature. Increasing the irradiation temperature to 575°F significantly decreased the amount of damage. Transition-temperature increases on the order of 250°F were developed by irradiation of 1×10^{19} neutrons (>1 Mev)/cm^2 under 200°F. Postirradiation heat-treatment produced recovery of properties after annealing at 650°F. Comparison of Charpy V and drop-weight nil-ductility shifts indicated good agreement between the two test methods.

In work at Argonne[123] on subsize tensile specimens of A-nickel and type 347 stainless steel, it was found that property changes induced by irradiation up to 4×10^{20} neutrons (>0.5 Mev)/cm^2 were qualitatively similar to those produced by cold working. However, no basis for direct correlation of changes was found. Table IV-11 indicates the effect of irradiation on properties. It was determined that the irradiation left the alloys more ductile than did cold work to a comparable ultimate strength. Radiation hardening was completely eliminated by a 1-hr anneal at 500°C, whereas temperatures of 600 to 800°C were required to anneal out cold-work hardening.

The effect of neutron irradiation on the tensile properties of Zircaloy-2 has been investigated at Chalk River.[124] Specimens of (1) annealed 13.1 per cent cold-worked and (2) 25.5 per cent cold-worked and tempered Zircaloy-2 were irradiated at 220 and 280°C with respective fast-neutron fluxes of 3.6×10^{19} and 2.7×10^{20} neutrons/cm^2. Postirradiation tensile tests performed at room temperature and 280°C showed that considerable hardening occurred in all the irradiated material. This change was characterized by an increase in the proportional limit, yield strength, and ultimate tensile strength, and a decrease in the total and uniform per cent elongations. The per cent changes in mechanical properties were greater in the annealed than in the cold-worked material. The tensile properties of irradiated 13.1 per cent cold-worked material were almost identical to those for the irradiated 25 per cent cold-worked

Table IV-11 EFFECT OF NEUTRON IRRADIATION ON SOME PROPERTIES OF A-NICKEL AND TYPE 347 STAINLESS STEEL[123]

	A-nickel specimens*			Type 347 stainless-steel specimens*		
		Irradiated			Irradiated	
	Unirradiated	2.4×10^{20} nvt fast flux	4.0×10^{20} nvt fast flux	Unirradiated	2.4×10^{20} nvt fast flux	4.0×10^{20} nvt fast flux
Specimens with 0.075-In.-Square Section						
Yield strength,† 1000 psi	17.1 ± 1.0	77.7(1)	91.2 ± 11.4(2)	33.2 ± 1.8	72.8 ± 3.2(2)	86.9 ± 1.4
Ultimate strength, 1000 psi	62.5 ± 1.7	95.3 ± 0.5(2)	106.0 ± 0.2	85.0 ± 1.5	102.9 ± 0.9	106.9 ± 0.5
Yield to tensile strength ratio	0.274	0.815(1)	0.860(2)	0.391	0.707(2)	0.813
Elongation,‡ %	33 ± 4	17 ± 1	17 ± 2	55 ± 2	34 ± 3	29 ± 2
Hardness, Rockwell B	39.8 ± 2.6(24)	93.5 ± 0.1(12)	99.3 ± 0.3(9)	73.7 ± 0.8(24)	95.7 ± 0.2(12)	99.0 ± 0.4(9)
Density, g/cm^3	8.875 ± 0.008	8.898 ± 0.003	8.866 ± 0.000	7.937 ± 0.005	7.953 ± 0.007	7.931 ± 0.003
Resistivity, μohm-cm	10.45 ± 0.22(4)	10.45(1)	10.20 ± 0.15	75.28 ± 0.20(3)	76.98(1)	74.27 ± 0.15
Specimens with 0.020- by 0.250-In. Section						
Yield strength,† 1000 psi	16.6 ± 2.3	82.8(1)	>61.2(1)	33.0 ± 1.1(5)	82.5 ± 1.2	83.8 ± 13.1
Ultimate strength, 1000 psi	56.0 ± 1.2	85.7 ± 0.8	89.0 ± 1.1	86.4 ± 1.6	105.8 ± 2.1	104.0 ± 1.6
Yield to tensile strength ratio	0.296	0.966(1)	>0.688(1)	0.382	0.780	0.806
Elongation,‡ %	45 ± 1	23 ± 4	13 ± 1	64 ± 6	37 ± 1	36 ± 2
Hardness, Rockwell 15T	71.2 ± 2.6(24)	87.8 ± 0.5(12)	85.6 ± 1.4(9)	68.4 ± 7.0(24)	88.4 ± 0.2(12)	84.0 ± 2.6(9)
Density, g/cm^3	8.885 ± 0.003	8.902 ± 0.003	8.875 ± 0.005	7.915 ± 0.012	7.965 ± 0.006	7.940 ± 0.001
Resistivity, μohm-cm	9.08 ± 0.14(4)	9.31(1)	9.44 ± 0.14	74.97 ± 0.63(3)	74.88(1)	75.59 ± 0.28

* Unless otherwise indicated in parentheses, averages are based on six measurements of control specimens and three measurements of irradiated specimens.

† Based on 0.2 per cent offset.

‡ 1-in. gauge length.

and tempered material for both levels of irradiation. No yield point appeared in irradiated annealed material tested at room temperature, but one did appear on testing at 280°C. For annealed and cold-worked Zircaloy-2 irradiated at 280°C, the radiation damage was found to anneal out after the material was heated for 1 hr at 450°C.

In a recent survey article,[114] Leeser states that further irradiation experiments should be undertaken to reduce "ignorance factors" now going into reactor designs. For example, only limited data are available on materials for special application, such as magnetic compounds, thermal insulators, and noble metals. Moreover, little is known about radiation stability of precipitation-hardening structural alloys exposed at or near aging temperatures.

(B. C. Allen)

References

1. F. W. Albaugh, Reactor and Fuels Research and Development Operation Monthly Report for August 1960, USAEC Report HW-66644-A, Hanford Atomic Products Operation, Sept. 15, 1960. (Classified)
2. F. W. Albaugh, Reactor and Fuels Research and Development Operation Monthly Report for July 1960, USAEC Report HW-66237-A, Hanford Atomic Products Operation, Aug. 15, 1960. (Classified)
3. B. Cox and T. Johnston, The Oxidation and Corrosion of Zirconium and Its Alloys. Part IX, British Report AERE-R-3256, June 1960.
4. J. H. Frye, Jr., et al., Metallurgy Division Annual Progress Report for Period Ending July 1, 1960, USAEC Report ORNL-2988, Oak Ridge National Laboratory, Sept. 30, 1960.
5. Westinghouse Electric Corp., Bettis Atomic

Power Laboratory, Zirconium Highlights, USAEC Report WAPD-ZH-24, May 1960.

6. A. P. Gavin, Irradiation of an Aluminum Alloy-Clad Ceramic Pellet-Fueled Plate, USAEC Report ANL-6143, Argonne National Laboratory, May 1960.
7. A. P. Gavin and C. C. Crothers, Irradiation of an Aluminum Alloy-Clad Aluminum-Uranium Alloy-Fueled Plate, USAEC Report ANL-6180, Argonne National Laboratory, July 1960.
8. R. L. Hodson and J. I. Fisher, Dispersed-Phase Strengthening of Corrosion-Resistant Aluminum, USAEC Report ANL-6188 (Final Report: ARF-2176-6), Argonne National Laboratory, May 6, 1960.
9. Oak Ridge National Laboratory, Gas-Cooled Reactor Project Quarterly Progress Report for Period Ending June 30, 1960, USAEC Report ORNL-2964, Aug. 22, 1960.
10. Martin Co., Nuclear Div., ERDL-NPFO Corrosion Testing of Inconel and Croloy 16-1 Heat Exchangers, Report MND-E-2326, March 1960.
11. L. H. McEwen, comp., Unclassified Research and Development Programs Executed for the Division of Reactor Development and the Division of Research, February 1960, USAEC Report HW-64307, Hanford Atomic Products Operation, Mar. 10, 1960.
12. Westinghouse Electric Corp., Bettis Atomic Power Laboratory, Materials Department Technical Progress Report for the Period March 26 to June 25, 1960, USAEC Report WAPD-MRK-6, June 25, 1960. (Classified)
13. Knolls Atomic Power Laboratory, Reactor Technology Report No. 14, Chemistry, USAEC Report KAPL-2000-11, September 1960.
14. W. D. Gilbert et al., Carbon Steel for the Hanford New Production Reactor, USAEC Report HW-58299(Rev.), Hanford Atomic Products Operation, Nov. 26, 1958.
15. Aerojet-General Nucleonics, Army Gas-Cooled Reactor Systems Program Semiannual Progress Report for January 1–June 30, 1960, USAEC Report IDO-28558, July 31, 1960.
16. General Atomic and Electric Boat Divs. of General Dynamics Corp., Maritime Gas-Cooled Reactor Program, Quarterly Progress Report for the Period Ending September 30, 1959, USAEC Report GA-1183.
17. C. F. Hale et al., High-Temperature Corrosion of Some Metals and Ceramics in Fluorinating Atmospheres, USAEC Report K-1459, Union Carbide Nuclear Co., K-25 Plant, Sept. 30, 1960.
18. O. Kubaschewski and B. E. Hopkins, Oxidation Mechanisms of Niobium, Tantalum, Molybdenum, and Tungsten, *J. Less-Common Metals*, 2(2-4): 172 (April-August 1960).
19. G. T. J. Mayo et al., Oxidation Behavior of Niobium-Chromium Alloys, *J. Less-Common Metals*, 2(2-4): 223 (April-August 1960).
20. B. B. Argent and B. Phelps, The Oxidation of Niobium-Titanium and Niobium-Molybdenum Alloys, *J. Less-Common Metals*, 2(2-4): 181 (April-August 1960).
21. R. Smith, The Development of Oxidation-Resistant Niobium Alloys, *J. Less-Common Metals*, 2(2-4): 191 (April-August 1960).
22. G. L. Miller and F. G. Cox, Development of Oxidation Resistance of Some Refractory Metals, *J. Less-Common Metals*, 2(2-4): 207 (April-August 1960).
23. W. D. Klopp, Oxidation Behavior and Protective Coatings for Columbium and Columbium-Base Alloys, Report DMIC-123(PB-151080), Defense Metals Information Center, Jan. 15, 1960.
24. P. Kofstad et al., Oxidation Studies of Niobium-Base Alloys, Technical (Scientific) Note No. 3 for April 1, 1959, to March 31, 1960, Report NP-8936, Central Institute for Industrial Research, Blindern, Norway, May 1960.
25. Key Elements Amend Columbium for High-Temperature Service, *Iron Age*, 186(4): 86 (July 28, 1960).
26. R. A. Jeffreys and J. D. Gadd, Development and Evaluation of High-Temperature Protective Coatings for Columbium Alloys, Second Quarterly Progress Report to WADD, Report TM-1621, Thompson Ramo Wooldridge Inc., Oct. 15, 1960.
27. F. F. Schmidt et al., Investigation of the Properties of Tantalum and Its Alloys, Battelle Memorial Institute, Oct. 17, 1960.
28. Sylvania-Corning Nuclear Corp., Aug. 31, 1960. (Unpublished)
29. S. Greenberg and W. E. Ruther, Aqueous Corrosion of Magnesium Alloys, USAEC Report ANL-6070, Argonne National Laboratory, May 1960.
30. Samuel Glasstone, comp., Quarterly Status Report on LAMPRE Program for the Period Ending August 20, 1960, USAEC Report LAMS-2462, Los Alamos Scientific Laboratory, Sept. 29, 1960.
31. W. J. Anderson and G. V. Sneesby, Carburization of Austentic Stainless Steel in Liquid Sodium, USAEC Report NAA-SR-5282, Atomics International, Sept. 1, 1960.
32. Atomics International, Annual Progress Report—AEC Unclassified Programs for Fiscal Year 1960, USAEC Report NAA-SR-5350, August 1960.
33. Oak Ridge National Laboratory, Oct. 6, 1960. (Unpublished)
34. John R. Weeks and Carl J. Klament, Reaction Between Sheet Surfaces and Zirconium in Liquid Bismuth, *Nuclear Sci. and Eng.*, 8(2): 133–147 (August 1960).
35. E. C. W. Perryman, A Review of Zircaloy-2 and Zircaloy-4 Properties Relating to the Design

Stress of CANDU Pressure Tubes, Canadian Report CRMet-937 (AECL-1048), June 1960.

36. Westinghouse Electric Corp., Bettis Atomic Power Laboratory, Pressurized-Water Reactor (PWR) Project Technical Progress Report for the Period April 24 to June 23, 1960, USAEC Report WAPD-MRP-86.
37. F. W. Albaugh, Reactor and Fuels Research and Development Operation Monthly Report for June, 1960, USAEC Report HW-65854-A, Hanford Atomic Products Operation, July 15, 1960. (Classified)
38. J. H. Schemel, New Alloy to Boost Reactor Efficiency, *Prod. Eng.*, 31(30): 9 (July 25, 1960).
39. W. C. Hayes and A. J. Birkle, Development of Ferritic Steels for High Temperature Sodium Service, USAEC Report NAA-SR-4832, Atomics International, May 15, 1960.
40. A. E. Dinerman, Cyclic Strain Fatigue of Inconel at 75 to 600°F, USAEC Report KAPL-2084, Knolls Atomic Power Laboratory, Aug. 15, 1960.
41. Oak Ridge National Laboratory, Aircraft Nuclear Propulsion Project Semiannual Progress Report for the Period Ending April 30, 1960, USAEC Report ORNL-2942, July 28, 1960. (Classified)
42. General Electric Co., Aircraft Nuclear Propulsion Dept., Aircraft Nuclear Propulsion Engineering Progress Report No. 36 for April 1 to June 30, 1960, USAEC Report APEX-36, June 1960. (Classified)
43. R. T. Begley and A. I. Lewis, Development of Niobium-Base Alloys, Report NP-8735, Westinghouse Research Laboratories, Apr. 15, 1960.
44. I. Perlmutter, Mechanical Properties Attainable by Alloying of Refractory Metals, *J. Less-Common Metals*, 2(2-4): 253–271 (April-August 1960).
45. P. E. Brookes et al., The Creep and High-Temperature Fatigue Properties of the Magnesium-Base Canning Alloy, Magnox A.12, *J. Inst. Metals*, 88: 500–508 (August 1960).
46. G. C. E. Olds and G. M. Michie, Creep-Resistant Magnesium Alloys for Nuclear Fuel Elements, *J. Inst. Metals*, 88: 493–499 (August 1960).
47. B. J. Seddon, comp., Aluminum Data Manual, British Report DEGR-86(R), Mar. 9, 1960.
48. N. G. Boriskina and I. I. Kornilov, Constitution Diagrams of Fe-Cr-Ti at Iron and Chromium Rich Side of the Alloy, *Izvest. Akad. Nauk S.S.S.R., Otdel. Tekh. Nauk Met. i Toplivo*, No. 1, pp. 50–58 (January-February 1960).
49. R. W. Guard and E. A. Smith, Constitution of Nickel-Base Ternary Alloys, Nickel-Molybdenum-Aluminum System, *J. Inst. Metals*, 88: 283–285 (February 1960).
50. R. T. Begley, Development of Niobium-Base Alloys, Third Quarterly Progress Report, Report A-2573Z(WEC), Westinghouse Electric Corp., Aviation Gas Turbine Div., Feb. 10, 1959.
51. H. Braun et al., Studies of Niobium-Tantalum Alloys, *J. Less-Common Metals*, 1: 413–419 (December 1959).
52. A. G. Knapton, The Niobium-Rhenium System, *J. Less-Common Metals*, 1: 480–486 (December 1959).
53. A. Ottenberg, Studies of the Gas Carburization of Niobium, Report LMSD-288234, Lockheed Aircraft Corp., January 1960.
54. J. P. Pemsler, Study of Gases in Metals: A Literature Survey, Report NMI-9800, Nuclear Metals, Inc., Aug. 17, 1959.
55. E. J. Rapperport, Refractory Metal Phase Diagrams, Quarterly Progress Report for the Period July 15, 1959, to October 15, 1959, Report NMI-9214, Nuclear Metals, Inc., Dec. 18, 1959.
56. G. L. Miller, ed., *Tantalum and Niobium*, Academic Press, Inc., New York, 1959.
57. D. W. Bare and O. N. Carlson, Phase Equilibrium and Properties of Yttrium-Titanium Alloys, *Metal Progr.*, 78(4): 206–208 (October 1960).
58. J. D. Ramsdell and E. D. Hull, Properties of Titanium-Vanadium-Zirconium Alloys, Report BM-RI-5604, Bureau of Mines, May 1960.
59. Yu. F. Bychkov et al., Characteristic Features of the Beta Phase Decay in Zirconium Alloys, *Inzhener. Fiz. Zhur., Akad. Nauk Belorus. S.S.R.*, 3(4): 95–98 (1960).
60. W. Chubb et al., Structural Materials for Thermal Nuclear Reactors Operating at About 1950°F with Air as a Coolant, USAEC Report BMI-X-159, Battelle Memorial Institute, July 20, 1960.
61. W. M. Campbell and E. C. W. Perryman, Atomic Energy of Canada Ltd., 1960. (Unpublished)
62. R. Resnick and L. S. Castleman, The Self-Diffusion of Columbium, *Trans. Met. Soc. AIME*, 218: 307–310 (April 1960).
63. W. D. Klopp and V. D. Barth, Diffusion Rates and Solubilities of Interstitials in Refractory Metals, Report DMIC-Memo-50(PB-161200), Defense Metals Information Center, Apr. 4, 1960.
64. D. W. Rudd et al., The Permeation of Hydrogen Through Hastelloy B, USAEC Report NAA-SR-4898, Atomics International, June 15, 1960.

64*a*. D. W. Rudd et al., The Permeation of Hydrogen Through Hastelloy B, USAEC Report NAA-SR-4898(Rev.1), Atomics International, February 1961.

65. G. T. Murray and G. Pincus, Permeability of Cladding Materials to Inert Gases (Progress Report No. 15), USAEC Report MRC-R156, Materials Research Corp., Apr. 22, 1960.
66. J. A. Stohr and L. Alfille, Apparatus for Studying the Diffusion of Rare Gases in Stainless Steel, French Report CEA-1294, 1959 (in French).
67. Y. Adda and J. Philibert, Study of Uranium-Titanium Diffusion, French Report CEA-1297, 1959 (in French).
68. J. Philibert and Y. Adda, Contribution to the

Study of Diffusion in a Polyphase System, French Report CEA-1300, 1959 (in French).

69. R. Boucher, Diffusion of Aluminum During the Transformation UAl_3-UAl_4 in the Solid State, French Report CEA-1298, 1959 (in French).
70. M. Moosé et al., Diffusion of Some Metals in Dilute Solution in Uranium, *Compt. rend.*, 250: 3171–3173 (May 9, 1960).
71. Y. Adda et al., Effect of Pressure on the Intermetallic Compound Formed by Diffusion Between Uranium and Copper, *Compt. rend.*, 250: 115–117 (Jan. 4, 1960).
72. N. L. Peterson and R. E. Ogilvie, Diffusion Studies in the Uranium-Niobium Systems, *Trans. Met. Soc. AIME*, 218: 439–444 (June 1960).
73. Israel Atomic Energy Commission, Literature Survey on Diffusion of Uranium-Aluminum, Uranium-Nickel, Nickel-Aluminum, and Uranium-Nickel-Aluminum, Israeli Report LS-63, August 1959.
74. S. Isserow et al., Power Reactor Program Progress Report to E. I. duPont de Nemours & Company for the Period March 1, 1959, Through March 31, 1959, USAEC Report NMI-4392, Nuclear Metals, Inc., July 27, 1959.
75. R. S. Barnes and D. J. Mazey, The Nature of Radiation-Induced Point Defect Clusters, British Report AERE-R-3348, June 1960.
76. R. S. Barnes, The Generation of Vacancies in Metals, *Phil. Mag.*, 5(8): 635 (1960).
77. M. J. Hordon and B. L. Averbach, X-Ray Measurements of Dislocation Density in Deformed Copper and Aluminum Single Crystals, USAEC Report NYO-7085, Massachusetts Institute of Technology, July 1, 1960.
78. C. J. Meechan et al., Thermally Activated Point Defect Migration in Copper, *Phys. Rev.*, 120: 411 (1960); also in USAEC Report NAA-SR-5377.
79. M. T. Robinson et al., Diffusion of Deuterium in Deuterium-Irradiated Copper, *J. Appl. Phys.*, 31: 1474 (1960).
80. A. F. Gabrysh et al., Study of Irradiation Effects and the $H^2 + H^2$ Buildup in Tantalum, *J. Appl. Phys.*, 31: 1785–1791 (1960).
81. H. R. Peiffer and F. Stevenson, Cold Work and Subsequent Electrical Resistivity Increases in Pure Aluminum, *Acta Met.*, 8: 494 (1960).
82. A. Grenall, Direct Observation of Fast Neutron Damage in Gold Films, USAEC Report NAA-SR-5062, Atomics International, July 15, 1960.
83. R. O. Simmons and R. W. Balluffi, Measurements of the Equilibrium Concentration of Lattice Vacancies in Silver Near the Melting Point, *Phys. Rev.*, 119: 600 (1960).
84. M. Doyama and J. S. Koehler, Quenching of Lattice Vacancies in Pure Silver, *Phys. Rev.*, 119: 939 (1960).
85. D. L. Gray and W. V. Cummings, Jr., An X-Ray Diffraction Study of Irradiated Molybdenum, *Acta Met.*, 8: 446 (1960).
86. A. A. Johnson, The Embrittlement of Molybdenum by Neutron Irradiation, *Phil. Mag.*, 5: 413 (1960).
87. L. M. Clarebrough and M. H. Loretto, Order-Disorder Phenomena in α-Brass. I. Development of Order, *Proc. Roy. Soc. (London)*, A257: 326 (1960).
88. L. M. Clarebrough et al., Order-Disorder Phenomena in α-Brass. II. Influence of Quenching, *Proc. Roy. Soc. (London)*, A257: 338 (1960).
89. L. M. Clarebrough et al., Order-Disorder Phenomena in α-Brass. III. Influence of Plastic Deformation, *Proc. Roy. Soc. (London)*, A257: 363 (1960).
90. A. I. Schindler and E. I. Salkovitz, Effect of Applying a Magnetic Field During Neutron Irradiation on the Magnetic Properties of Fe-Ni Alloys, *J. Appl. Phys.*, 31(Suppl.): 245S (1960).
91. J. Pauleve and D. Dautreppe, Orientation Superstructure Created by Neutron Irradiation in a Magnetic Field in the Alloy Fe-Ni (50%–50%), *Compt. rend.*, 250: 3804 (1960).
92. N. M. Omel'Yanovskaya, Radiation Effects on Magnetic Properties of Ferrite, *Kernenergie*, 3: 394 (1960).
93. G. Biorci et al., Effect of Neutron Bombardment on the Magnetic Properties of Iron and Nickel of Very High Permeability, Technical Note No. 2b, Report AFOSR-TN-60-309, December 1959.
94. G. Biorci et al., Effect of Neutron Bombardment on the Magnetic Properties of Iron and Nickel of Very High Permeability, Final Report No. 3b, Report AFOSR-TR-60-66, February 1960.
95. W. Bollmann, Electron-Microscopic Observations on Radiation Damage in Graphite, *Phil. Mag.*, 5(8): 621 (1960).
96. G. Mayer and M. Lecomte, Internal Energy and Elastic Constants for Silicon Irradiated with Fast Neutrons, *J. phys. radium*, 21: 242 (1960).
97. O. R. Gilliam, Investigations of Radiation Effects in Solids by Electron Spin Resonance, Progress Report for June 16, 1959 to March 15, 1960, USAEC Report TID-5786, University of Connecticut, Mar. 15, 1960.
98. R. M. Berman et al., Fission Fragment Damage to Crystal Structures, *J. Nuclear Materials*, 2 (2): 129–140 (June 1960).
99. R. L. Hines and R. Arndt, Radiation Effects of Bombardment of Quartz and Vitreous Silica by 7.5 to 59 Kev Positive Ions, *Phys. Rev.*, 119: 623 (1960).
100. R. A. Weeks and C. M. Nelson, Irradiation Effects and Short-Range Order in Fused Silica and Quartz, *J. Appl. Phys.*, 31: 1555 (1960).
101. G. S. Zhdanov et al., The Elastic Properties of Neutron-Irradiated Quartz, *Kristallografiya*, 3: 720 (1958); English translation in *Soviet Phys.-Cryst.*, 3: 726 (1960).
102. M. W. Thompson, How Focusing Collisions Af-

fect Radiation Damage, *Nucleonics*, 18: 135 (1960).

103. D. K. Holmes and G. Leibfried, Range of Radiation Induced Primary Knockons in the Hard Core Approximation, *J. Appl. Phys.*, 31: 1046 (1960).
104. A. C. Damask and G. J. Dienes, Theory of Vacancy Annealing in Impure Metals, *Phys. Rev.*, 120: 99 (1960).
105. L. A. Girifalco and V. G. Weizer, Vacancy Relaxation in Cubic Crystals, *J. Phys. Chem. Solids*, 12: 260 (1960).
106. A. Seeger and E. Mann, Beldungsenergien and Gitterverzerrungen von Zwishengitteratomen und Lerrstellen in Kubisch-Flachenzentrierten Kristallen, Insbesondere in Kupfer, *J. Phys. Chem. Solids*, 12: 326 (1960).
107. R. M. Walker, On the Production of Displaced Atoms by Thermal Neutrons, *J. Nuclear Materials*, 2(2): 147–151 (June 1960).
108. L. Crabs et al., Radiation Damage in Crystals, *Bull. classe sci., Acad. roy. Belg.*, 45: 891 (1959).
109. J. M. Planeix, Irradiation Induced Atomic Displacements in Metals, *Dissertation Abstr.*, 19 (12): 3271 (1959).
110. O. P. Manley, A Method of Evaluating Diffusion Coefficients in Crystals, *J. Phys. Chem. Solids*, 13: 244 (1960).
111. Yu. I. Remnev, On Stresses in Metals Under Irradiation, *Nauch. Doklady Vysshei Shkoly Fiz-Mat. Nauki*, 4: 141–142 (1958).
112. USAEC Conference on the Status of Radiation Effects Research on Structural Materials and the Implications to Reactor Design, USAEC Report TID-7588, October 1959.
113. J. A. Brinkman et al., eds., Proceedings of the Lattice Defects in Noble Metals Conference Held at Canoga Park, California, October 16 and 17, 1958, USAEC Report NAA-SR-3250, Atomics International, May 19, 1960.
114. Advances in Radiation Effects, *Nucleonics*, 18 (9): 63–86 (September 1960).
115. A. H. Cottrell, Effect of Nuclear Radiation on Engineering Materials, *J. Brit. Nuclear Energy Conf.*, 5: 64 (1960).
116. E. Germagnoli and S. Granata, On the Behavior of Lattice Vacancies in Pure Metals, *Energia nucleare*, 7: 309 (1960).
117. O. Hauser, The Effects of Fast Neutrons on Solid Bodies, *Kernenergie*, 1: 709 (1958).
118. E. M. Doss, Radiation Damage to Nonmetallic Materials, USAEC Report NAA-SR-Memo-1890, Atomics International, May 8, 1957.
119. C. Motoc, Some Aspects on the Effects of Neutrons on Solid Bodies, *Acad. rep. populare Romîne, Inst. fiz. atomică Inst. fiz., Studii cercetări fiz.*, 10: 533 (1960).
120. Sh. Sh. Ibragimov et al., The Structures and Properties of Some Metals and Steels After Irradiation with Fast Neutrons, *At. Energ.*, 8: 413–419 (May 1960) (in Russian).
121. H. Goldstein, *Fundamental Aspects of Reactor Shielding*, Addison-Wesley Publishing Co., Inc., Reading, Mass., 1959.
122. J. R. Hawthorne and L. E. Steel, The Effects of Neutron Irradiation on the Charpy V and Drop-Weight Test Transition Temperatures of Various Steels and Weld Metals, Report NRL-5479, Naval Research Laboratory, Mar. 3, 1960.
123. S. H. Paine et al., A Study of Irradiation Effects on Type A Nickel and Type 347 Stainless Steel Tensile Specimens, USAEC Report ANL-6102, Argonne National Laboratory, July 1960.
124. L. M. Howe and W. R. Thomas, The Effects of Neutron Irradiation on the Tensile Properties of Zircaloy-2, *J. Nuclear Materials*, 2(3): 248–260 (September 1960).

Section V

SPECIAL FABRICATION TECHNIQUES

Melting, Casting, Heat-Treatment, and Hot Working

National Lead Company of Ohio[1] has extended its work on the effect of furnace atmosphere (pressure level) on unalloyed uranium ingot chemistry. Particular attention was given to the ingot impurities, hydrogen, oxygen, and nitrogen. Three levels of pressure were imposed (30, 3, and less than 3×10^{-2} mm Hg abs.). In the most recent effort,[2] the character of the charge materials was also varied.

For the normal charge makeup (derbies and briquettes), National Lead noted that (1) hydrogen and oxygen increased with furnace pressure; (2) at a pressure of 3 mm Hg or higher, the nitrogen content increased with pressure; and (3) furnace pressure did not affect the carbon content. However, when the crucible charge was 100 per cent dingot scrap feed (this dingot scrap was low in oxygen but high in hydrogen, and the normal charges were lower in hydrogen and higher in oxygen), the carbon content increased significantly with a decrease in furnace pressure. Within an ingot, the oxygen concentration at the ingot top was lower than that at the bottom when the charge material was dingot scrap. No such effect was noted in the normal charges.

A bibliography that should be of considerable interest to the melter of refractory metals was compiled recently by Cernak et al.[3] It covers the subject of vacuum arc melting in a comprehensive manner. The bibliography also includes data published in 334 references from 1945 to 1949 on the related subjects of electrode preparation, furnace construction and operation, melting, vacuum techniques, and theories.

Successful research has been reported[4] on expendable graphite molds for metals with melting points in excess of 2100°C. Sound hafnium castings with good surfaces were obtained in molds prepared by a shortened and an improved curing cycle. Rigorous control in the curing cycle has reduced mold shrinkage from 4 per cent to 1 or 2 per cent. As might be expected, carbon pickup on the casting surface was high, exceeding 1000 ppm at the surface. However, at depths of 15 to 30 mils below the surface, carbon levels decreased to within 50 to 100 ppm of the electrode stock. Below 30 mils, the carbon content was essentially the same as that of the electrode material.

Several facets of the problem met in casting beryllium are being studied by the Beryllium Corporation.[5] Additions of tantalum nitride, tungsten carbide, and silver have been made to beryllium in order to obtain grain refinement and improved castings. On the basis of incomplete results, tantalum nitride appears ineffective, and tungsten carbide recovery is very low. However, the silver additions increased the fluidity of the molten beryllium and the soundness of the castings.

Molybdenum, niobium, tantalum, and tungsten sheet for air-frame or rocket-motor uses is the subject of a Defense Metals Information Center memorandum,[6] in which the present technology for producing sheet material is reviewed and commented upon. Interesting items in the appraisals are (1) the role of surface contamination as a detriment to the fabrication of sheet, (2) the still-unanswered need for reliable oxidation-resistant coatings, and (3) the opinion that tungsten is the only unalloyed refractory metal for which a sheet-rolling program can be justified.

The cold working (swaging and drawing) of uranium in the fabrication of wire and tubes has been reported.[7] Both ingot (vacuum melted) uranium and dingot (as reduced) uranium were

fabricated. In swaging, a mixture of Molykote and SAE 20 oil was the best lubricant; in drawing, both Fluorolube and Steelskin were effective if the surface of the uranium was oxidized. The best annealing cycle was 5 min in vacuum at 1100°F. Reductions totaling about 70 per cent between anneals and reductions as high as 20 per cent per pass in drawing could be made. No significant difference between the dingot or ingot material with respect to total reduction, reduction per pass, or annealing cycle was noted.

Rocky Flats[8] has been conducting studies on the use of different salts for the annealing of uranium with the stated purpose of finding an alternative (with improved water solubility) to the presently used Holden 660 mixture. After many criteria were considered (melting point, water solubility, corrosion characteristics, stability, and hydrogen concentration), the best alternative found contained approximately 34.5 wt.% K_2CO_3, 33.5 wt.% KCl, 31 wt.% Na_2CO_3, and 1 wt.% $MgCO_3$.

In research to establish methods of obtaining multitemperature extrusion conditions,[9] Nuclear Metals has worked with the following composites: (1) uranium clad with stainless steel or magnesium and (2) UO_2 clad with stainless steel or molybdenum. Both types 446 and 304 stainless steels were successfully clad on a fine-grained uranium core. On the other hand, little success was achieved with magnesium as the cladding material because of undesirable end effects and the poor core-clad interface. Notable in the attempts to extrude UO_2 in steel or molybdenum were the uniform increase in UO_2 density at low reductions and the lack of success with molybdenum-clad specimens at temperatures of 3000°F or higher.

In the fabrication of reactor hardware, Hanford has obtained from a commercial tube vendor (Tube Reducing Corporation, Passaic, N.J.) large zirconium process tubes that are unique because of their shape and size. The conditions to be met (542°F and 1050 psig) require that extensive nondestructive tests be conducted on the tubes. The testing and the production of the tubes are covered in some detail in a report by Knecht.[10]

Of considerably broader interest is the summary[11] of the various techniques that have been developed, modified, or used at Hanford to produce reactor fuel elements. Applications pertinent to cladding and clad fuels are discussed. These include (1) controlled plug and die sizing with metal and plastic dies; (2) forming of internal ribs on tubes by swaging; (3) controlled sinking and tapering by swaging; (4) deep forming of fuel-element hardware; (5) vacuum precision casting of various types of fuel-element hardware such as end caps and supports; (6) special closure methods, including swaging, extrusion closure utilizing the Dynapak, electron-beam welding, and seam welding; (7) attachment of supports by resistance spot and ultrasonic welding; and (8) precision forming of irregular shapes by spark machining.

Fabrication of shapes for reactor applications has been reported by Los Alamos.[12] An interest in materials for the containment of molten plutonium in the LAMPRE reactor has led to the development of fabrication techniques for tantalum. Extrusion, deep drawing, and ironing operations have been conducted to obtain the desired shapes. The importance of metal purity, tool design, and lubrication has been noted.

(E. L. Foster)

Cladding

Cladding by Rolling and Swaging

Continued emphasis is being placed on the preparation of uranium dioxide-fueled rod type elements by various swaging processes. Additional studies on roll cladding of uranium-aluminum and uranium-molybdenum are in progress.

Zircaloy-2-clad UO_2 rod type fuel elements were prepared at Hanford[13] by swaging for PRTR startup and critical-assembly tests. The UO_2 in this group of approximately 75 rods was compacted to an average density of 89 per cent of the theoretical density.

Other experiments were initiated to improve the as-swaged surface of the Zircaloy cladding by use of better die lubricants.[13] Electrofilm 77-5, a solid lubricant, was chemically applied to the impact surfaces of a set of dies. Although the lubricant broke off after several passes, the fuel-rod surfaces were noticeably improved. Improved techniques for applying the lubricant are being investigated.

Improvement of hot-swaged surfaces of fuel elements prepared at Hanford by modification of the swaging operation is also being studied.[14] These modifications include better temperature control, rebuilding the feeding device to prevent lateral movement during swaging, and relieving

the edges of the swaging dies to provide a softer blow.

Equipment has been installed at Savannah River to study vibratory compaction of UO_2 in stainless steel prior to swaging.[15] The tubes were loaded with −20-mesh Norton fused UO_2 while vibrating at 550 to 625 cycles/sec with an acceleration of 20 g. As-packed densities ranged from 70 to 76 per cent of the theoretical density. Vibratory compaction reduced the number of swaging operations necessary to achieve 90 per cent densities from 12 to 6. The combination of vibratory compaction and an improved hydraulic feed to the swager produced smoother fuel-rod surfaces.

Swaging is being investigated by Westinghouse[16] as a method for producing thermoelectric nuclear fuel elements. Prefabricated couple units were assembled in tubes for swaging. The couples were separated by Lavite spacers to facilitate swaging of several units in one operation.

Since welding techniques have been unsatisfactory, Hanford[11] is investigating cold swaging as a means for producing integral heat-transfer fins on the surface of tubular cladding stock. Both two- and four-die swaging has been successfully used with the dies machined and ground to the desired configuration. To date, the best results have been obtained with a thick-walled, fully annealed, type 1100 aluminum tube swaged around a mild-steel mandrel.

Roll cladding of uranium-aluminum alloy and UO_2-aluminum dispersion cores with aluminum cladding is being studied by Francis and Craig.[17] These fuels are being fabricated with and without burnable poisons. Fuels of less than 20 wt.% uranium were successfully clad with type 1100 aluminum with no core dog boning or rippling. Alloy cores with higher uranium content were uniformly clad with 6061 aluminum, a high-strength aluminum alloy. However, to prevent frame-to-cladding separation, the lower strength alloy was used for the frame. Examination of roll-clad dispersion fuels revealed embedding of the fuel particles in the cladding. Experience was gained with the use of boron, Gd_2O_3, Dy_2O_3, Ir_2O_3, iridium, and B_4C as burnable poisons.

A uranium-bearing Fiberglas core roll clad with an aluminum alloy is being studied by the Clevite Corporation.[18–21] Dog boning and rippling of the core were major problems in the fabrication of a 40 vol.% uranium-bearing Fiberglas core clad with type 1100 aluminum alloy at 1100°F.[17] An increase in the rolling temperature to 1175°F eliminated these effects, but the core still varied in thickness.[19] Type 6061 aluminum cover plates gave the best core integrity, but frames of the same alloy separated from the covers during rolling. The best procedure found to date was to use a type 1100 aluminum frame with a type 6061 cover and to reduce the composite 50 to 65 per cent by rolling at 1100°F.[19,20] Lowering the initial reduction from 30 to 20 per cent apparently prevented core fracturing, but preheating of the rolls had no effect.[21]

Nuclear Metals[22] produced two roll-clad strips of uranium–10 wt.% molybdenum with 0.015 in. of beryllium cladding. The core alloy was packed in a mild-steel container and completely surrounded by beryllium powder. The billet was evacuated and sealed, heated to 1950°F, and press forged at 100,000 psi. After the composite was removed from the jacket and inspected for cracks, it was rejacketed and unidirectionally rolled at 1950°F. The cladding was apparently crack-free. (E. S. Hodge)

Diffusion Bonding

A continuing investigation of diffusion bonding of dissimilar metals and alloys is being conducted by Castleman and coworkers.[23] The kinetics of growth of intermetallic layers in binary diffusion couples has been studied to test existing theory relating to anomalous behavior which had been reported for some systems. Anomalous behavior previously reported for the aluminum-nickel system included the presence in the diffusion zone of only two of the four thermodynamically stable phases and inhibition of intermetallic-layer growth to a surprising extent by application of pressure. It has been found in this study, however, that all four stable phases are actually present in the diffusion zone and that the effect of pressure is a consequence of an increase in the heat of activation for diffusion within the affected intermetallic phase. In the aluminum-nickel system, it had been indicated previously that application of pressure markedly increased intermetallic-layer growth and that, under some conditions, growth decreased with increasing temperature. Castleman and his coworkers have found that these anomalies are apparently due to striking structural alterations occurring during the extremely rapid growth of the predominant UAl_3 phase.

Studies have also been made of the aluminum-thorium and copper-zinc systems. A pressure effect on layer growth in the aluminum-thorium diffusion zones reported by other workers has been found to be insignificant. The mechanism of interdiffusion in ordered and disordered beta brass is currently being investigated. A related study is summarized under Diffusion Studies in Sec. IV of this Review.

A hot-pressing bonding process is being investigated as a possible backup bonding method (to gas-pressure bonding) for the production of Shippingport PWR Core 2 fuel elements.[24] This development work has shown that satisfactory dimensional control is achieved. However, the bonds obtained in the blanket type elements are not considered acceptable, although those obtained in seed type elements are of higher quality and appear satisfactory. Further sampling and evaluation will be performed, and the equipment capacity required for bonding half-length (55-in.-long) seed elements by this technique may be installed. The eutectic-diffusion-bonding technique originally developed by Bettis for making PWR Core 2 elements has been applied to the bonding of Zircaloy tubes to Zircaloy spacers.[25] Investigation of chromium, copper, iron, and nickel intermediate layers demonstrated that only nickel gave a bonded microstructure similar to that of the Zircaloy-2 parent metal. (D. C. Carmichael)

Coextrusion

An investigation was conducted by Bridgeport Brass[26] to determine the density and stoichiometry of coextruded UO_2 fuel rods clad with type 304 stainless steel. The rod samples had the high density of 97.5 per cent of the theoretical density and an oxygen-uranium ratio of 2.02. The billet was extruded in a 3.675-in.-diameter liner to a 0.785-in.-diameter rod. According to Bridgeport Brass, these results verify the feasibility of producing high-density, near-stoichiometric UO_2 by the hot-extrusion process.

Further development of a hot-coextrusion technique as a procedure for the economic production of stainless-steel- or Zircaloy-clad UO_2 fuel elements is being conducted at Nuclear Metals.[27,28] The multitemperature technique is being employed to obtain the necessary close match of relative stiffness or extrusion constant between the stainless steel and UO_2. In this process the materials to be extruded are heated separately to temperatures at which their constants are nearly equal, then quickly assembled and coextruded. At the present time, this involves heating, assembling, and extruding the UO_2 core at a temperature 500°F above the melting point of the stainless steel, whereas the stainless-steel cladding components are maintained at approximately 1500°F below the core temperature. This temperature difference gives the stainless steel an extrusion stiffness comparable to that of the oxide core. Preservation of this temperature gradient has been a problem because overheating the cladding and/or chilling the core results in a rough core-cladding interface. Stainless-steel-clad UO_2 fuel rods, ranging from 20 to 25 in. in length, have been hot coextruded with core diameters between 320 and 340 mils and cladding thicknesses between 30 and 40 mils. The UO_2 cores are 99 per cent of the theoretical density, with ideal stoichiometry.

It has become evident from past results of an investigation made by Nuclear Metals[22,29] that some of the major difficulties normally encountered in coextruding a beryllium-clad uranium fuel element are alleviated when the core is stiffened to match the stiffness of the cladding. This has been accomplished by the addition of molybdenum, for example, in the uranium–10 wt.% molybdenum core. (C. B. Boyer)

Canning

Methods for using sodium as the bonding material of full-length fuel elements are being studied at Atomics International.[30] This study is related to the fabrication development of uranium-alloy fuel elements for the Hallam Nuclear Power Facility. Extrusion and liquid pouring were investigated. Extrusion was found to be impractical because of mechanical difficulties in introducing a sufficient volume of sodium into a fuel rod. However, two full-length fuel rods were successfully bonded using the liquid-pouring technique. The first fuel rod contained dummy steel fuel slugs and a simulated sodium-potassium bond, and the second fuel rod contained natural uranium–10 wt.% molybdenum fuel and a sodium bond. Further study is needed on reproducibility of quality and the reduction of scrap losses. Improvements are necessary in the liquid-sodium apparatus to reduce maintenance and cleaning time. Also, satisfactory sodium purity is essential for the prevention of excessive corrosion of the cladding.

An advanced fuel-element design for the organic-moderated reactor, being considered by Atomics International,[30] incorporates a fluted tube as the cladding, a uranium-molybdenum alloy rod as the fuel, and a liquid metal as the bonding medium. In preliminary nuclear, thermal, and fabrication studies, the cladding material was assumed to be stainless steel, and sodium was selected as the liquid-metal bond. When sodium is in contact with an organic coolant (such as Santowax R) in concentrations between 1 and 8.5 per cent, it has been found that an accelerated pressure buildup occurs upon heating to 750°F. Other liquid-metal bonding media are to be investigated. Also, the high cross section of stainless steel may preclude its use as a cladding material for this concept.

Efforts to can thorium wafers in aluminum jackets by hot pressing have been unsuccessful. Hanford[31] had previously found that thorium plated with nickel, copper, and iron-nickel prior to canning showed no more uniformity of diffusion or bond strength than unplated thorium. When unplated cores were used, over half the canned assemblies were rejected because of poor bonds between the cores and jackets. Experiments which were run to determine the cause of the poor bonding indicated that it stemmed from materials occluded in the thorium during fabrication which volatilized during the canning operation.

Hot isostatic pressing of ThO_2 and UO_2-ThO_2 fuel plates clad with aluminum is reported by Phillips investigators.[17] Evacuated picture-frame packs, compacted under 8 tsi pressure at 590°C for 15 min, were used. No additional annealing was given the plates because bonding between core and cladding was not anticipated.

(E. G. Smith, Jr.)

Nonelectrolytic Chemical-Plating Techniques

Properties of nickel coatings on steel, formed by thermal decomposition of nickel carbonyl, have been studied.[32] In thicknesses greater than 10 μ, the coatings were resistant to 3 per cent NaCl solutions.

Chromium coatings prepared by the thermal decomposition of chromium dicumene on Zircaloy-2 were evaluated at Hanford.[14]

Work on the coating of nuclear fuel particles with niobium, chromium, molybdenum, vanadium, tungsten, and silicon during 1959 is summarized,[33] and a detailed evaluation of methods of preparing these coatings is presented[34] by Nuclear Materials & Equipment Corporation. In experiments designed to determine the conditions for preparing niobium–5 wt.% vanadium alloys,[35] UO_2 powder was coated with vanadium by hydrogen reduction of the chloride at 900°C. The feasibility of preparing silicon-coated UO_2 by hydrogen reduction of the chloride was demonstrated. In coating UO_2 with chromium by hydrogen reduction of $CrCl_2$, it was observed that incomplete coatings were obtained between 950 and 1000°C and that chromium had a tendency to completely surround the spheres above 1100°C. Chromium coatings prepared by the decomposition of chromium dicumene were bright, shiny, adherent, and continuous. Further improvements were made in the "vibrating-pan" reactor used by Nuclear Materials to coat nuclear fuel particles by chemical vapor-deposition reactions. Further progress was noted in the preparation of matrices by infiltrating the voids between particles by continuing the vapor-deposition reaction in a static bed of the particles.

Development work on pyrolytic graphite at High Temperature Materials, Inc., is reviewed by Yaffee.[36] Work on Al_2O_3-coated UO_2 and carbon-coated UC_2 up to mid-1960 is reviewed by Battelle.[37] Details are given on the evaluation in the Battelle Research Reactor of the coated particles that are being studied for the Pebble-Bed Reactor. Further details of the alumina-coating procedure are reported separately.[38]

Pyrolytic carbon coatings, prepared by thermal decomposition of acetylene at 1400°C on thorium-uranium carbide particles, were effective in protecting the particles from air oxidation and hydrolysis.[38]

The deposition of tungsten by hydrogen reduction of tungsten hexafluoride is receiving increased attention as a means of coating graphite for erosion and corrosion protection in a reducing atmosphere.[39–46] The reaction occurs readily at 400 to 700°C without the interfering formation of lower halides that occurs with hydrogen reduction of tungsten hexachloride. Factors influencing the adherence of vapor-deposited molybdenum coatings to metallic bases were studied at MIT.[47] Purity of materials and careful surface preparation were shown to be important.

(J. M. Blocher, Jr.)

Electroplating

A method for electrodepositing an adherent iron plate onto uranium has been patented.[48] Cladding is accomplished by soldering an aluminum sheath or some other protective coating to the iron layer.

Protection of uranium from reaction with aluminum cladding by electrodeposition of nickel, followed by thermal diffusion, has been studied at the Center of Nuclear Studies in France.[49] Using boron-free plating solutions, nickel deposits were heat-treated up to 100 hr at 700°C. An intermetallic uranium-nickel diffusion zone builds up which (1) avoids uranium-aluminum diffusion during subsequent tests with aluminum cans and (2) decreases the corrosion rate of the underlying uranium. The heat-treatment causes the formation of five to seven distinct layers in the diffusion layer which are identified as intermetallics such as UNi_5, UNi_2, and U_7Ni_9. The most brittle compound is the UNi_5 compound that occurs next to the pure nickel. Fracture always occurs in this brittle UNi_5 layer. All other intermetallics in the diffusion layer remain fixed to the uranium. Impurities in the uranium tend to collect between the uranium and the first intermetallic, U_6Ni.

Personnel at Knolls laboratory[50] have evaluated chromium-plated steels in high-temperature, high-purity waters. Large differences in corrosion protection occurred in steels from various commercial suppliers. They conclude that quality-control procedures must be worked out and that research is needed to define plating specifications more narrowly than is now possible. Until these controls and specifications are defined, chromium plating cannot be adopted for the corrosion protection of stressed parts.

The feasibility of coating small particles of uranium metal or oxide for corrosion protection has been investigated.[33] Small metallic-coated particles have high thermal conductivity and lower inherent cost than fabricated metal. Moreover, coated particles permit a combined use of materials that are incompatible in other forms. Moreover, if some coatings are penetrated by corrosion, the loss of active material is limited to the small particles involved. For these and other reasons, this exploratory research was undertaken. Methods were derived for coating UO_2 with nickel and copper by immersion and electrolysis; chromium by electrolysis; and niobium, chromium, molybdenum, and tungsten by hydrogen reduction of their chlorides. Some progress was also made toward the successful coating of uranium metal with electrodeposited copper and nickel.

(J. McCallum)

Ceramic Coatings

The techniques of application and the quality of Al_2O_3 coatings on UO_2 particles are being investigated at Battelle.[51,52] Batches of 45- to 50-mesh UO_2 particles were coated with 30 to 150 μ of Al_2O_3 by reacting aluminum chloride and water vapor in a fluidized bed. After heating at 1200°F in air and between 550 and 2500°F in forming gas, the quality was evaluated on the basis of weight change and alpha count. Particles having coatings of 160 μ or greater thickness passed both tests very well.

Westinghouse[53] is investigating the coating of UO_2 fuel wafers with pyrolytic carbon. By tumbling the wafers, adherent coatings up to about 25 μin. thick were obtained. Ten to 25 μin. of coating effectively inhibits reactions between fuel and Zircaloy-2 during isostatic pressure bonding.

(B. W. King)

Explosion Forming

A study is presently being conducted on the explosion forming of the refractory metals, molybdenum, tungsten, tantalum, and niobium, with special emphasis being placed on the forming of molybdenum.[54] The objectives of this program are (1) to develop techniques for explosively forming these refractory metals, (2) to investigate the effects of the detonation waves on these materials, (3) to determine the feasibility of using explosion forming as a technique for joining these metals, and (4) to obtain some measure of the deformation rate and its effect on the explosion forming of these refractory metals.

Tests have been conducted on the explosion cupping of molybdenum and molybdenum–0.5 wt.% titanium alloy panels. During this testing, a photogrid system was employed in an effort to determine the elongation of the metal at any one particular point during the forming process. The photogrid system was used in preference to an etched or scribed grid since, during some early testing with a scribed grid, it was found that fracturing occurred immediately at the scribe marks with no apparent elongation. After

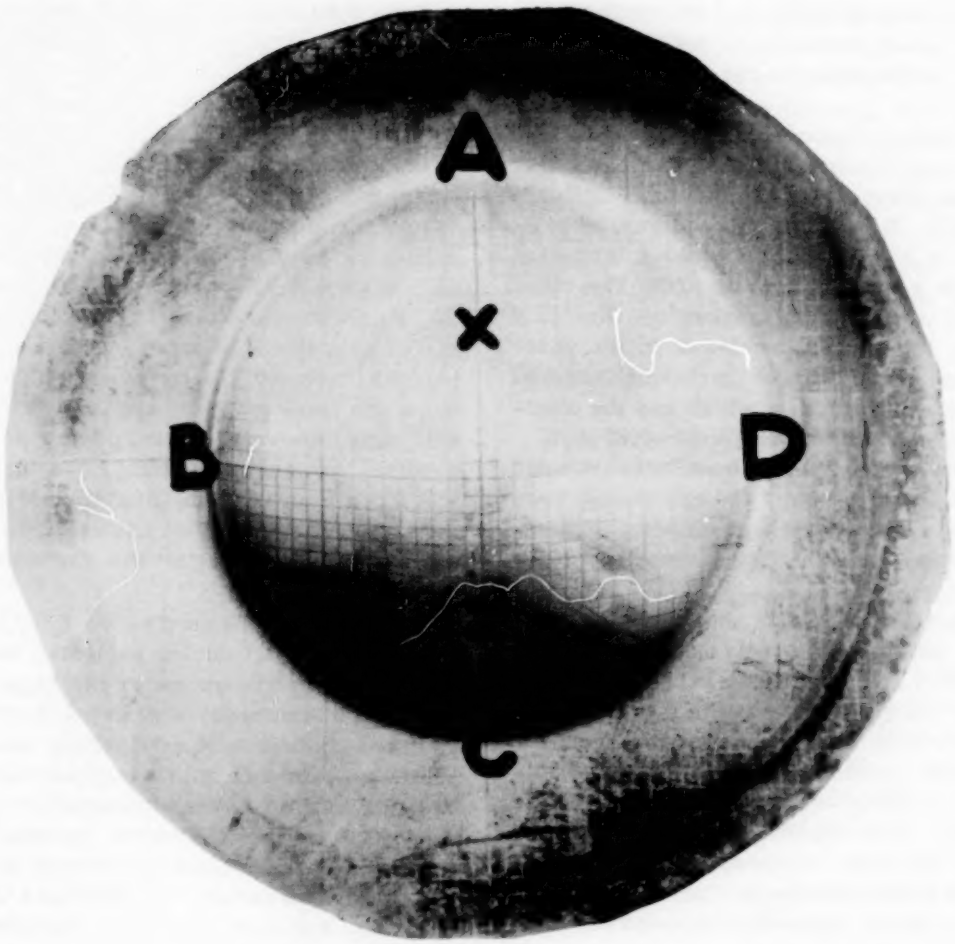

Figure 22— Explosively formed pure-molybdenum sheet.[54] The figure shows the grid and location of the markings on an explosively formed 0.040-in. pure-molybdenum sheet. The sheet was formed at 600°F using a 45-g charge of RDX.

the metal blank was exposed and printed, the photogrid was measured and checked for error. This examination revealed an error of only 1 per cent in a 1-sq in. section of gridding. After the grids had been checked for accuracy, the panels were marked at points where they were expected to bevel during the deformation process, at points that were expected to be at the center of the formed cup, and also halfway between the center and beveled edges of the cup. Figure 22 shows a metal blank marked in this manner after being explosively formed. Measurements were taken along a straight line, *A*, *X*, center, *Y*, and *C*, in order to determine the relative degree of elongation as the center of the cup was approached. Each individual measurement at a designated point was two grid lengths long and directed toward the center of the cup.

The energy-transmitting medium (325-mesh powdered alumina) and the standoff distance (6 in.) were held constant during these tests. The explosives used were 15 per cent dynamite and RDX, since these two explosives provided data for both the low and high ends of the detonation-rate scale. The weight of charge used during the test was varied according to the thickness of the metal blank being formed. Charge weight was varied between 15 and 25 g when forming 0.010-in. sheet, and between 40 and 45 g when forming 0.040-in. sheet. The charge weight used was limited to 45 g, since it was felt that a heavier charge would result in fracturing of the confinement tube used during this testing. Also,

the temperature at which the specimens were run was varied from 200 to 600°F. The grid showed no deleterious effects as a result of the tests.

The maximum individual elongation, defined as the elongation measured at one particular point, was found to be 25 per cent for pure molybdenum. This measurement was taken at the bevel of a 0.040-in.-thick sheet formed at 600°F with a 45-g charge of RDX. The other elongation measurements taken on this part were also the highest achieved in the pure-molybdenum series without fracturing the metal blank. The depth of draw, which was the maximum obtained in this series, was ~0.80 in.

The data obtained from these tests revealed that, as a rule, greater elongations were achieved by utilizing the high-velocity RDX explosive rather than the lower velocity 15 per cent dynamite.

A comparison of the data obtained from similar tests conducted on molybdehum–0.5 wt.% titanium alloy and those on the pure molybdenum showed only slight differences in the results.

Metallographic examination of the successfully formed specimens revealed a uniformly cold-worked structure typical of cold-rolled molybdenum. The microhardness values and superficial Rockwell hardness values of the explosively formed specimens are in fair agreement, both being approximately equivalent to Rockwell C30.

Those samples which fractured during forming were found to have some unusual features in the failure areas. Extensive internal splitting and fragmentation with an appearance of internal "blowup" was found to be characteristic of the shattered specimens. There is also some evidence that internal fracturing may occur even when it appears that the specimen has been formed successfully.

A study of explosive welding is presently being conducted to determine the feasibility of explosively welding high-temperature metals and those that are extremely difficult to weld by other processes.[55] The materials included in this study are as follows:

Molybdenum to molybdenum*
Beryllium to beryllium
BC 120 VCA titanium to BC 120 VCA titanium
Molybdenum* to type 310 stainless steel
Type 4340 steel to type 4340 steel
Niobium to type 310 stainless steel

Experiments involving the explosive welding of type 4340 steel to itself have been conducted to determine the proper surface treatment, medium, explosive, and standoff distance required to produce a satisfactory weld.

Surface preparation for explosive welding is of considerable importance. In all these tests the surfaces were cleaned by both rough and chemical methods to remove greases, oils, and oxides. Chemical treatments were found to be more desirable since they would etch the surface uniformly, whereas the roughening treatments resulted in erratic cleaning. The etchant that was found to produce the best welds was a 2-min etch in an aqua regia–cupric chloride solution. After etching, the metal was washed and dried before testing.

The medium to be used between the explosive charge and metal during explosive welding is determined by the geometry of the parts to be welded and their physical properties. This study required flat sheet-to-flat sheet welding. In initial experiments with water as the transfer medium, a central area of the specimen was not bonded. Other media, which included rubber, chipboard, and combinations of these with water, were also used during this program.

Various types of high explosives which were found to be efficient under conditions of confinement from air have been used. These included combinations of aluminized RDX-TNT.

The shape and weight of the charge were also varied in an attempt to weld the central portion of the metal samples. Disks and parallelepipeds were the shapes of greatest interest. Charge weight was varied from 32 to 200 g.

Standoff is needed to prevent the rupture of metal under test. The standoff distance and medium are somewhat dependent on each other since too great a standoff for a given charge results in insufficient pressure for satisfactory welding. During this experimentation, the standoff was varied from $\frac{1}{2}$ to 2 in. In a chipboard-water medium, a $\frac{1}{2}$- to $\frac{3}{4}$-in. standoff produced the best results. A metallographic examination of a specimen produced under these conditions revealed that the periphery was welded while the central portion was merely in intimate contact. Figure 23 shows a section of the explosively welded interface. The thin white layer of varying thickness is the weld interface. A mi-

*Molybdenum–0.5 per cent titanium, deoxidized arc-cast alloy.

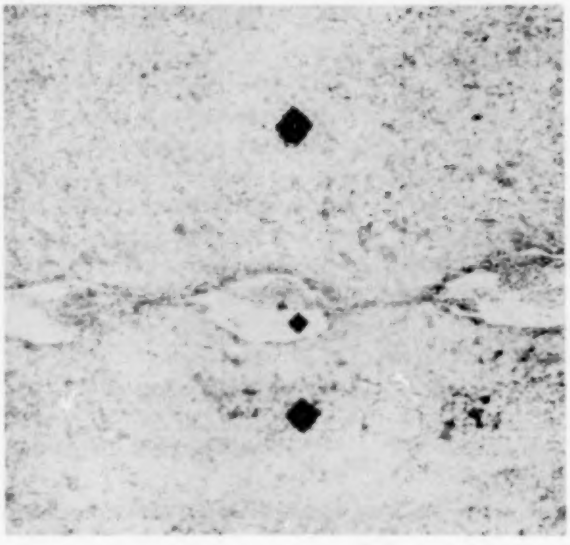

Figure 23 — Explosively welded interface of type 4340 steel.[55] (Magnification, 200 ×.)

crohardness survey of a section through the welded area indicated that the interface was approximately three times harder than the material on either side of it. The hardness at the interface was found to be 824 VPN or Rockwell C65. Tensile shear tests of the specimen indicated that the welds were stronger than the parent metal. The results of three of these tensile tests are shown in Table V-1.

Table V-1 RESULTS OF TENSILE TESTS OF EXPLOSIVELY WELDED SPECIMENS[55]

Specimen	Failure load, lb	Ultimate tensile strength,* psi
½-in. overlap	1190	80,000
1-in. overlap	2180	73,000
1-in. overlap	2660	88,000

*The values are based on a 0.030-in.-thick specimen. Since some thinning occurred in regions adjoining the welded area, failure took place in these areas. A more accurate tensile strength would be higher than those shown.

General conclusions that can be drawn from the results of explosive welding tests of type 4340 steel to itself are (1) type 4340 steel can be welded to itself with sufficient area to produce a weld as strong as the parent metal, (2) the areas of weld are not uniform on lapped surfaces, and (3) the welded interface has a high hardness and is martensitic in structure.

A bibliography on explosive metalworking containing over 200 references has been prepared.[56] It contains references to such explosive metalworking operations as forming, extruding, welding, hardening, and the compaction of metal powders. The report also contains references to experimental work concerned with the use of an electric spark discharge as the energy source for high-energy-rate metalworking.

(C. C. Simons)

Welding and Brazing

A variety of joining studies are being continued by personnel at Hanford.[57] These studies involve the use of high-frequency resistance welding for attaching spacing members to fuel elements and the use of magnetic-force butt welding for end capping. Both of these projects are concerned with nonmetallic fuel elements.

Work is being conducted at Oak Ridge on the problems involved in using welded niobium for extended periods of time at elevated temperatures.[58] A niobium alloy with a nominal 1 per cent zirconium content has been used in this work. The welds in this alloy will become embrittled when subjected to temperatures around 1500°F. The embrittlement or aging reaction is dependent upon time and temperature. Figure 24 illustrates some of the results that have been obtained on the aging behavior of niobium weldments. In addition to the aging studies reported[58] which involve weldments, considerable data are given on base-metal properties. This information will also be of interest to personnel involved with the welding of this alloy. The later work appears to indicate that the ratio of zirconium and oxygen contents in the alloy controls the aging behavior.

Studies made at Battelle on various aspects of tantalum welding have been reported. This work included studies of the causes of porosity in tantalum welds, methods of reducing the grain size of tantalum weld metal, and procedure developments for the fabrication of small heat exchangers.[59] It was found that porosity formation depends on the oxygen content of the material and the carbon-oxygen ratio. Ultrasonic vibration transmitted into arc-welded joints effectively reduced grain size in the weld metal.

(R. E. Monroe)

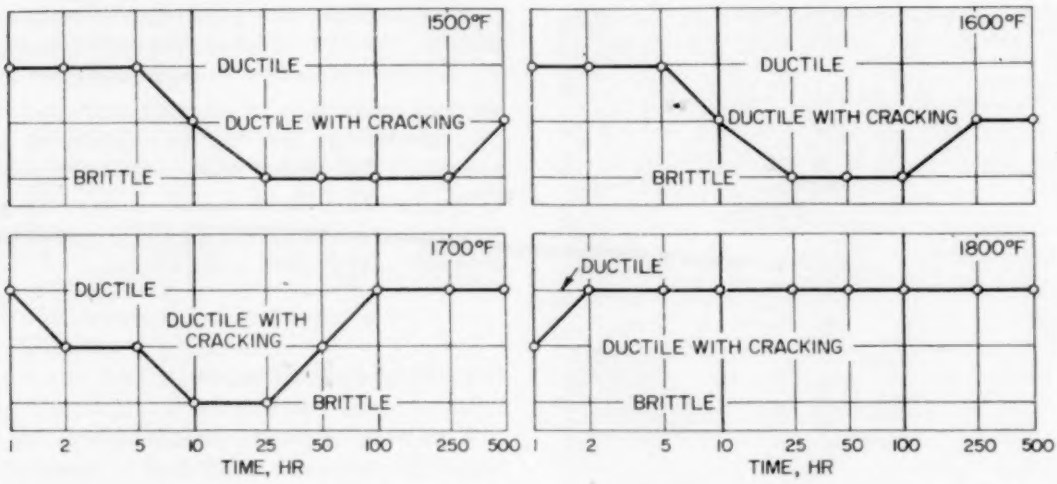

Figure 24—Influence of aging time at various temperatures on the bend-test behavior of Nb–1 per cent Zr alloy.[58]

Nondestructive Testing

Ultrasonics

The role experience plays in the efficiency of ultrasonic inspection is often emphasized. Brioni,[60] after discussing problems of interpretation, recommends the use of ultrasonic inspection of welds as a "preventive and supplementary function," using radiographs only at points of doubtful interpretation. In this way, Brioni claims to be able to inspect 30 to 40 meters of weld in 8 hr, compared with 8 to 10 meters inspected radiographically within the same period of time.

The problems of interpreting ultrasonic data, as well as those of coupling and aligning the probes with the test material, must be considered in automating ultrasonic inspection equipment. De Sterke[61] reports on a system in which three ultrasonic probes are used to inspect welds automatically. The ultrasonic energy is directed in such a way as to locate both transverse and longitudinal defects. Warnings of flaws are given by means of horns and lights, and the flaw area may be sprayed with paint, as is often done in automatic installations.

Some interesting projects under way at Argonne[58,62–64] include the measurement of elastic constants of single crystals (using equipment based on a system developed by Bell Telephone Laboratories at frequencies ranging from 12 to 150 Mc), Lamb-wave propagation, ultrasonic attenuation, and ultrasonic inspection of Zircaloy rod. Especially interesting is the search for a suitable solid seal capable of carrying shear waves into the specimen at temperatures up to 600°C and which will be easily removable without damaging the specimen or the fused-quartz buffer rod. A mixture of calcium carbonate and sodium silicate in solution has been used successfully with zirconium, and it is now being evaluated as a means of attaching uranium to the buffer.

The elastic constants of alpha zirconium[62] have been determined ultrasonically at 20°C. The values are as follows:

$$C_{11} = 1.4351 \times 10^{12} \text{ dynes/cm}^2$$
$$C_{12} = 0.7255 \times 10^{12} \text{ dynes/cm}^2$$
$$C_{33} = 1.6491 \times 10^{12} \text{ dynes/cm}^2$$
$$C_{13} = 0.6550 \times 10^{12} \text{ dynes/cm}^2$$
$$C_{44} = 0.3207 \times 10^{12} \text{ dynes/cm}^2$$

Hanford[65] has developed an immersion ultrasonic test that will detect small cracks on the inner surface of Zircaloy-2 tubing used for PRTR fuel-element cladding, but it is not sensitive to bonded inclusions or to wall-thickness variations. It is claimed that the ultrasonic method is the best for locating internal defects and that the best results are obtained with a 10-Mc focused lithium sulfate transducer. Internal test notches 0.001 to 0.006 in. deep by 3 in. long were easily detected. Surface char-

acteristics of the cladding influence the effectiveness of the test. Alignment of the transducer with the specimen is very critical.

Equipment has been developed[58] for simultaneously measuring reflection, transmission, and Lamb-wave propagation in thin metal sections. Their ultrasonic-attenuation comparator has completely variable frequency and voltage of pulse. These and other developments (such as the thickness-measuring device, which integrates a series of single measurements and displays the information on a counter instead of an oscilloscope) are typical of the advancement in the art of nondestructive testing by means of ultrasonics. (D. Ensminger)

Eddy-Current, Radiographic, and Other Techniques

Improvements in the resolution of eddy-current measurements by the application of low-frequency masking fields have been made by Argonne.[64] The technique has been applied successfully to the examination of Zircaloy-2 tubing for cracks. Time-delay, through-transmission techniques have also proved successful for flaw detection of aluminum tubing.

Gamma radiographic gauging of blanket wafers for density has been developed at Westinghouse.[66] By factoring out thickness variations through micrometer gauging, precisions of ±1.0 and 0.5 per cent are obtained for wafer density and loading. Automatic dimensional gauging at the rate of 1800 pieces per hour has been accomplished. The thickness of a copper bonding film has been determined by an X-ray fluorescence technique.

Gamma-ray spectroscopy has been used successfully to determine the enrichment of liquid samples.[67] Studies of photoemitting materials for use in neutron radiography are also being made at Argonne.[68] Rhodium and indium appear best at this stage of the work, based on exposure-speed rating and image resolution. In addition, rhodium has a favorably low response to the gamma radiation that usually accompanies a neutron beam.

A calorimetric method is being used at Argonne[64] to accurately determine the plutonium content of fuel elements. The heat generated by the radioactive decay of the plutonium is measured. Accuracies of greater than 1 per cent are claimed for this technique.

A technique has been devised at Sylvania[69] for the determination of uranium hydride and iron content in fuel slugs by measuring magnetic susceptibility at both liquid-nitrogen and room temperatures.

A report by Ruby and Gardner[70] contains a selected bibliography on the nondestructive assay of irradiated and unirradiated reactor fuel-element assemblies. Included are discussions, evaluations, and suggestions for further work. (D. R. Grieser)

References

1. J. W. Simmons, ed., Summary Technical Report for the Period April 1 to June 1, 1960, USAEC Report NLCO-810, National Lead Co. of Ohio, Aug. 11, 1960. (Classified)
2. J. W. Simmons, ed., Summary Technical Report for the Period July 1 to September 30, 1960, USAEC Report NLCO-820, National Lead Co. of Ohio, Oct. 28, 1960.
3. E. A. Cernak et al., Vacuum Arc Melting (A Bibliography), Report CNLM-1802-11, Pratt & Whitney Aircraft Div., United Aircraft Corp., Mar. 16, 1960.
4. Mark L. Wright, Quarterly Metallurgical Progress Report No. 7 for the Period April 1 to June 30, 1960, USAEC Report USBM-U-745, Bureau of Mines, Albany Metallurgy Research Center.
5. P. M. Cohen and R. C. Harris, Beryllium Casting, Phase II, Interim Technical Report No. 7 for the Period March 18 to June 17, 1960, Report NP-8911, Beryllium Corp.
6. Defense Metals Information Center, Development of Refractory Metal Sheet in the United States, Report DMIC-Memo-67(PB-161217), Sept. 20, 1960.
7. Nuclear Metals, Inc., Technical Progress Report to the AEC Reactor Division for the Period Ending June 30, 1959, USAEC Report NMI-1216, July 21, 1960.
8. S. R. Pocsik, Investigation of Salts for Use in Uranium Metal Heat-Treating Baths, USAEC Report RFP-191, Dow Chemical Co., Rocky Flats Plant, July 25, 1960.
9. E. S. Guidoboni et al., Multi-Temperature Extrusions, USAEC Report NMI-1229, Nuclear Metals, Inc., Mar. 14, 1960.
10. R. L. Knecht, Fabrication of the PRTR Zircaloy-2 High Pressure Process Tubes, USAEC Report HW-60358, Hanford Atomic Products Operation, July 31, 1959.
11. S. H. Bush, Unique Fabrication Processes Applied to Fuel Cladding Materials, USAEC Report HW-64335, Hanford Atomic Products Operation, Mar. 15, 1960.
12. G. S. Hanks and J. M. Taub, Fabrication of

Tantalum Capsules for LAMPRE-I Reactor, USAEC Report LAMS-2434, Los Alamos Scientific Laboratory, July 29, 1960.

13. L. H. McEwen, comp., Unclassified Research and Development Programs Executed for the Division of Reactor Development and the Division of Research, March 1960, USAEC Report HW-64865, Hanford Atomic Products Operation, Apr. 15, 1960.
14. F. W. Albaugh, Reactor and Fuels Research and Development Operation Monthly Report for June 1960, USAEC Report HW-65854-A, Hanford Atomic Products Operation, July 15, 1960. (Classified)
15. R. R. Hood and L. Isakoff, comps., Heavy-Water Moderated Power Reactors, USAEC Report DP-505, E. I. du Pont de Nemours & Co., Inc., July 1960.
16. G. R. Kilp et al., Thermoelectric Nuclear Fuel Element, Progress Report No. 22, USAEC Report WCAP-1565, Westinghouse Electric Corp., Bettis Atomic Power Laboratory, May 10, 1960.
17. W. C. Francis and S. E. Craig, Progress Report on Fuel-Element Development and Associated Projects, USAEC Report IDO-16574, Phillips Petroleum Co., Aug. 16, 1960.
18. R. H. Baskey, Fuel-Bearing Fiberglas in Aluminum-Base Fuel Elements, USAEC Report ORO-303, Clevite Corp., June 13, 1960.
19. R. H. Baskey, Fuel-Bearing Fiberglas in Aluminum-Base Fuel Elements, USAEC Report ORO-304, Clevite Corp., July 7, 1960.
20. R. H. Baskey, Fuel-Bearing Fiberglas in Aluminum-Base Fuel Elements, USAEC Report ORO-322, Clevite Corp., Sept. 12, 1960.
21. R. H. Baskey, Fuel-Bearing Fiberglas in Aluminum-Base Fuel Elements, USAEC Report ORO-316, Clevite Corp., Sept. 2, 1960.
22. Nuclear Metals, Inc., Fundamental and Applied Research and Development in Metallurgy, Progress Report for November 1959, USAEC Report NMI-2081, May 6, 1960.
23. L. S. Castleman and L. Seigle, Fundamentals of Diffusion Bonding, USAEC Report SEP-227, Sylvania Electric Products, Inc., Aug. 13, 1956.
24. Westinghouse Electric Corp., Bettis Atomic Power Laboratory, Pressurized-Water Reactor (PWR) Project Technical Progress Report for the Period June 24 to August 23, 1960, USAEC Report WAPD-MRP-87.
25. W. P. McQuillan, Diffusion Bonding: A New Way to Join Critical Parts, *Materials in Design Eng.*, 51(4): 14–16 (April 1960).
26. Bridgeport Brass Co., Process Development Quarterly Report for July–September 1959, USAEC Report BRB-53, June 20, 1960. (Classified)
27. J. G. Hunt and P. Loewenstein, The Fabrication of Clad Massive UO_2 Fuel Elements by Coextrusion, Quarterly Progress Report No. 3, USAEC Report NMI-2508, Nuclear Metals, Inc., Apr. 20, 1960.
28. J. G. Hunt and P. Loewenstein, The Fabrication of Clad Massive UO_2 Fuel Elements by Coextrusion, Quarterly Progress Report No. 4, USAEC Report NMI-2510, Nuclear Metals, Inc., June 6, 1960.
29. Nuclear Metals, Inc., Fundamental and Applied Research and Development in Metallurgy, Progress Report for December 1959, USAEC Report NMI-2082, May 6, 1960.
30. Atomics International, Annual Progress Report—AEC Unclassified Programs for Fiscal Year 1960, USAEC Report NAA-SR-5350, August 1960.
31. C. H. Bloomster, Hot Press Canning of Thorium, USAEC Report HW-36169, Hanford Atomic Products Operation, Mar. 24, 1955.
32. A. M. Verblovskii and A. L. Rotinian, Nickel Plating by Thermal Decomposition of Nickel Carbonyl Vapor, USAEC Translation AEC-tr-4132, July 1960.
33. Nuclear Materials and Equipment Corp., Final Report on Coating Fuel Elements, November 15, 1958, to November 14, 1959, USAEC Report NYO-2801.
34. Nuclear Materials and Equipment Corp., Quarterly Progress Report, November 16, 1959, to February 15, 1960, USAEC Report NYO-2804.
35. Nuclear Materials and Equipment Corp., Quarterly Progress Report, February 16, 1960, to May 15, 1960, USAEC Report NYO-9184.
36. Michael Yaffee, Pyrolytic Graphite Studied for Re-Entry, *Aviation Week and Space Technology*, 73(4): 26–28 (July 25, 1960).
37. Battelle Memorial Institute, Progress on Ceramic-Coated Fuel Particles at Battelle, presented at the AEC Information Meeting held at Battelle Memorial Institute, July 12, 1960, USAEC Report BMI-1468, Sept. 16, 1960.
38. M. F. Browning et al., Alumina Coating of UO_2 Shot by Hydrolysis of Aluminum Chloride Vapor, USAEC Report BMI-1471, Battelle Memorial Institute, Oct. 25, 1960.
39. W. E. Reid et al., Electrodeposition of Tungsten and Other Refractory Metals, Report NBS-6508, National Bureau of Standards, Aug. 14, 1959.
40. Tungsten Deposition Perfected, *Chem. Eng. News*, 37(40): 24 (Oct. 5, 1959).
41. NBS Plates Tungsten, *Chem. Eng. News*, 38(6): 59 (Feb. 22, 1960).
42. F. W. Hoertel, Vapor Deposition of Tungsten on Graphite Nozzle Inserts, Monthly Progress Report No. 5, for USN, Special Project Office, Order No. IPR SP-9-60-3, September 1960.
43. W. E. Reid and A. Brenner, Tungsten for High-Temperature Coatings, *Natl. Bur. Standards (U.S.), Tech. News Bull.*, 44(2): 32–33 (February 1960).
44. W. E. Reid et al., Electrodeposition of Tungsten and Other Refractory Metals (Vapor Deposition of Tungsten), Technical Report for August 1 to

December 31, 1959, Report NBS-6666, National Bureau of Standards, Jan. 2, 1960.

45. F. W. Hoertel, Vapor Deposition of Tungsten on Graphite Nozzle Inserts, Monthly Progress Report No. 1, Order No. IPR SP-9-60-3 (DMIC 37987), Bureau of Mines, May 1960.
46. W. E. Reid et al., Electrodeposition of Tungsten and Other Refractory Metals (Vapor Deposition of Tungsten), Technical Report for January 2 to May 31, 1960, Report NBS-6877, National Bureau of Standards, June 15, 1960.
47. S. T. Wlodek and J. Wulff, The Adhesion of Vapor-Deposited Molybdenum Coatings, *J. Electrochem. Soc.*, 107(6): 565–568 (June 1960).
48. A. G. Gray, Iron-Coated Uranium and Its Production, U. S. Patent 2,928,168, Mar. 15, 1960.
49. G. Baudin et al., Protection of Uranium by Electrodeposition of Nickel and Diffusion, French Report CEA-1299, 1959.
50. Knolls Atomic Power Laboratory, Reactor Technology Report No. 12, Metallurgy, USAEC Report KAPL-2000-9, March 1960.
51. R. W. Dayton and C. R. Tipton, Jr., Progress Relating to Civilian Applications During July 1960, USAEC Report BMI-1455, Battelle Memorial Institute, Aug. 1, 1960.
52. R. W. Dayton and C. R. Tipton, Jr., Progress Relating to Civilian Applications During June 1960, USAEC Report BMI-1448, Battelle Memorial Institute, July 1, 1960. (Classified)
53. Westinghouse Electric Corp., Bettis Atomic Power Laboratory, Pressurized-Water Reactor (PWR) Project Technical Progress Report for the Period April 24 to June 23, 1960, USAEC Report WAPD-MRP-86.
54. R. L. Wachtell, Explosive Forming of Refractory Metals, Report AD-229174, Chromalloy Corp., Sept. 1, 1959.
55. Vaisl Philipchuck and Frank Bois, Explosive Welding, Progress Report No. 3 for the Period July–September 1960, National Northern Division of American Potash and Chemical Corp., West Hanover, Mass., Oct. 14, 1960.
56. C. T. Olofson and F. W. Boulger, Bibliography on Explosive Metal Working, Report DMIC-Memo-51(PB-161201), Defense Metals Information Center, Apr. 7, 1960.
57. F. W. Albaugh, Reactor and Fuels Research and Development Operation Monthly Report for July 1960, USAEC Report HW-66237-A, Hanford Atomic Products Operation, Aug. 15, 1960. (Classified)
58. J. H. Frye, Jr., et al., Metallurgy Division Annual Progress Report for Period Ending July 1, 1960, USAEC Report ORNL-2988, Oak Ridge National Laboratory, Sept. 30, 1960.
59. S. M. Silverstein et al., Welding Tantalum for High-Temperature Systems, *Metal Progr.*, 77(6): 103–109 (June 1960).
60. Angelo Brioni, Considerations on the Use of Ultrasonics in the Non-Destructive Inspection of Weldings, USAEC Translation AEC-tr-4045, 1960.
61. A. de Sterke, Automatic Ultrasonic Testing of Welds, USAEC Translation AEC-tr-4021, 1960.
62. W. J. McGonnagle et al., Argonne National Laboratory, September 1960, unpublished work.
63. W. J. McGonnagle et al., Argonne National Laboratory, October 1960, unpublished work.
64. F. G. Foote et al., Metallurgy Division Annual Report for 1959, USAEC Report ANL-6099, Argonne National Laboratory.
65. P. L. Farnsworth and T. G. Lambert, Ultrasonic Inspection of PRTR Fuel Element Cladding, USAEC Report HW-64562, Hanford Atomic Products Operation, Apr. 1, 1960.
66. Westinghouse Electric Corp., Bettis Atomic Power Laboratory, Pressurized-Water Reactor (PWR) Project Technical Progress Report for the Period February 24 to April 23, 1960, USAEC Report WAPD-MRP-85.
67. N. S. Beyer, Argonne National Laboratory, September 1960, unpublished work.
68. H. Berger, Argonne National Laboratory, September 1960, unpublished work.
69. D. Wahl and A. Liboff, Magnetic Determination of Impurities in Uranium Fuel Slugs, USAEC Report SEP-167, Sylvania Electric Products, Inc., June 18, 1956.
70. S. L. Ruby and D. G. Gardner, Review of Research on Non-Destructive Analysis of Reactor Fuel Elements, Report STI/DOC/10, International Atomic Energy Agency, Vienna, 1959.

LEGAL NOTICE

This document was prepared under the sponsorship of the U. S. Atomic Energy Commission. Neither the United States, nor the Commission, nor any person acting on behalf of the Commission:

A. Makes any warranty or representation, expressed or implied, with respect to the accuracy, completeness, or usefulness of the information contained in this report, or that the use of any information, apparatus, method, or process disclosed in this report may not infringe privately owned rights; or

B. Assumes any liabilities with respect to the use of, or for damages resulting from the use of any information, apparatus, method, or process disclosed in this report.

As used in the above, "person acting on behalf of the Commission" includes any employee or contractor of the Commission, or employee of such contractor, to the extent that such employee or contractor of the Commission, or employee of such contractor prepares, disseminates, or provides access to, any information pursuant to his employment or contract with the Commission, or his employment with such contractor.

NUCLEAR SCIENCE ABSTRACTS

The U. S. Atomic Energy Commission, Office of Technical Information, publishes *Nuclear Science Abstracts (NSA)*, a semimonthly journal containing abstracts of the literature of nuclear science and engineering.

NSA covers (1) research reports of the U. S. Atomic Energy Commission and its contractors; (2) research reports of government agencies, universities, and industrial research organizations on a world-wide basis; and (3) translations, patents, books, and articles appearing in technical and scientific journals.

Complete indexes covering subject, author, source, and report number are included in each issue. These are cumulated quarterly, semiannually, and annually providing a detailed and convenient key to the literature.

Availability of *NSA*

SALE *NSA* is available on subscription from the Superintendent of Documents, U. S. Government Printing Office, Washington 25, D. C., at $18.00 per year for the semimonthly abstract issues and $15.00 per year for the four cumulated-index issues. Subscriptions are postpaid within the United States, Canada, Mexico, and all Central and South American countries, except Argentina, Brazil, British and French Guiana, Surinam, and British Honduras. Subscribers in these Central and South American countries, and in all other countries throughout the world, should remit $22.50 per year for subscriptions to semimonthly abstract issues and $17.50 per year for the four cumulated-index issues.

EXCHANGE *NSA* is also available on an exchange basis to universities, research institutions, industrial firms, and publishers of scientific information. Inquiries should be directed to the Office of Technical Information Extension, U. S. Atomic Energy Commission, P. O. Box 62, Oak Ridge, Tennessee.

TECHNICAL PROGRESS REVIEWS may be purchased from Superintendent of Documents, U. S. Government Printing Office, Washington 25, D. C. for $2.00 per year for each subscription or for $0.55 per issue. The use of the coupon below will facilitate the handling of your order.

POSTAGE AND REMITTANCE: Postpaid within the United States, Canada, Mexico, and all Central and South American countries except as hereinafter noted. Add $0.50 per year, or $0.15 per single issue, for postage to all other countries, including Argentina, Brazil, British and French Guiana, Surinam, and British Honduras. Payment should be by check, money order, or document coupons, and MUST accompany order. Remittances from foreign countries should be made by international money order, or draft on an American bank, payable to the Superintendent of Documents, or by UNESCO book coupons.

order form

SUPERINTENDENT OF DOCUMENTS
U. S. GOVERNMENT PRINTING OFFICE
WASHINGTON 25, D. C.

Enclosed:
document coupons ☐ check ☐ money order ☐

Charge to Superintendent of Documents No. _____

Please send a one-year subscription to

☐ REACTOR CORE MATERIALS
☐ POWER REACTOR TECHNOLOGY
☐ NUCLEAR SAFETY
☐ REACTOR FUEL PROCESSING

(Each subscription $2.00 a year; $0.55 per issue.)

SUPERINTENDENT OF DOCUMENTS
U. S. GOVERNMENT PRINTING OFFICE
WASHINGTON 25, D. C.

(Print clearly)

Name _____

Street _____

City _____ Zone ____ State _____